Development of an effective cell penetrating peptide: towards viable approaches to gene delivery and chemotherapy against cancer

by

Obdulia Covarrubias-Zambrano

A.S., Seward County Community College/Area Technical School, 2012
B.S., Kansas State University, 2015

AN ABSTRACT OF A DISSERTATION

submitted in partial fulfillment of the requirements for the degree

DOCTOR OF PHILOSOPHY

Department of Chemistry
College of Arts and Sciences

KANSAS STATE UNIVERSITY
Manhattan, Kansas

2019

Abstract

Cancer is not only the second leading cause of death worldwide, but this disease consists of more than 200 different and unique types of cancer, making it a major challenge to develop a cancer treatment that could be effective against multiple cancer types. Multiple alternatives for cancer treatment have been exploited, and the use of therapeutic peptides (molecules capable of acting as neurotransmitters, hormones, ion channel ligands, or anti-infective/anti-cancer drugs) is among the most promising approaches. For this reason, our study focuses on developing a peptide that could be used as a nanocarrier to reach cancerous cells in a targeted manner. Here, a peptide was modified by replacing an amino acid at a specific location that would modify the peptide structure that could facilitate cellular uptake. Four peptides containing microtube-associated sequences (MTAS) and/or nuclear localization signals (NLS) were modified and synthesized following the solid phase peptide synthesis (SPPS) protocol. After cellular uptake experiments, WTAS peptide (MTAS segment containing an amino acid replaced with Trp "W"), resulted in the most effective cell penetrating peptide. Fixed and live confocal studies demonstrated that WTAS was able to penetrate cells within a couple seconds after exposure, and it was further transported to the cell nucleus in the GL26 cancerous cell within a few minutes after penetrating the cell. Interestingly enough, WTAS seemed to lose its ability to penetrate the cell nucleus when it was tested on SIM-A9, a non-cancerous cell line. More studies must be conducted to clearly demonstrate whether WTAS is capable to penetrate cell nuclei in cancer cells only.

Furthermore, WTAS was used to develop a second peptide that could be an improved anti-cancer therapeutic peptide. D-SA-K_6L_9-AS is a highly toxic therapeutic peptide that had been previously synthesized in our research group. For our next approach, following the SPPS

procedure, we synthesized a longer version of both peptides, WTAS and D-SA-K_6L_9-AS to create WTAS-D-SA-K_6L_9-AS. After successfully synthesizing this peptide, it was characterized by HPLC and MS. Cytotoxicity effects were compared to those of D-SA-K_6L_9-AS alone on B16F10 and GL26 cell lines, and results demonstrated that toxicity levels did not change after the addition of the WTAS peptide. Also, confocal studies determined that WTAS-D-SA-K_6L_9-AS still had the ability to target the mitochondria after penetration of the cell and could also reach the cell nucleus in the GL26 cell line. This behavior reflects a unique characteristic common to both peptides. Lastly, fluorescence microscope experiments determined that WTAS-D-SA-K_6L_9-AS kills cells in the GL26 cell line via the necrosis pathway.

WTAS was further used to develop a novel gene delivery nanocarrier composed of WTAS peptide as the primary nanocarrier and poly(β-amino ester) (PBAE) polymer as the secondary nanocarrier. PBAE polymer, a nontoxic and biodegradable polymer, was used to improve the stability of WTAS peptide while facilitating the transportation into cells. After assembling and characterizing the nanocarrier, cell cytotoxicity studies were determined in three cell lines, SIM-A9, B16F10, and GL26. Finally, cell transfection was achieved by utilizing the self-assembling PBAE-WTAS nanocarrier and plasmid DNA genetically modified to express GFP (green fluorescent protein). Results demonstrated effective transfection of the GL26 cell line within 48 hours after loading the cells with the nanocarrier. This nanocarrier can be optimized by including targeting reagents in conjunction with designer plasmids against various diseases.

Development of an effective cell penetrating peptide: towards viable approaches to gene delivery and chemotherapy against cancer

by

Obdulia Covarrubias-Zambrano

A.S., Seward County Community College/Area Technical School, 2012
B.S., Kansas State University, 2015

A DISSERTATION

submitted in partial fulfillment of the requirements for the degree

DOCTOR OF PHILOSOPHY

Department of Chemistry
College of Arts and Sciences

KANSAS STATE UNIVERSITY
Manhattan, Kansas

2019

Approved by:

Major Professor
Stefan H. Bossmann

Copyright

© Obdulia Covarrubias-Zambrano 2019.

Abstract

Cancer is not only the second leading cause of death worldwide, but this disease consists of more than 200 different and unique types of cancer, making it a major challenge to develop a cancer treatment that could be effective against multiple cancer types. Multiple alternatives for cancer treatment have been exploited, and the use of therapeutic peptides (molecules capable of acting as neurotransmitters, hormones, ion channel ligands, or anti-infective/anti-cancer drugs) is among the most promising approaches. For this reason, our study focuses on developing a peptide that could be used as a nanocarrier to reach cancerous cells in a targeted manner. Here, a peptide was modified by replacing an amino acid at a specific location that would modify the peptide structure that could facilitate cellular uptake. Four peptides containing microtube-associated sequences (MTAS) and/or nuclear localization signals (NLS) were modified and synthesized following the solid phase peptide synthesis (SPPS) protocol. After cellular uptake experiments, WTAS peptide (MTAS segment containing an amino acid replaced with Trp "W"), resulted in the most effective cell penetrating peptide. Fixed and live confocal studies demonstrated that WTAS was able to penetrate cells within a couple seconds after exposure, and it was further transported to the cell nucleus in the GL26 cancerous cell within a few minutes after penetrating the cell. Interestingly enough, WTAS seemed to lose its ability to penetrate the cell nucleus when it was tested on SIM-A9, a non-cancerous cell line. More studies must be conducted to clearly demonstrate whether WTAS is capable to penetrate cell nuclei in cancer cells only.

Furthermore, WTAS was used to develop a second peptide that could be an improved anti-cancer therapeutic peptide. D-SA-K_6L_9-AS is a highly toxic therapeutic peptide that had been previously synthesized in our research group. For our next approach, following the SPPS

procedure, we synthesized a longer version of both peptides, WTAS and D-SA-K_6L_9-AS to create WTAS-D-SA-K_6L_9-AS. After successfully synthesizing this peptide, it was characterized by HPLC and MS. Cytotoxicity effects were compared to those of D-SA-K_6L_9-AS alone on B16F10 and GL26 cell lines, and results demonstrated that toxicity levels did not change after the addition of the WTAS peptide. Also, confocal studies determined that WTAS-D-SA-K_6L_9-AS still had the ability to target the mitochondria after penetration of the cell and could also reach the cell nucleus in the GL26 cell line. This behavior reflects a unique characteristic common to both peptides. Lastly, fluorescence microscope experiments determined that WTAS-D-SA-K_6L_9-AS kills cells in the GL26 cell line via the necrosis pathway.

WTAS was further used to develop a novel gene delivery nanocarrier composed of WTAS peptide as the primary nanocarrier and poly(β-amino ester) (PBAE) polymer as the secondary nanocarrier. PBAE polymer, a nontoxic and biodegradable polymer, was used to improve the stability of WTAS peptide while facilitating the transportation into cells. After assembling and characterizing the nanocarrier, cell cytotoxicity studies were determined in three cell lines, SIM-A9, B16F10, and GL26. Finally, cell transfection was achieved by utilizing the self-assembling PBAE-WTAS nanocarrier and plasmid DNA genetically modified to express GFP (green fluorescent protein). Results demonstrated effective transfection of the GL26 cell line within 48 hours after loading the cells with the nanocarrier. This nanocarrier can be optimized by including targeting reagents in conjunction with designer plasmids against various diseases.

Table of Contents

List of Figures

List of Tables

Acknowledgements

This accomplishment is not mine alone! Getting to this point is not only because of the hard work and dedication I have put from my part throughout these years, but it is also due to the help, advice, guidance, support, and motivation from very important people in my life. It is a true blessing to have all these people in my life, and I would like to take a moment to acknowledge them for making this moment a reality.

First and foremost, I would like to specially and sincerely thank my major professor, advisor, and mentor, Dr. Stefan H. Bossmann. Thank you for giving me the opportunity to be part of the Bossmann group, thank you for believing in me even when I couldn't do it myself, and thank you for not letting me quit when I felt like doing so. Thank you for all your encouragement, support, and guidance during these 4 years. But most importantly, thank you for being the best role model and example of what a great, intelligent, kind, caring, patient, and supportive mentor and boss you are! Thank you for being the best mentor to all of us! Truly, your support, encouragement, and guidance are the reason why I made it until the end. It has been a real blessing and honor to work with you and to have you in my life! THANK YOU!

I would also like to thank Katrin Bossmann, for all her love, support, and guidance during this time. Thank you for always checking on me, to make sure I was doing okay. Thank you for taking your time to listen to me when things got overwhelmed. And big thank you for always proof-reading and polishing my writing!

I also want to thank my current and previous committee members: Dr. Daryl Troyer, Dr. Emily McLaurin, Dr. Ping Li, Dr. Christine Aikens, Dr. Jianzhong Yu, Dr. Paul E. Smith and Dr. Anna Zinovyeva for their time, suggestions, and support through this journey.

A big thank you goes to Dr. Tej Shrestha and Marla Pyle for their help and guidance to teach me cell culture, transfection, and cell experiment techniques.

I would like to thank all former and current members of the Bossmann group! A big thanks to Lauren, for becoming my study partner and making the suffering of those exams and cumes easier! Thank you for becoming such a close friend and for making this PhD journey fun! And of course, I would like to thank my undergraduates Maria Montes-Gonzalez and Vannessa Hernandez for all your help in the lab, it was a pleasure to work with exceptional mentees who made research exciting and fun to teach.

Also, I want to thank the professors, faculty, and staff from the Department of Chemistry. A special thank you goes to Tobe Eggers and James Hodgson for facilitating our research work with your work.

I would also like to thank all the teachers, advisors, and mentors that believed in me since high school. I am the first person in my family to attend college, and this was made possible because even since high school I was blessed with a teacher who opened the door and guided me to the next level. These are people who truly marked my life and are close to my heart: Coach Lori Navarro, Mrs. Owens, Mrs. Boles, Mrs. Westerman, Rhonda L. Kinser, Dr. William Bryan, Dr. Todd Carter, Ms. Anita Cortez, Dr. Dorith Rotenber, and Dr. Karen Alviar.

Last but not least, I would like to thank my wonderful, loving, and supportive family!

My biggest fans and role models, my loving parents Julian and Obdulia Covarrubias! They are the reason why I am here, and the ones responsible for the woman I have grown to be. They taught me to get up and keep going after falling, to never give up no matter how hard it gets, and to always be the best person I can be. To love unconditionally and never forget my

roots and where I come from. Through hard work and sacrifices, they have given the best life to my 3 brothers and myself. The best parents ever! Muchas gracias Papi & Mami! Los amo!

My best friend, loving, patient, and supportive husband, Ricardo Perez! Thank you for being with me through my entire Ph.D., first as a friend and now as my husband. Thank you for praying for and with me when things got difficult. Thank you for always reminding myself who I am and listening to me complaint after a long day of work. Thank you for the long hours you listened to me practice presentations and helped me prepared for them. Specially thank you for your patience and guidance especially during these last few months, and for reminding me to take a break, have fun and enjoy life once in a while. Thank you for becoming my biggest support during harsh times. Thank you for loving me unconditionally! Te amo!

Thank you to my lifelong best friend and partner in crime for the last 25 years, Jose Covarrubias. My time here in Manhattan could not have been the same without you. Thank you for always being with me during good and not so good times. Thank you for always loving and caring for me, and for becoming that protective little brother you are. Also, thank you for introducing me to Dr. Bossmann! Doing science with you has been a true blessing! I love having you as my best friend, little brother, and collaborator! Also, I would like to than my two oldest brothers, Julian and Salvador Covarrubias. They always pushed Jose and I to attend college and earn a degree, which was something they were not able to do. Also, thanks to my two sisters-in-law who became the sisters I always dreamed of, Miriam and Nena Covarrubias. Thank you for becoming part of my life and for all your love and support. Lastly, thanks to my friends from Manhattan, who became a family away from home, my Bluemont Church Family!

Thanks to God for blessing me with these people in my life and allowing all this to happen!

Dedication

"There is only one thing that makes a dream impossible to achieve: the fear of failure"

Paulo Coelho

I dedicate my doctoral dissertation to my little troublemakers and biggest motivation to always be the best example of life I can be, my loving little boys, who more than my nephews are like my own kids: *Bryan, Julian Jr., Jonathan, Axel, and Gabriel Covarrubias*. Their unconditional love and the way they admire the work I do as a scientist was so inspiring to me, especially when they told me once that they wanted to be like me when they grow up. I hope with all my heart that when they grow up, they will be inspired to work hard, achieve all their dreams, and dream big, just like I have done!

Chapter 1 - Nanotechnologies to Improve the Pharmacological Profile of Therapeutic Peptides

1. Abstract

Therapeutic peptides (TPs) are a class of molecules with interesting biological properties, being able to act as **neurotransmitters, hormones, ion channel ligands, growth factors or anti-infectives**. Taking into account their attractive pharmacological profile, therapeutic peptides represent a valid starting point for the development of new drugs. This is encouraged by their lower manufacturing costs compared with protein-based biopharmaceuticals and it is confirmed by the increasing number of peptides in the preclinical phase and clinical trials.

On the other hand, bringing these compounds into the pharmaceutical market is difficult due to some important intrinsic limitations of TPs: low biostability, cytotoxicity at high concentrations and the difficulty in reaching the site of infection at active concentrations. All these limitations make the marketing of TPs a research challenge. For these reasons, advances in nanotechnology have allowed us to counteract these disadvantages. In particular, conjugation and/or the coating of a TP to inorganic/organic nanoparticles (NPs) represent a valid choice for protecting TPs against degradation and for serving as a delivery system. This is possible due to the ability of NPs to be functionalized with a great variety of biocompatible molecules and to be easily synthesized in a variety of shapes and sizes. In addition, the coating/conjugation of TPs to NPs allows to increase the active concentration of TPs at the target site and/or to provide a gradual release of the drug, thus reducing the number of administrations. Therefore, the progress of nanotechnologies, combined with the biological properties of these peptides, represent the new frontier of pharmacology and medicine.

2. Introduction

2.1 Pros and Cons of Therapeutic Peptides

Therapeutic peptides contain up to 50 amino acids, which corresponds to > 10^{35} possible peptide sequences. Because of their versatility and tunability, and the experience that was gained during a century of research, peptide therapeutics are considered highly selective, biocompatible and reasonably safe[1-3]. Major problems arise from rapid proteolytic degradation, peptide **a**bsorption (e.g. to serum proteins), (bio)**d**istribution, **m**etabolism, and **e**xcretion (ADME)[4] and in-vivo pharmacological barriers[1]. These effects have severely limited clinical translation, especially when delivery to the brain[5] and/or tumors/metastases[5,6] has been attempted.

Here, we will address the challenges and opportunities of using nanotechnology-based approaches to improve the pharmacological profile[3] of therapeutic peptides[7,8]. Historically, peptides have been developed to target G-protein coupled receptors[9] and other extracellular targets, ion channels and enzymes, such as proteases and kinases[10-14]. In these areas, major competition by small-molecule drugs exist, which can be synthesized more efficiently and are more cost-efficient[15,16]. Furthermore, high-throughput screening methods for small-molecule drugs exist that can identify lead compounds from large libraries[17,18]. These disadvantages have been relatively recently addressed by developing renewable methods for peptide synthesis[19], and incorporation of non-natural building blocks[20,21] and the design of peptide/drug hybrids[22-26]. A major advantage of therapeutic peptides in comparison with small molecule drugs is that they are capable of effectively targeting protein:protein interactions (PPIs), especially if these interactions depend on numerous spatially-distinct low affinity interactions, in opposite to PPIs that depend on pockets or concentrated binding foci[1,10,27-30]. Further application of peptide therapeutics comprise cell signaling[31], and inhibition of cell function[32].

"According to the *Global Peptide Therapeutics Market & Clinical Trials Insight 2022* report[33], there are more than 100 peptide-based drugs commercially available, and 688 of them are in the clinical pipeline and have a variety of different delivery strategies." [1]

2.2 Proteolytic Instability

Intracellular peptidases are capable of degrading more than 99% of the peptides that are either released by the proteasome or were able to enter the cell[34] within minutes[3]. The following proteases have been identified as key players in these processes: Tripeptidyl peptidase II (TPPII)[35], Thimet oligopeptidase (TOP)[36,37], Neurolysin[38], Nardilysin (insulin-degrading enzyme)[39] and Prolyl oligopeptidase[40]. The peptides generated by peptidases are further converted into free amino acids by aminopeptidases, including puromycin-sensitive aminopeptidase, leucine aminopeptidase, cysteinylaminopeptidase, insulin-regulated aminopeptidase, bleomycin hydrolase, aminopeptidase A and aminopeptidase B[41,42]. In serum, metallo- and Ca^{2+}-dependent proteases are present, as well as and heparin (e.g. thrombin, factor Xa) and plasmin[43]. Important interstitial proteases comprise collagenolytic enzymes include matrix metalloproteinases, cathepsin K, and neutrophil elastase[44].

To enhance the pharmacological profile of linear therapeutic peptides, the following strategies have been explored:

1) Chemical Modification of Peptides
2) Synthesis of Cyclic Peptides
3) Supramolecular Aggregation of Therapeutic Peptides
4) Development of Nanocarriers for Therapeutic Peptides

2.3 Uptake Mechanisms of Nanoparticles in Cells

The uptake of peptides, proteins, and nanostructures by cells occurs by means of various pathways, depending on their size and, to a lesser degree, on their shape, albeit the discussions about shape are somewhat clouded by persisting problems of reproducibility in nanostructure synthesis[1]. The three principal pathways of endocytosis can be distinguished as non-specific uptake, pinocytosis, and phagocytosis[1,45-52]. (Figure 1) Non-specific uptake occurs via direct penetration, the formation of transmembrane pores, or passive diffusion[48-52]. Pinocytosis (cellular drinking) consists of the uptake of fluid and dissolved (macro)molecules via small vesicles (< 0.15 μm in diameter)[45]. Depending on the size of the object that is ingested via pinocytosis, macropinocytosis, clathrin- and caveolin-mediated endocytosis, and clathrin- and caveolin-independent endocytosis can be distinguished[46]. Phagocytosis, which proceeds via the formation of phagosomes (> 0.25 μm in diameter)[46,47] is utilized for the assimilation of microorganisms and cell debris and mainly performed by phagocytes (i.e., monocytes/ macrophages, neutrophils, dendritic cells). Phagosomes undergo fusion and fission events with components of the endocytotic pathway. Eventually mature phagolysosomes are formed, in which their content is enzymatically degraded[53]. Macropinocytosis depends on actin formation. Macropinosomes are large intracellular vesicles[54,55].

Clathrin-mediated endocytosis belongs to the group of receptor-mediated endocytotic processes. It is distinctly faster than phagocytosis, micropinocytosis, and caveolin-dependent endocytosis. In virtually all mammalian cells, clathrin-mediated endocytosis is responsible for nutrient uptake, for instance cholesterol-laden low-density lipoprotein particles that target the low-density lipoprotein receptor and iron-rich transferrin that binds to transferrin receptors[56,57]. Caveolae are flask-shaped invaginations of the plasma membrane. Caveolin-mediated

endocytosis is dependent on cholesterol-rich microdomains (lipid rafts, 40-50nm in diameter)[58,59]. Caveolin-1 is a dimeric protein that binds cholesterol for lipid homeostasis[60]. Clathrin- and caveolin-independent endocytotic mechanisms are less understood than receptor-mediated uptake processes. The general paradigm is that they also arise from cholesterol-rich microdomains and proceed via sorting processes of membrane proteins, glycoproteins, and/or glycolipids[58,59]. All pinocytotic and phagocytotic processes have in common that the proteins and nanoparticles end up in membrane-bound compartments. Therefore, appropriate "escape strategies" have to be designed to avoid enzymatic degradation of the delivered payload in late endosomes, which are formed by means of fusion between endosomes and lysosomes[3,61,62].

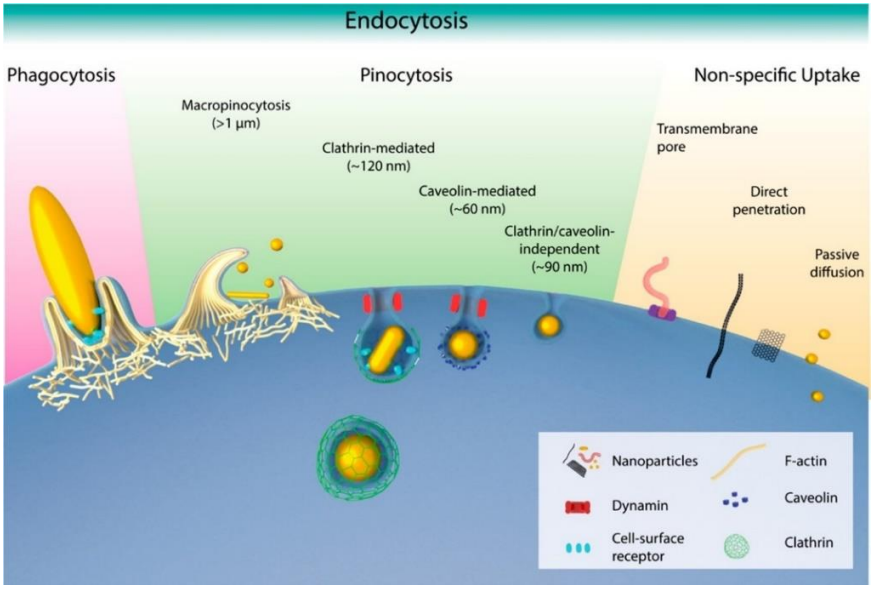

Figure 1. Schematic representation of different endocytotic mechanisms.
Large (micrometer-sized) particles may be actively incorporated via phagocytosis. Areas of high curvature on anisotropic particles, such as large ellipsoids, can contact cells and be more favorably phagocytosed. Smaller particles can be internalized through multiple distinct mechanisms, namely, macropinocytosis (>1 μm), clathrin-mediated endocytosis (~120 nm), clathrin- and caveolae-independent endocytosis, or caveolae-mediated endocytosis (~60 nm). Besides active transport, nanoparticles may also enter the cell passively via diffusion or passive uptake by van der Waals or steric interactions through the plasma membrane. This can include piercing of the cell membrane by areas of very high curvature (e.g., carbon nanotubes or graphene edges)."[63] Reprinted with permission from (Kinnear C, Moore TL, Rodriguez-Lorenzo L, Rothen-Rutishauser B, Petri-Fink A. Form Follows Function: Nanoparticle Shape and Its Implications for Nanomedicine. Chem Rev (Washington, DC, U S). 2017;117(17):11476-521. doi: 10.1021/acs.chemrev.7b00194). Copyright (2017) American Chemical Society.

2.4 Interactions of Peptides with Cell Membranes

In opposite to cell-penetrating peptides, bilayer-disrupting peptides are therapeutic peptides, which kill cells by means of one of four principal mechanisms of bilayer membrane disruption that are depicted in Figure 1[48]. Upon reaching the required threshold concentration, the peptides either insert into the bilayer membrane structure and form either barrel stave pores[49], toroidal pores[50], or disordered toroidal pores[51]. For barrel stave and toroidal pores, it is required that the lengths of the peptide sequence after assuming its 3D structure are long enough to span the entire diameter of the bilayer membrane[48]. If that is not possible, disordered toroidal pores can be formed[51]. One important alternative to pore-forming mechanisms is the carpet mechanism[52], in which the therapeutic peptides adsorb parallel to the bilayer. Upon reaching the threshold concentration, micellization of membrane components and entire membrane sections can be observed. These processes can disintegrate bilayer membranes very efficiently[48].

3. Cell Penetrating Peptides

The discovery of cell penetrating peptides (CPPs) is one of the major breakthroughs in transportation of peptides, proteins, and nanostructures through cell membrane. Transport of these large molecules, aggregates, and clusters was challenging due to their size and biophysical properties[64]. In 1988, Frankel and Pabo discovered the rapid uptake of a purified *trans*-activator protein (TAT) from HIV virus type 1 by HL3T1 cells[65]. Its rapid uptake was later to be discovered to occur through endocytosis[66]. In 1997, Vives et al. discovered that the domain responsible for cellular uptake was a region that consisted of 13 amino acids (GRKKRRQRRRPPQ)[67]. Park et al. then successfully shortened the TAT peptide to the 9-mer RKKRRQRRR in 2002 [68,69]. Nowadays, CPPs are relatively short peptide sequences with 5-30 amino acids that can go through tissue and cell membranes, either by direct penetration (energy independent) or endocytosis (energy

dependent)[66,69]. CPPs are unique, since not only they can penetrate cells, but they can also transport a variety of cargos, including proteins, peptides, small drugs, nanoparticles, as well as genetic information like DNA and siRNA[69]. Despite being a breakthrough due to their efficiency to penetrate cells and transport payloads, the first generation of CPPs did not show a significant specificity for any targeted tissue, which is a major drawback for their intended application of delivering cargo to cancer/metastases or pathogens[2,69]. Therefore, in order to enhance cellular uptake to specific sites, scientists have developed stimuli-response CPPs, which stimuli can be responsive to pH or stress variation as well as enzymic activity[70]. For example, a CPP was designed and synthesized to form an α-helical structure that became pH responsive by substituting all lysine with histidines[71]. This study demonstrated that at physiological pH, the peptide remained at a neutral charge, and when exposed to acidic conditions, its net charge became positive, which then activated the ability to penetrate cells[70]. In general, cationic, hydrophobic, and amphipathic CPPs can be distinguished.

Classification	Peptide	Sequence	Reference
Cationic	TAT (HIV-1 TAT protein, TAT_{48-60})	GRKKRRQRRRPPQ	(67)
	TAT (HIV-1 TAT protein, TAT_{49-57})	RKKRRQRRR	(68)
	Penetratin $pAntp_{43-58}$	RQIKIWFQNRRMKWKK	(73, 74)
	Polyarginines	R_n	(75)
	Polylysines	K_n	(76)
	DPV1047	VKRGLKLRHVRPRVTRMDV	(77)
	[D]-K6L9	LKlLKkLlkKLLkLL	(52, 78)
	NLS	CGYGPKKKRKVGG	(79)

	cyclic [W(RW)$_4$]	[WRWRWRWRW]	(80)
	NrTP5	YkqchkkGGkkGsG	(81)
	hPP3	KPKRKRRKKKGHGWSR	(82)
Amphiphatic	Transportan	GWTLNSAGYLLG GWTLNSAGYLLGKINLKALAALAKKIL	(83, 84)
	MPG	GALFLGFLGAAGSTMGAWSQPKKKRKV	(85)
	Pep-1	KETWWETWWTEWSQPKKKRKV	(85)
	VP22	NAATATRGRSAASRPTQR	(86)
	MPG	GALFLGFLGAAGSTMGAWSQPKKKRKV	(85)
	pVEC	LLIILRRRIRKQAHAHSK	(87)
	BPrPp (1-26)	MVKSKIGSWILVLFVAMWSDVGLCKKRP	(88)
	ARF (1-22)	MVRRFLVTLRIRRACGPPRVRV	(89)
	VT5	DPKGDPPKGV(TV)$_5$GKGDPKPD	(90)
	MAP	KLALKLALKALKAALKLA	(91)
	p28	LSTAADMQGVVTDGMASGLDKDYLKPDD	(91)
	Bac 7 (Bac$_{1-24}$)	RRIRPRPPRLPRPRPRPLPFPRPG	(92)
Hydrophobic	C105Y	CSIPPEVKFNKPFVYLI	(93)
	PFVYLI	PFVYLI	(94)
	Pep-7	SDLWEMMMVSLACQY	(95)
	VP22	DAATATRGRSAASRPTERPRAPARSASRPRRVD	(96)

Table 1. Cell-Penetrating Peptides (CPPs), ordered by biophysical properties[2,69,72]

4. Chemical Stabilization Strategies for Therapeutic Peptides

4.1 Chemical Modification

Numerous chemical stabilization strategies of therapeutic peptides are discussed in the literature. All of these modifications are designed to decrease their vulnerability to proteolytic cleavage and, therefore, to enhance their circulation lifetimes. Among the simplest chemical modifications are N-terminal acetylation or glycosylation, and C-terminal amidation[97]. Other strategies comprise N-methylation[98], integration of D-amino acids[78,99-101], β-amino acids[102], β–

and γ–amino acids[103], and incorporation of non-native amino acids and pseudo-peptide bonds[104]. Complete D-amino acid variants, synthesized as "retro-inverso" peptides[105-107], exhibit significantly enhanced in-vivo stability (>10 times higher circulation lifetimes)[108,109]. However, decreased delivery activity of retro-inverso peptides has been observed in-vivo[110].

It has been established that the presence of sulfated or phosphorylated tyrosine residues and linkage of N-terminal glutamic acid via the γ-carboxy group decreases proteolytic activity as well[111]. A widely established strategy to enhance peptide stability is the attachment of polyethylene glycol (PEG)[112]. This chemical modification increases peptide hydrophilicity and reduces immunogenicity[113]. This concept was successfully demonstrated by investigating HIV-1 fusion inhibitors[114] and BH3 peptide[115,116], which showed significant improvements in half-lives, compared to the not chemically modified peptides[114-116]. The major drawbacks of chemical modifications are that the increase in half-lives seldom exceeds a factor of five, and that chemical modification can either impair or modify peptide function[1,3].

4.2 Cyclic Peptides

Cyclization is a viable strategy to suppress exoproteolytic activity by eliminating terminal peptide bonds and to decrease endoproteolytic activity by creating rigidity in the formed macrocycle[99,117]. The most effective targeting peptides to date are the group of iRGD-derivatives, which have been pioneered by Ruoslahti[58,118-126]. The development of the cyclic iRGD follows the discovery of the tripeptide sequence Arg-Gly-Asp (RGD)[127] that is the most acclaimed recognition motif for αv integrins. The latter are members of a family of 24 receptors that facilitate cellular adhesion to and migration on extracellular matrix proteins[128]. $\alpha_v\beta_3$ is one of the αv integrins that RGD is able to target. It is highly expressed on endothelial cells of tumor neovasculature, as well as on the surface of some tumor cells[128]. However, RGD is also able to target $\alpha_v\beta_1$, $\alpha_v\beta_5$, $\alpha_v\beta_6$,

$\alpha_v\beta_8$, $\alpha_5\beta_1$, $\alpha_8\beta_1$, and $\alpha_{IIb}\beta_3$, which is the cause for limited targeting efficacy[128,129]. Nevertheless, RGD-mediated targeting has been extensively explored for cancer imaging and drug delivery[130,131]. Cyclic RGD-derivatives offer the advantage of enhanced stability and binding strength to αv integrins[130,132]. In 2009, Ruoslathi et al. published the cyclic peptide iRGD (i=internalizing) CRGDK/RGPD/EC), which is capable of effective cell/tissue penetration in addition to tumor-targeting by means of RGD[133]. The family of cyclic iRGD derivatives has proven superior to other targeting peptides in tumor-targeted delivery of small molecules, antibodies, and nanoparticles[120-124,133,134]. The enhanced performance of iRGD can be explained by demonstrating that it follows consecutive steps[133]. In the first step, the RGD motif on the N-terminal region of iRGD recognizes $\alpha_v\beta_3$ or $\alpha_v\beta_5$ integrins. iRGD is then proteolytically cleaved to reveal the cryptic C-end Rule (CendR) motif (R/KXXR/K, X=any amino acid)[133]. Thus, the N-terminal half fragment of iRGD (CRGDK/R) is enabled to bind to neuropilin-1 (NRP-1), which facilitates cellular uptake, vascular leakage, and deep penetration into extravascular tumor tissue[118]. The family of neuropilines (NRPs) are trans-membrane receptors required for axon guidance and vascular development. They feature a carboxy-terminal, which recognize growth factors and other hormones through a carboxy (C)-terminal (CendR binding motif). Peptides featuring this motif trigger receptor-mediated endocytosis. Interestingly, CendR-mediated endocytosis resembles macropinacytosis. It has been labeled a “bulky transport pathway”. Cho et al. have demonstrated in 2019 that both the N- and C-termini of iRGDC can be tethered to either a FRET-pair to enable imaging or the combination of a fluorescent dye (cyanine 5.5) and a cisplatin prodrug, thus creating a theranostic reagent based on iRGD[134].

Year	Peptide	Sequence	References
2009	iRGD	CRGDK/RGPD/EC	(133)
2013	Cys-iRGDC (iRGDC)	C X'CRGDK/RGPD/EC (X' = 6-aminohexanoic acid)	(122, 134)
2013	Cys-X-iRGD (iRGDC)	CX'GGSGGSGGCRGDK/RGPD/EC (X' = 6-aminohexanoic acid)	(122)

Table 2. The iRGD Family

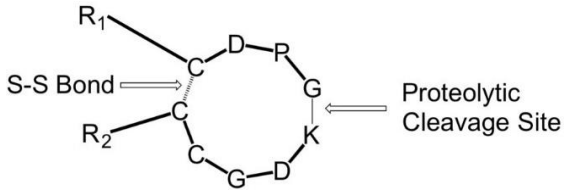

Figure 2. General structure of the iRGD Family.
iRGD contains a proteolytic cleavage site and a disulfide bond, which undergoes reductive cleavage[133]. On both, the N- and C- termini, functional tethers and/or diagnostic or therapeutic payloads can be attached[134].

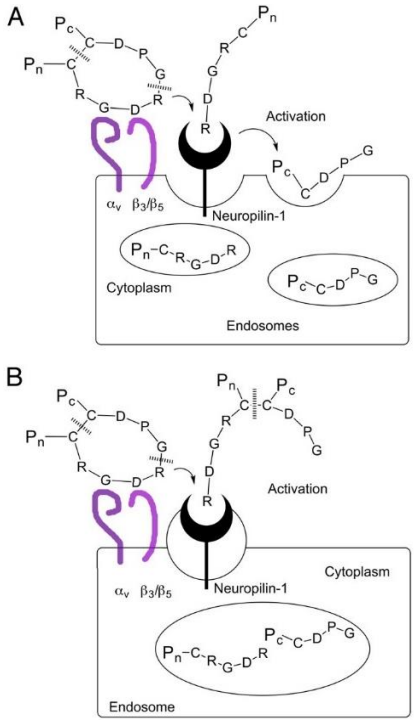

Figure 3. Proposed mechanisms for iRGD uptake.
A) Extracellular proteotic and reductive cleavage, followed by endosomal uptake;
B) extracellular proteotic cleavage, followed by neuropilin-1-triggered endosomal uptake and intracellular reductive cleavage. P_c: payload at the C-terminal end; P_n: payload at the n-terminal end[134].

5. Delivery to the Central Nervous System

The blood-brain-barrier (BBB)[2,135] is an essential biological semipermeable membrane that shields the brain and central nervous system (CNS) from peripheral circulating blood[136]. The BBB is formed by complex interaction between vascular endothelium, pericytes, and astrocytes. It is characterized by tight junctions and the absence of fenestrations, as well as high proteolytic activity and the existence of efflux pumps. Consequently, the BBB effectively restricts transport for numerous solutes[136]. Naturally, this also means that numerous therapeutic compounds cannot cross the BBB into the CNS[137]. Passive transport of gases, water, and other small molecules (e.g. ethanol) is quite effective. Passive transport of larger molecules is governed by molecular size, polarity (logP) and charge. A general rule (with numerous exceptions) is that molecules that are able to cross the BBB by means of passive diffusion should have a molecular weight of 400-500, log P = 1-2, and basic pH[138-140]. However, the shape of molecules and especially peptides can be quite a decisive factor[141]. CPPs hold enormous promise for delivery across the BBB, in spite of negative experiences in the past[2,142]. Schwarze et al. demonstrated in 1999 that Tat is able to deliver conjugated β-galactosidase into the mouse brain[143]. This finding is regarded as the beginning of designing Tat-derivatives and other peptides for enhanced BBB crossing[144-146]. As Table 3 indicates, numerous peptides have been inspired by peptide shuttles that were designed by evolutionary processes to deliver essential nutrients across the BBB. For instance, transport peptides capable of triggering receptor-mediated transcytosis (RMT) involving nicotine acetyl-choline (nAChRs)[147], transferrin (TfR)[148], low-density lipoprotein (LDLR) or low-density lipoprotein receptor-related protein-1 (LRP-1)[147,149] were designed to deliver payloads to the CNS. The discovery that endogeneous ligands are transported through the BBB[150] sparked an intensive search for suitable peptides, which are summarized in Table 3. The 16-residue peptide CDX,

derived from the snake neurotoxin candoxin, binds to nicotine acetyl-choline receptors (nAChRs), which facilitates transcytosis[151]. It is noteworthy that the retro-inverso isomer (^{re}CDX) (= the inverted sequence of D-amino acids) displayed superior transcytosis efficacy compared to ^{L}CDX when crossing to BBB of glioblastoma-bearing nude mice[151], because of its significantly higher stability against proteolytic degradation. However, it should be noted that glioblastomas usually cause at least a partial breakdown of the BBB, especially in later stages[152]. The transferrin receptor TfR internalizes can be targeted by peptides B6, CRT, THR, and T7, which have been discovered through phage displays[153-156]. All four peptides mimic the transferrin-iron complex, which is naturally shuttled by TfR through the BBB.

Proposed Transport(s)	Peptide BBB Shuttles	Sequence	Ref.
nAChRs	RVG29	YTIWMPENPRPGTPCDIFTNSRGKRASNG	(157)
	^{L}CDX	FKESWREARGTRIERG	(151)
	^{re}CDX	GreirtGraerwsekf	(130)
LRP/LDLR	Angiopep-2	TFFYGGSRGKRNNFKTEEY	(158)
	ApoB (3371–3409)	SSVIDALQYKLEGTTRLTRKRGLKLATALSLSNKFVEGS	(159)
	ApoE (159–167)$_2$	(LRKLRKRLL)$_2$	(160)
TfR	B6	CGHKAKGPRK	(154)
	T7	HAIYPRH	(153)
	THR	THRPPMWSPVWP	(156)
	^{re}THR	Pwvpswmpprht	(161)
Leptin Receptor	Leptin 30	YQQILTSMPSRNVIQISND-LENLRDLLHVL	(162)
GSH transporter	GSH	γ-l-glutamyl-CG	(161)
GM1	G23	HLNILSTLWKYRC	(162)
AMT	Tat(47-57)	YGRKKRQRRR	(163)

	SynB1	RGGRLSYSRRRFSTSTGR	(164)
Active transport	PepNeg	SGTQEEY	(165)

Table 3. Peptides capable of transcytosis through the Blood-Brain-Barrier.
Abbreviations: AMT, adsorptive-mediated transport; GM1, monosialotetrahexosylganglioside; GSH, glutathione; KCa channel, calcium-activated potassium channel; LDLR, low-density lipoprotein receptor; LRP-1, low-density lipoprotein receptor-related protein-1; nAChRs, nicotine acetyl-choline receptors; TfR, transferrin receptor.

6. Antibody-Mediated Uptake of Therapeutic Peptides

Antibodies hold considerable promise for targeting "soft targets", which do not exhibit structures that are druggable using small molecule drugs[166,167]. They can be generated by means of the well-established hybridoma technology or phage displays[168,169]. Although the general technology is well-established, the industrial production of antibodies with consistent quality standards can be challenging at times[170]. Whereas targeting epitopes at the surface of cells is straightforward, targeting cytosolic targets requires uptake[166]. These antibodies can be taken up by phagocytotic cells, sometimes causing off-target effects[171]. This problem can be addressed by utilizing smaller antibody fragments devoid of Fc regions such as antigen binding fragments (Fab), single chain variable fragment (S_cF_v), and nanobodies[166]. As discussed above, smaller antibody derivatives will be cleared from circulation much more rapidly than native antibodies[3,166]. It should be mentioned that antibody-targeting of cellular surface receptors often leads to receptor-mediated endocytosis[172]. However, this is not an option for an antibody with a target in the cytosol, mitochondria, endoplasmatic reticulum, or nucleus[166].

Once cytosolic antibodies are taken up via endocytosis, the endosomes are fused with lysosomes, which facilitate cathepsin-mediated degradation of protein-content. Therefore, antibodies/ antibody-fragments have to escape from the endosomes to remain active in the cytoplasm[173]. There are several solutions to this problem (see Figure 4). The antibody(fragment)

can either be microinjected[174,175] , or delivered via electroporation[176,177], which is only feasible in-vitro, or attached to a delivery vehicle or a peptide sequence allowing rapid uptake by the cell and/or endosomal escape (Table 1)[166].

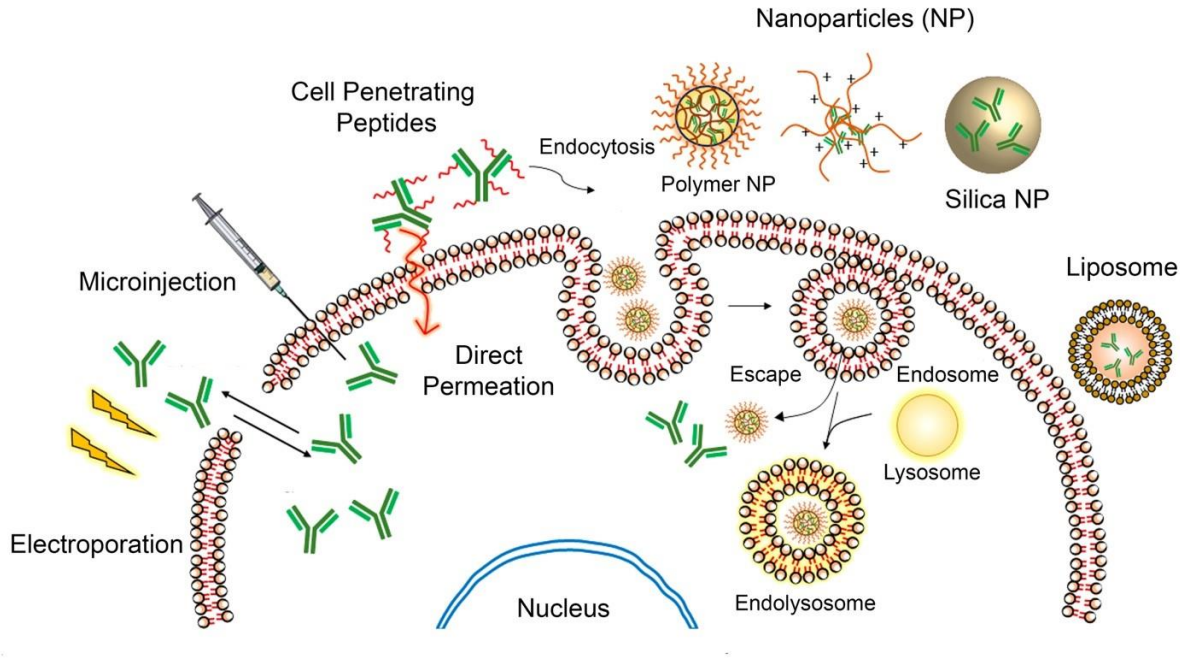

Figure 4. Mechanism of cellular entry by peptides, antibodies, and nanoparticles. Adapted with permission from (Singh K, Ejaz W, Dutta K, Thayumanavan S. Antibody Delivery for Intracellular Targets: Emergent Therapeutic Potential. Bioconjugate Chem. 2019, doi: 10.1021/acs.bioconjchem.9b00025.). Copyright (2019) American Chemical Society[166].

7. Nanoscopic Delivery Systems for Antibodies, Antibody Fragments, and Peptides Using Mesoporous Silica Nanoparticles

7.1 Delivery of Antibodies and Antibody Fragments

This decade has experienced the rise of mesoporous silica nanoparticles (MSN) as drug delivery agents[178,179]. MSN possess the following intrinsic advantages with respect to drug delivery: they are fully biocompatible, possess excellent surface functionalization capabilities, and pore volume tunability[178]. In addition, the inherent rigidity of the material can protect encapsulated antibodies against pH-changes and enzymatic degradation[180]. For instance, IgG

antibodies (immune-globulins) can be absorbed in MSN pores[181]. This is possible because the pores of MSN, which are synthesized via micelle-templated methods, can be tuned from 2-50 nm [178]. A typical IgG is 13.7 nm in length and 8.4 nm in height[182]. MSNs are also used for the purpose of delivering therapeutic peptide sequences, which requires gatekeepers for triggered drug release[183-186]. Furthermore, circulation lifetimes are significantly increased, because MSN/antibody aggregates are larger than antibodies/fragments alone. Typically, MSN designed for the adsorption of antibodies, e.g. Anti-phospho-Akt[181], are about 20 nm in diameter[184]. Uptake via energy-dependent endocytotic pathways, such as through clathrin pits and actin filaments is observed. The third class of MSN are hollow dendritic mesoporous silica nanospheres featuring a singular hole per particle of 25-50nm in diameter, which can be filled either with peptides or proteins[187,188].

7.2 Delivery of Therapeutic Peptide Sequences

As shown in Figure 5, the design of mesoporous silica nanoparticles (MSN) can be adapted to specifications for the purpose of delivering therapeutic peptides[189]. The templated synthesis of MSNs by means of condensation of siloxane-precursors permits the adaptation of MSN sizes and pore sizes to the chosen cellular uptake mode[63]. Furthermore, MSN can be synthesized around core materials, for instance magnetic iron oxide for the purpose of magnetotransfection and MRI[189-191]. The absorption of therapeutic peptides within the channels of the MSN (after template/surfactant exchange) follows a concentration gradient. It can be aided by optimizing the charge of the exterior and/or interior of the MSN by reaction with APTES ((3 Aminopropyl) triethoxysilane and other aminosilanes) [191,192]. “Gatekeepers” are necessary to prevent the MSN cargo from leaching out during transport[183-186]. As shown in Figure 5, molecular valves and environmentally-responsive polymer coatings are among the most popular gatekeepers (189). All

gatekeepers have in common that they permit the release of the payload once they have been activated. Furthermore, stealth ligands can be attached, which decelerate the recognition and subsequent clearance of the MSN by the reticuloendothelial system, as well as targeting ligands (peptides or antibody (fragments), see above)[189].

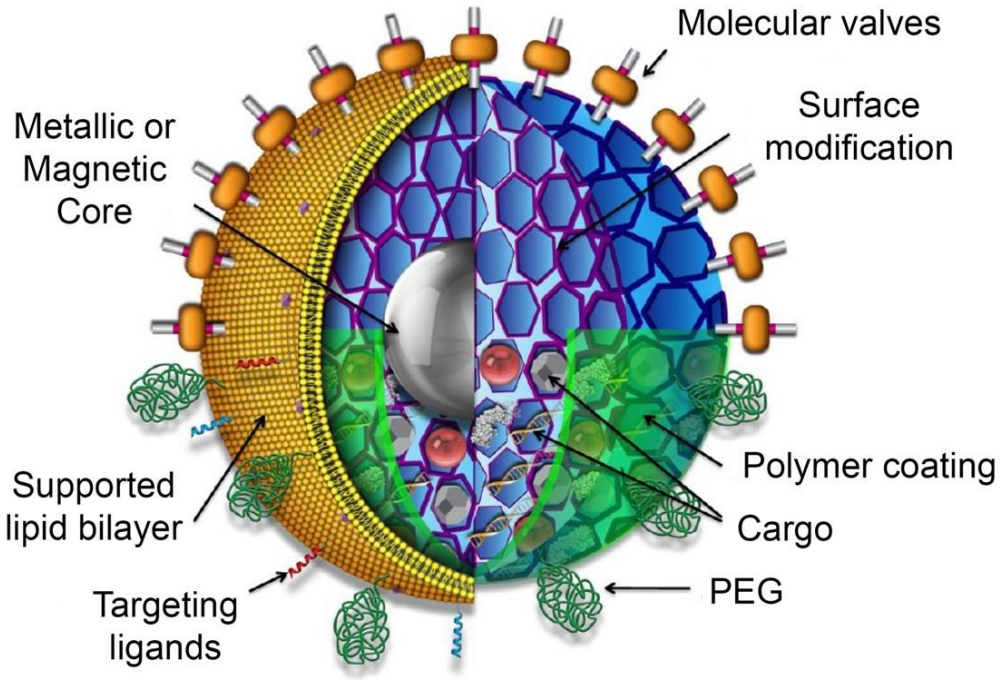

Figure 5. "Schematic of a multifunctional mesoporous silica nanoparticle showing possible core/shell design, surface modifications, and multiple types of cargos."
Adapted with permission from (Tarn D, Ashley CE, Xue M, Carnes EC, Zink JI, Brinker CJ. Mesoporous Silica Nanoparticle Nanocarriers: Biofunctionality and Biocompatibility. Accounts of Chemical Research. 2013;46(3):792-801. doi: 10.1021/ar3000986.) Copyright (2013) American Chemical Society.[189]

The endosomal protease cathepsin B, which is overexpressed in numerous solid tumors[193,194], can cleave the tetrapeptide GF-LG[195]. This cleavage motif can be used in conjunction with a biocompatible polymer (Poly-N-isopropyl-acrylamide (PNIPAM) or PEG diacrylate (PEGDA)) to construct a gatekeeper that can be enzymatically activated during endocytosis[196].

This concept was successfully demonstrated in HeLa cells and 3T3-J2 fibroblasts through releasing doxorubicin and subsequent cell death[196]. Torre et al. utilized T22 peptide to target C-X-C chemokine receptor type 4 (CXCR-4) expressing lymphoma cells to deliver MSNs into the cytosol via receptor-mediated endocytosis[197]. The targeting ability of T22 was significantly decreased in the presence of AMD3100 (antagonist of CXCR-4), demonstrating that T22 competes for CXCR-4 with AND3100[197]. Again, these examples should be regarded as proof-of-principle for very efficient drug-delivery designs. The challenge that remains is to optimize these systems for targeting diseases (especially cancer) in human patients.

7.3 Liposomes

Liposomes are very simple models of cells. They are spherical and feature phospholipid bilayers, which can be either single or multi-layered, and an aqueous buffer filled core[198,199]. Although they are biocompatible and biodegradable, classic liposomes often do not permit the release of antibodies, therapeutic peptides, or drugs with sufficient spatio-temporal control[200]. Therefore, during the last four decades[200,201], efforts have been made to develop liposomes triggerable by pH changes in tissue[202], redox mediators (e.g. ROS in cancers) [203], light to permit photo-triggerable release[204], and temperature (e.g. hyperthermia)[205]. Furthermore, PEGylation has significantly prolonged the circulation-half-life of liposomes[206]. Although PEGylated liposomes can remain in circulation significantly longer[207], the efficacy of drug delivery is still hampered by the absence of targeting mechanisms and very varying extravasation efficacy in human patients, in comparison to mouse models[208,209]. Therefore, the next logical step is to attach ligands, peptides, and antibody (fragments) for specific targeting[206]. However, this “active targeting approach” is either dependent on the availability of targets in blood, at the cell walls of blood vessels, or after extravasation. Unfortunately, tumor heterogeneity is the major roadblock to extravasation and

consequent drug delivery[1]. Several nanotherapeutics making use of liposomal formulations have reached the market (Doxil/Caelix, Johnson & Johnson; AmBisome, Gilead; Myocet, Cephalon)[210]. In order to overcome endosomal entrapment and enzymatic degradation, several (model) liposomal systems have been developed: CD44 is a transmembrane glycoprotein (P-glycoprotein) that facilitates receptor-mediated endosomal uptake[211]. Utilizing anti-CD44 antibody decorated liposomes composed of DOPC (1,2-dioleoyl-sn-glycero-3-phosphocholine), DOPE (2-dioleoyl-sn-glycero-3-phosphoethanolamine), cholesterol, and antibody-labeled 1,2-distearoyl-sn-glycero-3-phosphoethanolamine-N-[succinimidyl (poly-ethylene glycol)-3400] (DSPE-PEG_{3400}-NHS), bearing an anti-interleukin 6 receptor (IL6R) antibody as payload, Guo et al. were able to inhibit IL6R-Stat3 signaling in tumor bearing mice[212].

A multifunctional nanocarrier system capable of controlling intercellular trafficking was developed by Yamada et al.[92]: The cell-membrane penetrating peptide stearyl-octaarginine (R8) (Table 1) was used in conjunction with the cholestenyl ester-labeled fusogenic peptide GALA (WEAALAEALAEALAEHLAEALAEALEALAA). GALA adopts a random coil structure at neutral pH, but changes to an amphipathic α-helical structure at lower pH, which is typical for endosomes[213]. Based on this pH-induced change of structure, GALA is a very efficient disruptor of endosomal membranes, leading to fast endosomal escape[213]. Both peptide sequences were anchored using hydrophobic labels in the liposomes' bilayer, which was composed of the surfactant DOPE (1,2-dioleoyl-sn-glycero-3-phosphoethanolamine) and cholesterol hemisuccinate[214]. Whereas liposome-mediated delivery of protein and peptide payload via endocytosis and endosomal escape usually requires 4-24h incubation time, this nanoplatform is capable of completing both steps to 99% of cells within 30-120 min! An alternative strategy to promote fast endosomal escape is to utilize a photosensitizer to trigger ROS (reactive oxygen

species)-mediated degradation of the endosomal membrane, thus facilitating endosomal escape[215]. Interestingly, payload delivery by means of membrane fusion, thus avoiding endocytosis, was achieved by a liposome comprised of DSPE-4A (attached with R4 and DSPE-Hy-PEG2k (attached with benzaldehyde) [216]. Basel et al. have demonstrated an alternative drug delivery concept by designing caged hypertonic liposomes that can be activated via proteolytic cleavage of the consensus sequence SGRSA, which was incorporated into a "cage" of polyacrylic acid chains. Once the "bar" of this "cage" is cleaved by the protease, the hypertonic liposome releases its payload immediately. The challenge of this approach is the timing of the proteolytic attack. The authors suggest targeting membrane-bound proteases that are located at the surface of cancer cells (e.g. MMP9 on CD44[217] and MMP14[218]) to enable drug release in the immediate vicinity of tumors[219].

7.4 Limitations of Liposomal Delivery Systems

Although liposomal delivery systems are widely used and a great commercial success[200,210], they are suffering from intrinsic drawbacks: their encapsulation efficiencies are very low, especially for hydrophilic payloads. Liposomes are not long-term stable and, therefore, cannot be stored for very long. Liposomes can be destabilized while in circulation by interaction with serum proteins, which – in addition – promote opsonization. As this is true for virtually all nanostructures, corona formation decreases targeting efficacy by "burying" the targeting antibody (fragments) or peptides under layers of adsorbed proteins. Furthermore, even stealth-liposomes are recognized by the reticuloendothelial system and cleared[220,221].

8. Supramolecular Peptide Nanostructures/Hydrogels

Technically, supramolecular peptide nanostructures for biomedical applications are hydrogels, or at least closely related with this vast group of materials[222]. Hydrogels can form

networks, which are at least partially hydrated. These networks can be formed through covalent of or non-covalent interactions. The latter comprise ionic interactions, hydrogen bonds, or hydrophobic interactions[223]. The resulting hydrogels can be classified as amorphous, semi-crystalline, or crystalline[222]. The individual components from which hydrogels are formed can be either nonionic or ionic (anionic, cationic), ampholytic (containing both acidic and basic functional groups), or zwitterionic (polybetaines, containing both, positive and negative charges, but not necessarily the same number of them). With respect to this review, hydrogels formed from peptides belong to the group of hydrogen-forming natural peptides, even if the peptides discussed here are designer peptides. Synthetic polymers are usually formed by means of chemical polymerization[1]. Numerous synthetic hydrogel systems have been designed for drug delivery[1], which would exceed the capacity of this review. Here, we will focus on peptides that were designed for self-assembly as a strategy to slow down proteolytic degradation and thus significantly enhance circulation time[3].

9. Supramolecular Nanofibers

9.1 Crossing the Blood-Brain-Barrier

As discussed above, one of the most challenging tasks of drug delivery is the requirement to cross the blood brain barrier[224]. Multiple nanocarriers like liposomes and polymers have been synthesized for delivery to the brain, but no vector has been uniquely successful to date[136] However, the use of peptides for drug delivery across the BBB hold promise. Mazza et al. have demonstrated that transport into the brain using peptide nanofibers can be achieved[225] by designing an amphiphilic peptide-derivative featuring a highly positive charged and hydrophobically labeled terminus (palmitoyl-GGGAAAKRK)[225]. This peptide-derivative self-assembled into peptide nanofibers (PNFs). This self-assembling process generated flexible and elongated nanofibers, which were then incubated with 0.05% trypsin-EDTA to determine possible carboxypeptidase-

mediated degradation sites. Images were captured using TEM at different time points. These experiments demonstrated complete proteolytic degradation after 14 days[225]. PNFs were then labeled with Nile Red (hydrophobic fluorescent dye), and then incubated for 24 hours with primary neurons isolated from rat brains. Here, fluorescent microscopy demonstrated the presence of PNFs in the cytoplasm of these cells. Finally, a pilot *in vivo* study was designed to demonstrate localization and possible degradation of PNFs in rats' brains. Rats were intracranially injected with fluorescently labeled PNFs (VivoTag 680 XL), and the occurring fluorescent signal was measured for 15 days using an IVIS fluorescence imaging camera. A strong signal was detected for up to seven days, which almost disappeared after 15 days, but remained close to the site of injection. More mechanistic studies are required to further verify the underlying paradigm, according to which the peptide nanofiber that was not only able to reach the brain, but also was degraded overtime by plasma membranes. This would mean that potential cellular toxicity is strongly reduced by limiting the accumulation of this nanocarrier in the brain[225].

10. Cancer Chemotherapy

Chemotherapy is the most used treatment against cancer[226]. However, it is far from optimal due to the lack of tissue specificity, thus causing severe side effects, as well as generally low concentrations of drugs released at the tumor site, thus abetting the development of drug resistance. One of the most interesting applications of self-assembled peptides is an injectable hydrogel formulation, which can place the chemotherapeutic agents next to the target tissues for a higher local concentration release over time[227,228]. Previously, a peptide with alternating ionic hydrophilic and hydrophobic amino acids was reported to form stable β-sheet structures, which was called KLD12 (KLDLKLDLKLDL)[228]. Later, KLD was used to design a protease-sensitive hydrogel with a cleavable region, which facilitated drug release mediated by trypsin[228]. Yishay-Safranchik

et al. developed injectable *in situ*-forming hydrogels designed from self-assembled KLD motifs to control the release of doxorubicin (DOX) or Smac-derived pro-apoptotic peptide (SDPP (AVPIAQ)) for cancer treatment. These motifs were designed to be separated into two β-sheet peptides by the following spacers: 3- or 4- glycine (G) spacers or 4- glycine and a phenylalanine (F) spacer. These spacer modifications were intended to increase the gel formation rate, and the use of phenylalanine was intended to improve drug loading and stability by increasing the hydrophobicity of the hydrogel. Results demonstrated that addition of G spacers decreased the time for gel formation to 3 and 4 minutes after adding PBS, while addition of G and F increased the gel formation rate to only 2 minutes after addition of PBS. Cell penetration was confirmed on SK-OV-3 (ovarian cancer) cells after they were incubated for 24 hours with hydrogels loaded with SDPP labeled with a fluorescent dye. After 24 hours of incubation 80-90% of cells were fluorescent. Cytotoxicity of DOX being released from KLD-based hydrogels was then analyzed through MTT assays. Results demonstrated that within 24 hours of incubation, 50% cells treated with free DOX were alive, while 60% remained alive for DOX-loaded KLD hydrogels, which remained similar even after 48 and 72 hours. Results demonstrate that DOX release from hydrogels is controlled, since cytotoxic activity was maintained.

Toft et al. have designed peptide amphiphiles (PA), composed of hydrophobic, hydrogen-bonding, and hydrophilic domains that self-assemble to form cylindrical nanofibers. This supramolecular system has shown promising results to be used as potential cancer therapeutic[229]. A cationic peptide sequence $(KLAKLAK)_2$ was designed to interact with lipid membranes as well as lyse either plasma or mitochondrial membranes[229]. By conjugation of KLAK to lauric acid $[C_{16}A_4G_3(KLAKLAK)_2]$ cylindrical nanostructures capable of disrupting cell membranes were assembled. This is very interesting because in this case, KLAK peptide is both the delivery vector

and the therapeutic peptide sequence[17]. The drawback of this is that peptides are easily degraded, as discussed above[227]. To protect peptides from proteolysis this therapeutic-delivery vehicle was modified with pegylated peptide (PEG), to create a protective corona[229]. After KLAK was co-assembled to PEG, enzymatic degradation was measured using the protease trypsin. Results demonstrated that percentage of intact KLAK peptide increased as the concentration of PEG peptide increased. Then, cytotoxicity was compared for KLAK alone and KLAK/PEG peptides using MTT assays (reduction of 3-(4,5-dimethylthiazol-2-yl)-2,5-diphenyltetrazolium) by metabolic NAD(P)H-dependent cellular oxidoreductase[25]. MTT assays revealed similar toxicity of both peptides on three cell lines of human breast cancer. Lastly, using mouse breast cancer models, KLAK and KLAK/PEG were administered via intraperitoneal injections. Cell proliferation was measured using immunohistological staining for bromodeoxyuridine, which showed a lower proliferation for tumors treated with KLAK/PEG[229]. These experiments can be regarded as proof-of-principle that biodegradable nanocarriers can be designed using peptides as key ingredients.

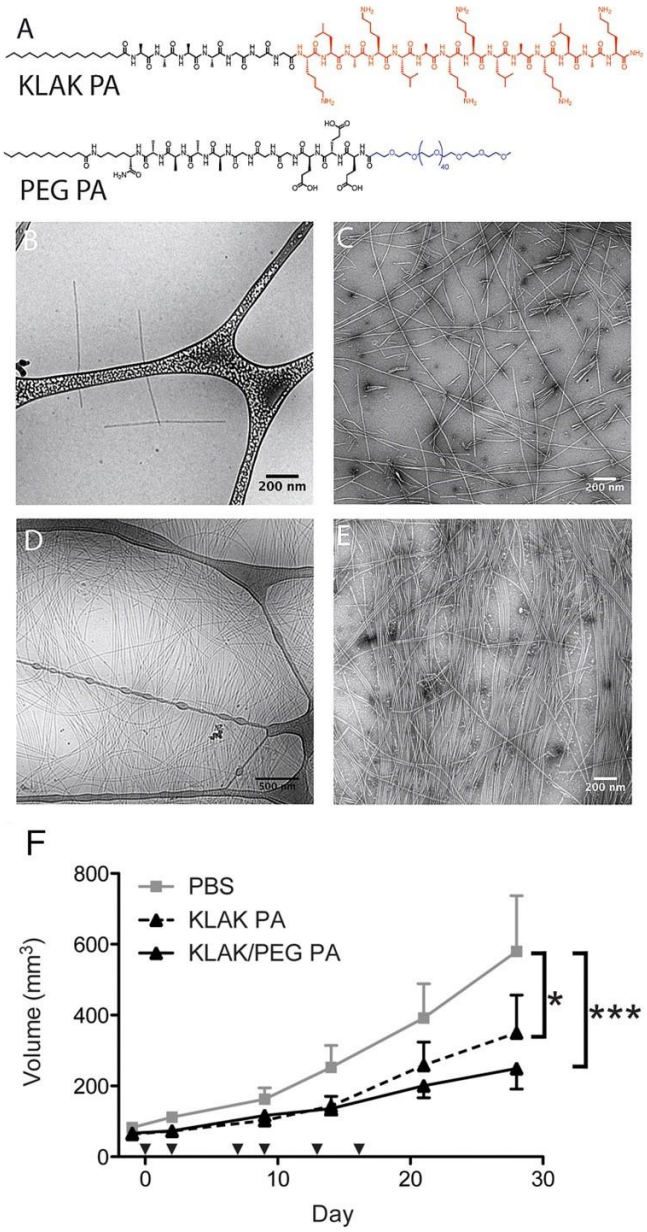

Figure 6. Characterization of Peptide Amphiphiles (PA).
A) Chemical structure of "KLAK PA" with the sequence palmitoyl-A4G3(KLAKLAK)2 and "PEG PA" with the sequence PEG2000-E3G3A4K(C12). Cryo-TEM of KLAK PA alone (B). KLAK with PEG (D) shows a significant difference in average length. Conventional TEM images show fiber formation for both KLAK alone (C) and KLAK PA with PEG PA (E). (F) The growth of MDA-MB-231 human breast cancer orthotopic tumors is inhibited by intraperitoneal treatment (inverted arrows) of KLAK PA nanostructures. Both the KLAK- and KLAK/PEG PA-treated tumors were statistically smaller, as determined by "two-way ANOVA." Adapted with permission from (Toft DJ, Moyer TJ, Standley SM, Ruff Y, Ugolkov A, Stupp SI, Cryns VL. Coassembled Cytotoxic and Pegylated Peptide Amphiphiles Form Filamentous Nanostructures with Potent Antitumor Activity in Models of Breast Cancer. ACS Nano. 2012;6(9):7956-65. doi: 10.1021/nn302503s.) Copyright (2012) American Chemical Society.[229]

11. Peptide Nanosponges

The Bossmann Group has designed peptide nanosponges for drug delivery across physiological barriers and targeting of defensive cells in peripheral blood[25,230,231]. They consist of poly-K or poly-R segments (n=5, 10, 15, or 20), a consensus sequence for a protease (e.g. DEVDGC for the executioner caspases 3, 6, and 7), as well as a trigonal linker capable of reacting with the linear peptides via Michael addition. Peptide nanosponges based on poly-K or poly-R units form spontaneously in aqueous buffers. Formulations can be also amended by mixing various amounts of poly-D nanosponge with either poly-K-, or poly-R-based sponges[231]. Due to charge attraction between the poly-D- and the poly-K-segments, nanosponge-like structures are formed featuring nanoscopic water droplets. Another feature of these nanostructures is that hydrophobic labels (e.g. cholesterol, steroid drugs, or hydrophobic dyes (e.g. cyanine 7.0)) can be attached to the N-terminal ends of the peptide sequences. This allows the incorporation of hydrophobic drugs, or the formation of cholesterol-nanodomains, which can be used for the physical adsorption of hydrophobic drugs. Another strategy that has been successfully tested for the treatment of glioblastoma[25] is to extend the linear peptide sequences by up to 10 D, E, or S units, which are then used to bind hydrophilic drugs via esterase-cleavable bonds. This concept has been proven successful for treating glioblastoma cell cultures with perillyl alcohol[25].

12. Polymer-based Nanoparticles

Whereas the degree of protection of antibodies and peptides by inorganic nanoparticles is usually greater, polymer-based nanoparticles are much more flexible and can be easily tuned in molecular weight, particle size, and surface functionality[232]. Furthermore, both targeting and therapeutic peptides can be easily attached to side chains in polymeric formulations. It should be noted that soft nanostructures may be able to spread out on a cell membrane, which would increase

the strength of interaction with the latter and could trigger either membrane-integration, endosomal uptake or direct transport through the membrane[63].

As discussed above for supramolecular peptide aggregates and hydrogels, polymer-based nanoparticles are also divided in two groups: nanostructures formed by means of non-covalent and covalent interaction. It should be noted that the boundaries between all delivery systems based on organic structures are somewhat blurred.

13. Polymer-based Nanoparticles Based on Noncovalent Interactions

Noncovalent complexation strategies are usually based on electrostatic interactions, although specific binding motifs, such as avidin-biotin, have already been successfully explored[233]. For instance, biotinylated poly(propylacrylic acid) (PPAAc) and a biotinylated anti-CD3 antibody have been combined with streptavidin to form a ternary nanostructure, which was taken up by Jurkat lymphoma cells via receptor-mediated endocytosis[234]. It was speculated that endolysosomal release was facilitated by the PPAAc-"proton sponge". In a similar manner, poly(lactic-co-glycolic acid) (PLGA) based nanocarriers have been employed to protect anti-annexinA2 (AnxA2) antibody[235]. However, in this case the encapsulated antibody was much better retained by the formulation, resulting in the slow release of active antibody over 12 days.

14. Gene Transfection

Non-viral nanocarriers have been developed and investigated, due to side effects and toxicity of viral nanocarriers[227]. For a non-viral gene delivery to be efficient, the vector must target specific cell receptors, protect DNA from degradation, deliver DNA into the nucleus, and disrupt endosomal membranes, a major biological barrier faced in gene delivery approaches[227,236]. For this approach, fusogenic peptides have been developed, which have gained attention as a promising gene delivery nanocarrier. Fusogenic peptides (FP) are virus- based amphiphilic peptides capable

of interacting with phospholipid membranes for membrane fusion and/or lysis[236] (Scheme 6). Among others, GALA, a 30 amino acid residue (WEAALAEALAEALAEHLAEALAEALEALAA) and pH-sensitive peptide (see above), was synthesized and shown to be an effective membrane fusion peptide at pH 5. In order to further improve this peptide, due to anionic properties that limited the association with DNA, KALA and RALA, fusogenic peptides were developed, which in each case the glutamic acid was substituted with lysine or arginine, respectively[17]. However, Nouri et al constructed a recombinant biopolymer for each FP, in order to determine which peptide is more efficient for gene delivery[236]. In this study, membrane disruption, cell toxicity, and transfection experiments were conducted. Results demonstrated that biopolymer containing GALA FP peptide had lower cell toxicity, better ability to disrupt membranes, as well as better transfection efficiencies compared to the rest[18]. Even though GALA has limited association with DNA individually, once it is used to form a biopolymer, it has been shown to be a better suitable nanocarrier for gene delivery.

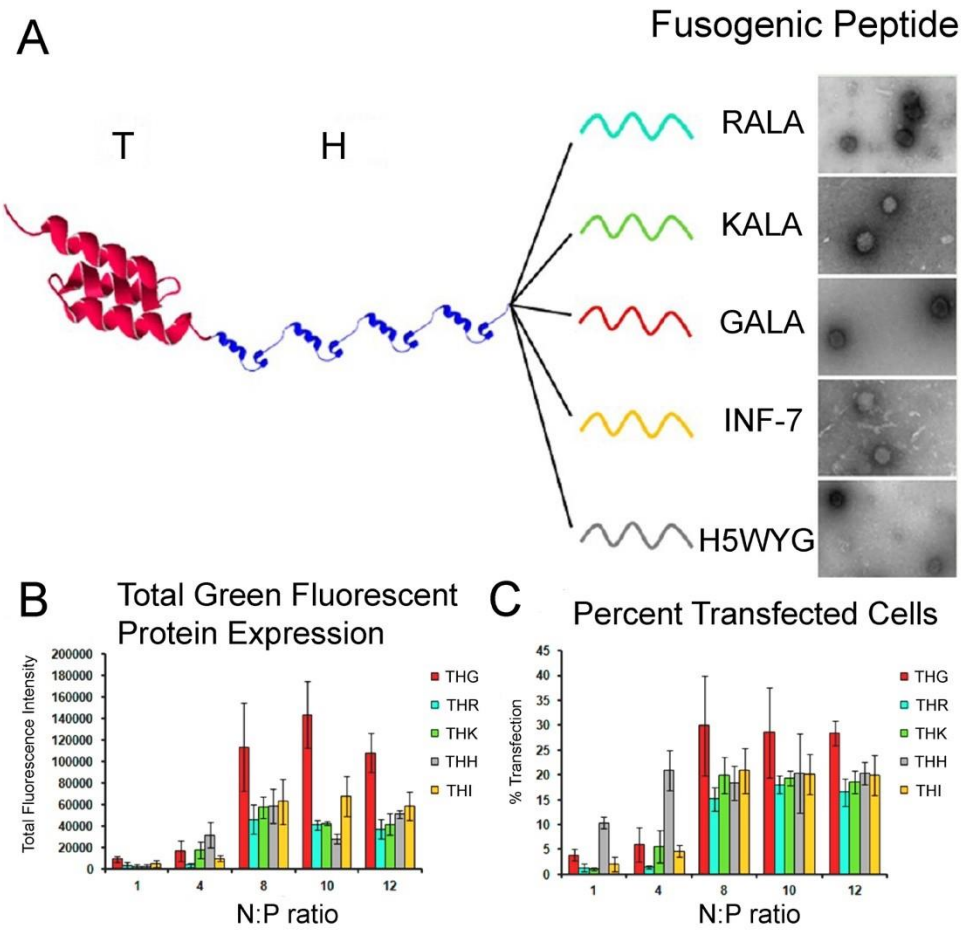

Figure 7. Recombinant biopolymers, RALA, KALA, GALA, INF-7, and H5WYG.
A) "Schematic representation of recombinant biopolymers composed of a targeting motif (T), four repeating units of histone H2A with an inherent nuclear localization signal (H) (MVDNKFNKEMRNAYWEIALLPNLNNQQKRAFITSLYDDPSQSANLLAEKKLNDAQAP KGGGGSGGGGSGRKRSGRSKQGGKARAKAKTRSSRAGLQFPVGRVHRLLRKSGRGKQ GGKARAKAKTRSSRAGLQFPVGRVHRLLRKSRGKQGGKARAKAKTRSSRAGLQFPVG RVHRLLRKSGRGKQGGKARAKAKTRSSRAGLQFPVGRVHRLLRKGGG) and a fusogenic peptide (e.g., INF7 (GLFEAIEGFIENGWEGMIDGWYG), GALA (WEAALAEALAEALAEHLAEALAEALEALAA), KALA (WEAKLAKALAKALAKHLAKALAKALKAGEA), RALA (WEARLARALARALARHLARALARALRAGEA), and H5WYG (GLFHAIAHFIHGGWHGLIHGWYG)). The 3D structures of T and one repeat of histone H2A are predicted by SWISS-MODEL program. B) A bar chart that quantitatively demonstrates total green fluorescence intensity of transfected SKOV-3 cells with biopolymer/pEGFP complexes. C) A bar chart that quantitatively demonstrates percent transfected cells with biopolymer/pEGFP complexes at different N:P ratios."
Adapted with permission from (Nouri FS, Wang X, Dorrani M, Karjoo Z, Hatefi A. A Recombinant Biopolymeric Platform for Reliable Evaluation of the Activity of pH-Responsive Amphiphile Fusogenic Peptides. Biomacromolecules. 2013;14(6):2033-40. doi: 10.1021/bm400380s.) Copyright (2013) American Chemical Society.[236]

Polyethyleneimine (PEI) has been widely used as delivery vector because it is positively charged at physiological pH and can form complexes with DNAs and RNAs. Effective endosomal escape is fast because PEI is a "proton sponge" at endosomal pH, which destabilized the endosomal membrane[237]. Similarly, PEI is used to associate with negatively charged proteins, such as anti-lamin antibodies. Nuclear lamins interact with membrane-associated proteins to form the nuclear lamina on the interior of the nuclear envelope[238]. In a similar approach, anti-synuclein antibody containing polybutylcyanoacrylate nanoparticles were taken up via low-density lipoprotein receptor mediated endocytosis.

15. Targeting Peptides to Improve Uptake and Delivery

Besides facilitating the transportation and delivery of payloads, peptides can also be used to develop a specific targeting nanocarrier. Therapeutic agents have been identified to be effective against pathogens, but most of the time they are toxic to healthy cells too, just like with chemotherapy. Therefore, the development of a vehicle that will be activated to release the therapeutic agents only after reaching the targeted tissue is crucial. Multiple nanocarriers have been developed with effective targeting mechanisms using peptides. Peptides sequences have been designed to target specific enzymes that play essential roles for pathogens to survive, which was effectively applied to deliver drug to specific tissues, like brain tumors[224]. This idea has been exploited to develop nanocarriers that could target challenging tissues, like bones. Jiang et al. developed a drug delivery system to target bone tissue exclusively. The nanocarrier was composed of PLGA-based nanoparticles linked to a fluorescent label poly-aspartic acid peptide sequence, which has been demonstrated to bind effectively to hydroxyapatite (a mineral found in bones)[224,239]. For this study, ex vivo experiments were conducted to determine binding of nanoparticle to multiple tissues. Mouse tibia, brain, heart, liver, spleen, kidney, lung, and

gastrointestinal tract tissues were exposed to poly-Asp nanoparticle, and results demonstrated that nanoparticle bound specifically to bone tissue[239]. It was found that the simple peptide sequence DDDDDDC was capable of targeting bone cells via binding to hydroxyapatite. This finding has the potential of leading to a very effective delivery for the (chemo)therapy of various bone cancers.

16. Conclusion

Therapeutic peptides, as well as antibody fragments and antibodies, are constantly increasing in importance as components of smart therapeutics that can effectively target and treat diseases[1,3,5,31,66,79,85,145,148]. Chemical strategies for enhancing the efficacies and/or circulation/residence times of peptides and proteins are straightforward. They comprise chemical derivatization, such as PEGylation[97], and the synthesis of retro-inverso peptides[142], which are much more stable against proteolytic degradation[2,3]. Nanoparticle-based strategies work well in further decreasing proteolytic degradation due to increase in size[1]. However, this can also be carefully counterbalanced with clearance of nanoparticles from circulation by the reticuloendothelial system, because nanoscopic structures have the size of viruses (and larger structures of bacteria)[97]. Furthermore, they are known to trigger immune-responses, which increase their uptake even more[240]. When selecting the type of nanoformulation, six factors should be carefully considered: Which physiological barriers does the nanoformulation have to cross? What is the intended mechanism of cellular uptake (phagocytosis, pinocytosis, or non-specific uptake)? What level of protection does your payload require? Do you desire immediate or timed release? What is the fate of the nanoformulation after the payload has been delivered? What off-target effects do you anticipate? The answers to these questions will guide you through the plethora of nanodelivery systems to an intelligent tailored solution for your drug delivery problem.

17. References

[1]Acar H, Ting JM, Srivastava S, La Belle JL, Tirrell MV. Molecular engineering solutions for therapeutic peptide delivery. *Chem Soc Rev*. **2017**, 46(21):6553-69.

[2]Gallo M, Defaus S, Andreu D. 1988-2018: Thirty years of drug smuggling at the nano scale. Challenges and opportunities of cell-penetrating peptides in biomedical research. *Arch Biochem Biophys*. **2019**, 661:74-86.

[3]Zuconelli CR, Brock R, Adjobo-Hermans MJW. Linear Peptides in Intracellular Applications. *Curr Med Chem*. **2017**, 24(17):1862-73.

[4]Di L. Strategic Approaches to Optimizing Peptide ADME Properties. *AAPS J*. **2015**, 17(1):134-43.

[5]Raucher D. Tumor targeting peptides: novel therapeutic strategies in glioblastoma. *Curr Opin Pharmacol.* **2019**, 47:14-9.

[6]Liu X, Wu F, Ji Y, Yin L. Recent Advances in Anti-cancer Protein/Peptide Delivery. *Bioconjugate Chem*. **2019**, 30(2):305-24.

[7]Acar H, Srivastava S, Chung EJ, Schnorenberg MR, Barrett JC, LaBelle JL, Tirrell M. Self-assembling peptide-based building blocks in medical applications. *Adv Drug Delivery Rev*. **2017**, 110-111:65-79.

[8]Blanco E, Shen H, Ferrari M. Principles of nanoparticle design for overcoming biological barriers to drug delivery. *Nat Biotechnol*. **2015**, 33(9):941-51.

[9]Kim K-M. Conceptual progress for the improvements in the selectivity and efficacy of G protein-coupled receptor therapeutics: an overview. *Biomol Ther*. **2017**, 25(1):1-3.

[10]Wells JA, McClendon CL. Reaching for high-hanging fruit in drug discovery at protein-protein interfaces. *Nature (London, U K).* **2007**, 450(7172):1001-9.

[11]Cesa LC, Mapp AK, Gestwicki JE. Direct and Propagated Effects of Small Molecules on Protein-Protein Interaction Networks. *Front Bioeng Biotechnol*. **2015**, 3:119.

[12]Cheng AC, Coleman RG, Smyth KT, Cao Q, Soulard P, Caffrey DR, Salzberg AC, Huang ES. Structure-based maximal affinity model predicts small-molecule druggability. *Nat Biotechnol*. **2007**, 25(1):71-5.

[13]Maes M, Loyter A, Friedler A. Peptides that inhibit HIV-1 integrase by blocking its protein-protein interactions. *FEBS J*. **2012**, 279(16):2795-809.

[14]Stumpf MPH, Thorne T, de Silva E, Stewart R, An HJ, Lappe M, Wiuf C. Estimating the size of the human interactome. *Proc Natl Acad Sci USA*. **2008**, 105(19):6959-64.

[15]Iyer VV. A Review of Stapled Peptides and Small Molecules to Inhibit Protein-Protein Interactions in Cancer. *Curr Med Chem*. **2016**, 23(27):3025-43.

[16]Semenova G, Chernoff J. Targeting PAK1. *Biochem Soc Trans*. **2017**, 45(1):79-88.

[17]Dalecki AG, Malalasekera AP, Schaaf K, Kutsch O, Bossmann SH, Wolschendorf F. Combinatorial phenotypic screen uncovers unrecognized family of extended thiourea inhibitors with copper-dependent anti-staphylococcal activity. *Metallomics*. **2016**, 8(4):412-21.

[18]Haeili M, Moore C, Davis CJC, Cochran JB, Shah S, Shrestha TB, Zhang Y, Bossmann SH, Benjamin WH, Kutsch O, Wolschendorf F. Copper complexation screen reveals compounds with potent antibiotic properties against methicillin-resistant Staphylococcus aureus. *Antimicrob Agents Chemother*. **2014**, 58(7):3727-36, 11 pp.

[19]Isidro-Llobet A, Kenworthy MN, Mukherjee S, Kopach ME, Wegner K, Gallou F, Smith AG, Roschangar F. Sustainability Challenges in Peptide Synthesis and Purification: From R&D to Production. *J Org Chem*. **2019**, Ahead of Print.

[20]Behnam MAM, Graf D, Bartenschlager R, Zlotos DP, Klein CD. Discovery of Nanomolar Dengue and West Nile Virus Protease Inhibitors Containing a 4-Benzyloxyphenylglycine Residue. *J Med Chem*. **2015**, 58(23):9354-70

[21]Gfeller D, Michielin O, Zoete V. SwissSidechain: a molecular and structural database of non-natural sidechains. *Nucleic Acids Res*. **2013**, 41(D1):D327-D32.

[22]Jabbari E, Yang X, Moeinzadeh S, He X. Drug release kinetics, cell uptake, and tumor toxicity of hybrid VVVVVVKK peptide-assembled polylactide nanoparticles. *Eur J Pharm Biopharm*. **2013**, 84(1):49-62.

[23]Lee D, Zhao J, Yang H, Xu S, Kim H, Pacheco S, Keshavjee S, Liu M. Effective delivery of a rationally designed intracellular peptide drug with gold nanoparticle-peptide hybrids. *Nanoscale*. **2015**, 7(29):12356-60.

[24]Li S, Roberts RW. A novel strategy for in vitro selection of peptide-drug conjugates. *Chem Biol*. **2003**, 10(3):233-9.

[25]Yapa AS, Shrestha TB, Wendel SO, Kalubowilage M, Yu J, Wang H, Pyle M, Basel MT, Toledo Y, Ortega R, Malalasekera AP, Thapa PS, Troyer DL, Bossmann SH. Peptide Nanosponges Designed for the Delivery of Perillyl Alcohol to Glioma Cells. *ACS Appl Bio Mater*. **2019**, 2(1):49-60.

[26]Abayaweera GS, Wang H, Shrestha TB, Yu J, Angle K, Thapa P, Malalasekera AP, Maurmann L, Troyer DL, Bossmann SH. Synergy of iron chelators and therapeutic peptide sequences delivered via a magnetic nanocarrier. *J Funct Biomater*. **2017**, 8(3):23/1-/18.

[27]London N, Raveh B, Schueler-Furman O. Druggable protein-protein interactions - from hot spots to hot segments. *Curr Opin Chem Biol*. **2013**, 17(6):952-9.

[28]Morelli X, Bourgeas R, Roche P. Chemical and structural lessons from recent successes in protein-protein interaction inhibition (2P2I). *Curr Opin Chem Biol*. **2011**, 15(4):475-81.

[29]Moellering RE, Cornejo M, Davis TN, Del Bianco C, Aster JC, Blacklow SC, Kung AL, Gilliland DG, Verdine GL, Bradner JE. *Direct inhibition of the NOTCH transcription factor complex. Nature (London, U K)*. **2009**, 462(7270):182-8.

[30]Walensky LD, Kung AL, Escher I, Malia TJ, Barbuto S, Wright RD, Wagner G, Verdine GL, Korsmeyer SJ. Activation of Apoptosis in Vivo by a Hydrocarbon-Stapled BH3 Helix. *Science (Washington, DC, U S).* **2004**, 305(5689):1466-70.

[31]Stone TA, Deber CM. Therapeutic design of peptide modulators of protein-protein interactions in membranes. *Biochim Biophys Acta, Biomembr*. **2017**, 1859(4):577-85.

[32]Ferrucci V, Pennino FP, Siciliano R, Asadzadeh F, Zollo M. A competitive cell-permeable peptide impairs Nme-1 (NDPK-A) and Prune-1 interaction: therapeutic applications in cancer. *Lab Invest*. **2018**, 98(5):571-81.

[33]https://www.researchandmarkets.com/reports/4600544/global-peptide-therapeutics-market-dosage-price.

[34]Neefjes J, Jongsma MLM, Paul P, Bakke O. Towards a systems understanding of MHC class I and MHC class II antigen presentation. *Nat Rev Immunol*. **2011**, 11(12):823-36.

[35]Rockel B, Kopec KO, Lupas AN, Baumeister W. Structure and function of tripeptidyl peptidase II, a giant cytosolic protease. *Biochim Biophys Acta, Proteins Proteomics*. **2012**, 1824(1):237-45.

[36]Ray K, Hines CS, Coll-Rodriguez J, Rodgers DW. Crystal Structure of Human Thimet Oligopeptidase Provides Insight into Substrate Recognition, Regulation, and Localization. *J Biol Chem*. **2004**, 279(19):20480-9.

[37]Kessler JH, Khan S, Seifert U, Le Gall S, Chow KM, Paschen A, Bres-Vloemans SA, de Ru A, van Montfoort N, Franken KLMC, Benckhuijsen WE, Brooks JM, van Hall T, Ray K, Mulder A, Doxiadis IIN, van Swieten PF, Overkleeft HS, Prat A, Tomkinson B, Neefjes J, Kloetzel PM, Rodgers DW, Hersh LB, Drijfhout JW, van Veelen PA, Ossendorp F, Melief CJM. Antigen processing by nardilysin and thimet oligopeptidase generates cytotoxic T cell epitopes. *Nat Immunol*. **2011**, 12(1):45-53.

[38]Checler F, Ferro ES. Neurolysin: From Initial Detection to Latest Advances. *Neurochem Res*. **2018**, 43(11):2017-24.

[39]Chesneau V, Foulon T, Cohen P, editors. Nardilysin **2004**: *Elsevier*.

[40]Babkova K, Korabecny J, Soukup O, Nepovimova E, Jun D, Kuca K. Prolyl oligopeptidase and its role in the organism: attention to the most promising and clinically relevant inhibitors. *Future Med Chem*. **2017**, 9(10):1015-38.

[41]Akkad N, Schatz M, Dengjel J, Tenzer S, Schild H. Census of cytosolic aminopeptidase activity reveals two novel cytosolic aminopeptidases. *Med Microbiol Immunol*. **2012**, 201(4):463-73.

[42]Byzia A, Szeffler A, Kalinowski L, Drag M. Activity profiling of aminopeptidases in cell lysates using a fluorogenic substrate library. *Biochimie*. **2016**, 122:31-7.

[43]Böttger R, Hoffmann R, Knappe D. Differential stability of therapeutic peptides with different proteolytic cleavage sites in blood, plasma and serum. *PLOS ONE*. **2017**, 12(6):e0178943.

[44]Fields GB. Interstitial Collagen Catabolism. *J Biol Chem*. **2013**, 288(13):8785-93.

[45]Torrice M. Does Nanomedicine Have a Delivery Problem? *ACS Cent Sci*. **2016**, 2(7):434-7.

[46]Ruoslahti E. Specialization of tumour vasculature. *Nat Rev Cancer*. **2002**, 2(2):83-90.

[47]Maeda H, Nakamura H, Fang J. The EPR effect for macromolecular drug delivery to solid tumors: Improvement of tumor uptake, lowering of systemic toxicity, and distinct tumor imaging in vivo. *Adv Drug Delivery Rev*. **2013**, 65(1):71-9.

[48]Melo MN, Ferre R, Castanho MARB. Antimicrobial peptides: linking partition, activity and high membrane-bound concentrations. *Nat Rev Microbiol*. **2009**, 7(3):245-50.

[49]Baumann G, Mueller P. Molecular model of membrane excitability. *J Supramol Struct*. **1974**, 2(5-6):538-57.

[50]Ludtke SJ, He K, Heller WT, Harroun TA, Yang L, Huang HW. Membrane Pores Induced by Magainin. *Biochemistry*. **1996**, 35(43):13723-8.

[51]Leontiadou H, Mark AE, Marrink SJ. Antimicrobial Peptides in Action. *J Am Chem Soc*. **2006**, 128(37):12156-61.

[52]Pouny Y, Rapaport D, Mor A, Nicolas P, Shai Y. Interaction of antimicrobial dermaseptin and its fluorescently labeled analogs with phospholipid membranes. *Biochemistry*. **1992**, 31(49):12416-23.

[53]Rai V, Abdo J, Alsuwaidan AN, Agrawal S, Sharma P, Agrawal DK. Cellular and molecular targets for the immunotherapy of hepatocellular carcinoma. *Mol Cell Biochem*. **2018**, 437(1-2):13-36.

[54]Pang H-B, Braun GB, Friman T, Aza-Blanc P, Ruidiaz ME, Sugahara KN, Teesalu T, Ruoslahti E. An endocytosis pathway initiated through neuropilin-1 and regulated by nutrient availability. *Nat Commun*. **2014**, 5:4904.

[55]Voltan AR, Alarcon KM, Fusco-Almeida AM, Soares CP, Mendes-Giannini MJS, Chorilli M. Highlights in Endocytosis of Nanostructured Systems. *Curr Med Chem*. **2017**, 24(18):1909-29. .

[56]Duncan R. Polymer conjugates as anticancer nanomedicines. *Nat Rev Cancer*. **2006,** 6(9):688-701.

[57]Keefe AJ, Jiang S. Poly(zwitterionic)protein conjugates offer increased stability without sacrificing binding affinity or bioactivity. *Nat Chem*. **2012**, 4(1):59-63.

[58]Ruoslahti E, Bhatia SN, Sailor MJ. Targeting of drugs and nanoparticles to tumors. *J Cell Biol*. **2010**, 188(6):759-68.

[59]Dreher MR, Liu W, Michelich CR, Dewhirst MW, Yuan F, Chilkoti A. Tumor Vascular Permeability, Accumulation, and Penetration of Macromolecular Drug Carriers. *J Natl Cancer Ins*t. **2006**, 98(5):335-44..

[60]Penchala SC, Miller MR, Pal A, Dong J, Madadi NR, Xie J, Joo H, Tsai J, Batoon P, Samoshin V, Franz A, Cox T, Miles J, Chan WK, Park MS, Alhamadsheh MM. A biomimetic approach for enhancing the in vivo half-life of peptides. *Nat Chem Biol*. **2015**, 11(10):793-8.

[61]Erazo-Oliveras A, Muthukrishnan N, Baker R, Wang T-Y, Pellois J-P. Improving the endosomal escape of cell-penetrating peptides and their cargos: strategies and challenges. *Pharmaceuticals*. **2012**, 5:1177-209.

[62]Brock DJ, Kondow-McConaghy HM, Hager EC, Pellois J-P. Endosomal Escape and Cytosolic Penetration of Macromolecules Mediated by Synthetic Delivery Agents. *Bioconjugate Chem*. **2019,** 30(2):293-304.

[63]Kinnear C, Moore TL, Rodriguez-Lorenzo L, Rothen-Rutishauser B, Petri-Fink A. Form Follows Function: Nanoparticle Shape and Its Implications for Nanomedicine. *Chem Rev (Washington, DC, U S)*. **2017**, 117(17):11476-521.

[64]Sternson L. Obstacles to polypeptide delivery. *Annals of the New York Academy of Sciences.* **1987**, 507(1):19-21.

[65]Frankel AD, Pabo CO. Cellular uptake of the tat protein from human immunodeficiency virus. *Cell (Cambridge, Mass)*. **1988**, 55(6):1189-93.

[66]Ramsey JD, Flynn NH. Cell-penetrating peptides transport therapeutics into cells. *Pharmacology & therapeutics*. **2015**, 154:78-86.

[67]Vives E, Brodin P, Lebleu B. A truncated HIV-1 Tat protein basic domain rapidly translocates through the plasma membrane and accumulates in the cell nucleus. *J Biol Chem*. **1997**, 272(25):16010-7.

[68]Park J, Ryu J, Kim K-A, Lee HJ, Bahn JH, Han K, Choi EY, Lee KS, Kwon HY, Choi SY. Mutational analysis of a human immunodeficiency virus type 1 Tat protein transduction domain which is required for delivery of an exogenous protein into mammalian cells. *J Gen Virol*. **2002**, 83(5):1173-81.

[69]Guidotti G, Brambilla L, Rossi D. Cell-Penetrating Peptides: From Basic Research to Clinics. *Trends Pharmacol Sci*. **2017**, 38(4):406-24.

[70]Tesauro D, Accardo A, Diaferia C, Milano V, Guillon J, Ronga L, Rossi F. Peptide-Based Drug-Delivery Systems in Biotechnological Applications: Recent Advances and Perspectives. *Molecules*. **2019**, 24(2):351.

[71]Zhang Q, Tang J, Fu L, Ran R, Liu Y, Yuan M, He Q. A pH-responsive α-helical cell penetrating peptide-mediated liposomal delivery system. *Biomaterials*. **2013**, 34(32):7980-93.

[72]Gagat M, Zielinska W, Grzanka A. Cell-penetrating peptides and their utility in genome function modifications (review). *Int J Mol Med*. **2017**, 40(6):1615-23.

[73]Joliot A, Pernelle C, Deagostini-Bazin H, Prochiantz A. Antennapedia homeobox peptide regulates neural morphogenesis. *Proc Natl Acad Sci U S A*. **1991**, 88(5):1864-8.

[74]Derossi D, Joliot AH, Chassaing G, Prochiantz A. The third helix of the Antennapedia homeodomain translocates through biological membranes. *J Biol Chem*. **1994**, 269(14):10444-50.

[75]Futaki S, Suzuki T, Ohashi W, Yagami T, Tanaka S, Ueda K, Sugiura Y. Arginine-rich peptides: an abundant source of membrane-permeable peptides having potential as carriers for intracellular protein delivery. *J Biol Chem*. **2001**, 276(8):5836-40.

[76]Fajac I, Grosse S, Briand P, Monsigny M. Targeting of cell receptors and gene transfer efficiency: a balancing act. *Gene Ther*. **2002**, 9(11):740-2.

[77]De Coupade C, Fittipaldi A, Chagnas V, Michel M, Carlier S, Tasciotti E, Darmon A, Ravel D, Kearsey J, Giacca M, Cailler F. Novel human-derived cell-penetrating peptides for specific subcellular delivery of therapeutic biomolecules. *Biochem J*. **2005**, 390(2):407-18.

[78]Braunstein A, Papo N, Shai Y. In vitro activity and potency of an intravenously injected antimicrobial peptide and its DL amino acid analog in mice infected with bacteria. *Antimicrob Agents Chemother*. **2004**, 48(8):3127-9.

[79]Ragin AD, Morgan RA, Chmielewski J. Cellular Import Mediated by Nuclear Localization Signal Peptide Sequences. *Chem Biol*. **2002**, 9(8):943-8.

[80]Nasrolahi Shirazi A, Tiwari R, Chhikara BS, Mandal D, Parang K. Design and Biological Evaluation of Cell-Penetrating Peptide-Doxorubicin Conjugates as Prodrugs. *Mol Pharmaceutics*. **2013**, 10(2):488-99.

[81]Rodrigues M, Andreu D, Santos NC. Uptake and cellular distribution of nucleolar targeting peptides (NrTPs) in different cell types. *Biopolymers*. **2015**, 104(2):101-9.

[82]Wang H, Ma J, Yang Y, Zeng F, Liu C. Highly Efficient Delivery of Functional Cargoes by a Novel Cell-Penetrating Peptide Derived from SP140-Like Protein. *Bioconjugate Chem*. **2016**, 27(5):1373-81.

[83]Pujals S, Giralt E. Proline-rich, amphipathic cell-penetrating peptides. *Adv Drug Delivery Rev.* **2008**, 60(4-5):473-84.

[84]Pooga M, Hallbrink M, Zorko M, Langel U. Cell penetration by transportan. *FASEB* J. **1998**, 12(1):67-77.

[85]Milletti F. Cell-penetrating peptides: classes, origin, and current landscape. *Drug Discovery Today*. **2012**, 17(15-16):850-60.

[86]Elliott G, O'Hare P. Intercellular trafficking and protein delivery by a herpesvirus structural protein. *Cell*. **1997**, 88(2):223-33.

[87]Elmquist A, Hansen M, Langel U. Structure-activity relationship study of the cell-penetrating peptide pVEC. *Biochim Biophys Acta, Biomembr*. **2006**, 1758(6):721-9.

[88]Magzoub M, Sandgren S, Lundberg P, Oglecka K, Lilja J, Wittrup A, Eriksson LEG, Langel U, Belting M, Graeslund A. N-terminal peptides from unprocessed prion proteins enter cells by macropinocytosis. *Biochem Biophys Res Commun.* **2006**, 348(2):379-85.

[89]Johansson HJ, El-Andaloussi S, Holm T, Maee M, Jaenes J, Maimets T, Langel U. Characterization of a Novel Cytotoxic Cell-penetrating Peptide Derived From p14ARF Protein. *Mol Ther*. **2008**, 16(1):115-23.

[90]Oehlke J, Krause E, Wiesner B, Beyermann M, Bienert M. Extensive cellular uptake into endothelial cells of an amphipathic β-sheet forming peptide. *FEBS Lett.* **1997**, 415(2):196-9.

[91]Oehlke J, Scheller A, Wiesner B, Krause E, Beyermann M, Klauschenz E, Melzig M, Bienert M. Cellular uptake of an α-helical amphipathic model peptide with the potential to deliver polar compounds into the cell interior non-endocytically. *Biochim Biophys Acta, Biomembr*. **1998**, 1414(1-2):127-39.

[92]Yamada T, Christov K, Shilkaitis A, Bratescu L, Green A, Santini S, Bizzarri AR, Cannistraro S, Gupta TKD, Beattie CW. p28, A first in class peptide inhibitor of cop1 binding to p53. *Br J Cancer*. **2013**, 108(12):2495-504.

[93]Rhee M, Davis P. Mechanism of Uptake of C105Y, a Novel Cell-penetrating Peptide. *J Biol Chem*. **2006**, 281(2):1233-40.

[94]Marks JR, Placone J, Hristova K, Wimley WC. Spontaneous Membrane-Translocating Peptides by Orthogonal High-Throughput Screening. *J Am Chem Soc*. **2011**, 133(23):8995-9004.

[95]Gao C, Mao S, Ditzel HJ, Farnaes L, Wirsching P, Lerner RA, Janda KD. A cell-penetrating peptide from a novel pVII-pIX phage-displayed random peptide library. *Bioorg Med Chem*. **2002**, 10(12):4057-65.

[96]Zavaglia D, Favrot MC, Eymin B, Tenaud C, Coll JL. Intercellular trafficking and enhanced in vivo antitumour activity of a non-virally delivered P27-VP22 fusion protein. *Gene Ther*. **2003**, 10(4):314-25.

[97]Werle M, Bernkop-Schnuerch A. Strategies to improve plasma half life time of peptide and protein drugs. *Amino Acids*. **2006**, 30(4):351-67.

[98]Chatterjee J, Gilon C, Hoffman A, Kessler H. N-Methylation of Peptides: A New Perspective in Medicinal Chemistry. *Acc Chem Res.* **2008**, 41(10):1331-42.

[99]Tugyi R, Uray K, Ivan D, Fellinger E, Perkins A, Hudecz F. Partial D-amino acid substitution: Improved enzymatic stability and preserved Ab recognition of a MUC2 epitope peptide. *Proc Natl Acad Sci U S A.* **2005**, 102(2):413-8.

[100]Rosenfeld Y, Sahl H-G, Shai Y. Parameters Involved in Antimicrobial and Endotoxin Detoxification Activities of Antimicrobial Peptides. *Biochemistry*. **2008**, 47(24):6468-78.

[101]Makovitzki A, Fink A, Shai Y. Suppression of Human Solid Tumor Growth in Mice by Intratumor and Systemic Inoculation of Histidine-Rich and pH-Dependent Host Defense-like Lytic Peptides. *Cancer Res.* **2009**, 69(8):3458-63.

[102]Ahmed S, Kaur K. The proteolytic stability and cytotoxicity studies of L-aspartic acid and L-diaminopropionic acid derived β-peptides and a mixed α/β-peptide. *Chem Biol Drug Des.* **2009**, 73(5):545-52.

[103]Frackenpohl J, Arvidsson PI, Schreiber JV, Seebach D. The outstanding biological stability of β- and γ-peptides toward proteolytic enzymes: an in vitro investigation with fifteen peptidases. *ChemBioChem*. **2001**, 2(6):445-55.

[104]Gentilucci L, De Marco R, Cerisoli L. Chemical modifications designed to improve peptide stability: incorporation of non-natural amino acids, pseudo-peptide bonds, and cyclization. *Curr Pharm Des*. **2010**, 16(28):3185-203.

[105]Goodman M, Chorev M. On the concept of linear modified retro-peptide structures. *Acc Chem Res*. **1979**, 12(1):1-7.

[106]Srinivasan M, Wardrop RM, Whitacre CC, Kaumaya PTP, editors. A CD28 CDR3 peptide analog inhibits CD4+ T-cell proliferation in vitro2000: Kluwer Academic Publishers.

[107]Fischer PM. The design, synthesis and application of stereochemical and directional peptide isomers: a critical review. *Curr Protein Pept Sci.* **2003**, 4(5):339-56.

[108]Pujals S, Fernandez-Carneado J, Ludevid MD, Giralt E. D-SAP: a new, noncytotoxic, and fully protease resistant cell-penetrating peptide. *ChemMedChem*. **2008**, 3(2):296-301.

[109]Youngblood DS, Hatlevig SA, Hassinger JN, Iversen PL, Moulton HM. Stability of Cell-Penetrating Peptide-Morpholino Oligomer Conjugates in Human Serum and in Cells. *Bioconjugate Chem*. **2007**, 18(1):50-60.

[110]Verdurmen WPR, Bovee-Geurts PH, Wadhwani P, Ulrich AS, Haellbrink M, van Kuppevelt TH, Brock R. Preferential Uptake of L- versus D-Amino Acid Cell-Penetrating Peptides in a Cell Type-Dependent Manner. *Chem Biol (Cambridge, MA, U S)*. **2011**, 18(8):1000-10.

[111]Otvos L, Jr., Cappelletto B, Varga I, Wade JD, Xiang ZQ, Kaiser K, Stephens LJ, Ertl HCJ. The effects of post-translational side-chain modifications on the stimulatory activity, serum stability and conformation of synthetic peptides carrying T helper cell epitopes. *Biochim Biophys Acta, Mol Cell Res*. **1996**, 1313(1):11-9.

[112]Hamley IW. PEG-Peptide Conjugates. *Biomacromolecules*. **2014**, 15(5):1543-59.

[113]Harris JM, Chess RB. Effect of PEGylation on pharmaceuticals. *Nat Rev Drug Discovery*. **2003**, 2(3):214-21.

[114]Danial M, van Dulmen THH, Aleksandrowicz J, Potgens AJG, Klok H-A. Site-Specific PEGylation of HR2 Peptides: Effects of PEG Conjugation Position and Chain Length on HIV-1 Membrane Fusion Inhibition and Proteolytic Degradation. *Bioconjugate Chem*. **2012**, 23(8):1648-60.

[115]Dozier JK, Distefano MD. Site-specific pegylation of therapeutic proteins. *Int J Mol Sci*. **2015**, 16(10):25831-64.

[116]Nischan N, Chakrabarti A, Serwa RA, Bovee-Geurts PHM, Brock R, Hackenberger CPR. Stabilization of Peptides for Intracellular Applications by Phosphoramidate-Linked Polyethylene Glycol Chains. *Angew Chem, Int Ed*. **2013**, 52(45):11920-4.

[117]White CJ, Yudin AK. Contemporary strategies for peptide macrocyclization. *Nat Chem*. **2011**, 3(7):509-24.

[118]Teesalu T, Sugahara KN, Kotamraju VR, Erkki R. C-end rule peptides mediate neuropilin-1-dependent cell, vascular, and tissue penetration. *Proc Natl Acad Sci U S A*. **2009**, 106(38):16157-62, S/1-S/15.

[119]Roth L, Agemy L, Kotamraju VR, Braun G, Teesalu T, Sugahara KN, Hamzah J, Ruoslahti E. Transtumoral targeting enabled by a novel neuropilin-binding peptide. *Oncogene*. **2012**, 31(33):3754-63.

[120]Alberici L, Roth L, Sugahara KN, Agemy L, Kotamraju VR, Teesalu T, Bordignon C, Traversari C, Rizzardi G-P, Ruoslahti E. De Novo Design of a Tumor-Penetrating Peptide. *Cancer Res*. **2013**, 73(2):804-12.

[121]Teesalu T, Sugahara KN, Ruoslahti E. Tumor-penetrating peptides. *Front Oncol*. 2013;3:216.

[122]Pang H-B, Braun GB, She Z-G, Kotamraju VR, Sugahara KN, Teesalu T, Ruoslahti E. A free cysteine prolongs the half-life of a homing peptide and improves its tumor-penetrating activity. *J Controlled Release*. **2014,** 175:48-53.

[123]Sugahara KN, Braun GB, Hurtado de Mendoza T, Kotamraju VR, French RP, Lowy AM, Teesalu T, Ruoslahti E. Tumor-Penetrating iRGD Peptide Inhibits Metastasis. *Mol Cancer Ther*. **2015**, 14(1):120-8.

[124]Ewert KK, Kotamraju VR, Majzoub RN, Steffes VM, Wonder EA, Teesalu T, Ruoslahti E, Safinya CR. Synthesis of linear and cyclic peptide-PEG-lipids for stabilization and targeting of cationic liposome-DNA complexes. *Bioorg Med Chem Lett*. **2016**, 26(6):1618-23.

[125]Nel A, Ruoslahti E, Meng H. New insights into "permeability" as in the enhanced permeability and retention effect of cancer nanotherapeutics. *ACS Nano*. **2017**, 11(10):9567-9.

[126]Sharma S, Kotamraju VR, Molder T, Tobi A, Teesalu T, Ruoslahti E. Tumor-Penetrating Nanosystem Strongly Suppresses Breast Tumor Growth. *Nano Lett*. **2017**, 17(3):1356-64.

[127]Pierschbacher MD, Ruoslahti E. Cell attachment activity of fibronectin can be duplicated by small synthetic fragments of the molecule. *Nature (London)*. **1984**, 309(5963):30-3.

[128]Sheldrake HM, Patterson LH. Strategies To Inhibit Tumor Associated Integrin Receptors: Rationale for Dual and Multi-Antagonists. *J Med Chem*. **2014**, 57(15):6301-15.

[129]Liu S. Radiolabeled Cyclic RGD Peptide Bioconjugates as Radiotracers Targeting Multiple Integrins. *Bioconjugate Chem*. **2015**, 26(8):1413-38.

[130]Temming K, Schiffelers RM, Molema G, Kok RJ. RGD-based strategies for selective delivery of therapeutics and imaging agents to the tumour vasculature. *Drug Resistance Updates*. **2005**, 8(6):381-402.

[131]Danhier F, Le Breton A, Préat V. RGD-Based Strategies To Target Alpha(v) Beta(3) Integrin in Cancer Therapy and Diagnosis. *Molecular Pharmaceutics*. **2012**, 9(11):2961-73.

[132]Schottelius M, Laufer B, Kessler H, Wester H-J. Ligands for Mapping αvβ3-Integrin Expression in Vivo. *Accounts of Chemical Research*. **2009**, 42(7):969-80.

[133]Sugahara KN, Teesalu T, Karmali PP, Kotamraju VR, Agemy L, Girard OM, Hanahan D, Mattrey RF, Ruoslahti E. Tissue-Penetrating Delivery of Compounds and Nanoparticles into Tumors. *Cancer Cell*. **2009**, 16(6):510-20.

[134]Cho H-J, Park S-J, Lee Y-S, Kim S. Theranostic iRGD peptide containing cisplatin prodrug: Dual-cargo tumor penetration for improved imaging and therapy. *J Controlled Release*. **2019**, 300:73-80.

[135]Kirschner N, Brandner JM. Barriers and more: functions of tight junction proteins in the skin. *Annals of the New York Academy of Sciences*. **2012**, 1257(1):158-66.

[136]Serlin Y, Shelef I, Knyazer B, Friedman A. Anatomy and physiology of the blood–brain barrier. *Seminars in Cell & Developmental Biology*. **2015**, 38:2-6.

[137]Daneman R, Prat A. The blood-brain barrier. *Cold Spring Harbor Perspect Biol.* **2015**, 7(1):1-24.

[138]Oldendorf WH. Lipid Solubility and Drug Penetration of the Blood Brain Barrier. *Proceedings of the Society for Experimental Biology and Medicine.* **1974**, 147(3):813-6.

[139]Banks WA, Kastin AJ. Peptides and the blood-brain barrier: Lipophilicity as a predictor of permeability. *Brain Research Bulletin*. **1985**, 15(3):287-92.

[140]Chikhale EG, Ng KY, Burton PS, Borchardt RT. Hydrogen bonding potential as a determinant of the in vitro and in situ blood-brain barrier permeability of peptides. *Pharm Res*. **1994**, 11(3):412-19.

[141]Begley DJ. Strategies for delivery of peptide drugs to the central nervous system: exploiting molecular structure. *Journal of Controlled Release*. **1994**, 29(3):293-306.

[142]Varghese NM, Senthil V, Saxena SK. Nanocarriers for brain specific delivery of anti-retro viral drugs: challenges and achievements. *J Drug Targeting*. **2018**, 26(3):195-207.

[143]Schwarze SR, Ho A, Vocero-Akbani A, Dowdy SF. In vivo protein transduction: Delivery of a biologically active protein into the mouse. *Science (Washington, D C).* **1999**, 285(5433):1569-72.

[144]Santra S, Yang H, Stanley JT, Holloway PH, Moudgil BM, Walter G, Mericle RA. Rapid and effective labeling of brain tissue using TAT-conjugated CdS:Mn/ZnS quantum dots. *Chemical Communications*. **2005**, (25):3144-6.

[145]Rao KS, Reddy MK, Horning JL, Labhasetwar V. TAT-conjugated nanoparticles for the CNS delivery of anti-HIV drugs. *Biomaterials*. **2008**, 29(33):4429-38.

[146]Liu L, Guo K, Lu J, Venkatraman SS, Luo D, Ng KC, Ling E-A, Moochhala S, Yang Y-Y. Biologically active core/shell nanoparticles self-assembled from cholesterol-terminated PEG–TAT for drug delivery across the blood–brain barrier. *Biomaterials*. **2008**, 29(10):1509-17.

[147]Zhao Y, Li D, Zhao J, Song J, Zhao Y. The role of the low-density lipoprotein receptor-related protein 1 (LRP-1) in regulating blood-brain barrier integrity. *Rev Neurosci (Berlin, Ger).* **2016,** 27(6):623-34.

[148]Qian ZM, Li H, Sun H, Ho K. Targeted drug delivery via the transferrin receptor-mediated endocytosis pathway. *Pharmacol Rev*. **2002**, 54(4):561-87.

[149]Go G-W, Mani A. Low-density lipoprotein receptor (LDLR) family orchestrates cholesterol homeostasis. *Yale J Biol Med*. **2012**, 85(1):19-28.

[150]Sánchez-Navarro M, Teixidó M, Giralt E. Jumping Hurdles: Peptides Able To Overcome Biological Barriers. *Acc of Chem Research*. **2017**, 50(8):1847-54.

[151]Zhan C, Li B, Hu L, Wei X, Feng L, Fu W, Lu W. Micelle-Based Brain-Targeted Drug Delivery Enabled by a Nicotine Acetylcholine Receptor Ligand. *Angewandte Chemie Inter Edition*. **2011**, 50(24):5482-5.

[152]Dubois LG, Campanati L, Righy C, D'Andrea-Meira I, Spohr TCLdSE, Porto-Carreiro I, Pereira CM, Balça-Silva J, Kahn SA, DosSantos MF, Oliveira MdAR, Ximenes-da-Silva A, Lopes MC, Faveret E, Gasparetto EL, Moura-Neto V. Gliomas and the vascular fragility of the blood brain barrier. *Front in cel neuroscience*. **2014**, 8:418-.

[153]Yu M-Z, Pang W-H, Yang T, Wang J-C, Wei L, Qiu C, Wu Y-F, Liu W-Z, Wei W, Guo X-Y, Zhang Q. Systemic delivery of siRNA by T7 peptide modified core-shell nanoparticles for targeted therapy of breast cancer. *European Jour of Pharm Sciences*. **2016**, 92:39-48.

[154]Liu Z, Gao X, Kang T, Jiang M, Miao D, Gu G, Hu Q, Song Q, Yao L, Tu Y, Chen H, Jiang X, Chen J. B6 Peptide-Modified PEG-PLA Nanoparticles for Enhanced Brain Delivery of Neuroprotective Peptide. *Bioconjugate Chemistry*. **2013**, 24(6):997-1007.

[155]Kang T, Jiang M, Jiang D, Feng X, Yao J, Song Q, Chen H, Gao X, Chen J. Enhancing Glioblastoma-Specific Penetration by Functionalization of Nanoparticles with an Iron-Mimic Peptide Targeting Transferrin/Transferrin Receptor Complex. *Molecular Pharmaceutics*. **2015**, 12(8):2947-61.

[156]Prades R, Guerrero S, Araya E, Molina C, Salas E, Zurita E, Selva J, Egea G, López-Iglesias C, Teixidó M, Kogan MJ, Giralt E. Delivery of gold nanoparticles to the brain by conjugation with a peptide that recognizes the transferrin receptor. *Biomaterials*. **2012**, 33(29):7194-205.

[157]Phoolcharoen W, Prehaud C, van Dolleweerd CJ, Both L, da Costa A, Lafon M, Ma JKC. Enhanced transport of plant-produced rabies single-chain antibody-RVG peptide fusion protein across an in cellulo blood–brain barrier device. *Plant Biotechnology Journal*. **2017**, 15(10):1331-9.

[158]Demeule M, Beaudet N, Régina A, Besserer-Offroy É, Murza A, Tétreault P, Belleville K, Ché C, Larocque A, Thiot C, Béliveau R, Longpré J-M, Marsault É, Leduc R, Lachowicz JE, Gonias SL, Castaigne J-P, Sarret P. Conjugation of a brain-penetrant peptide with neurotensin provides antinociceptive properties. *The Journal of Clinical Investigation*. **2014**, 124(3):1199-213.

[159]Sorrentino NC, D'Orsi L, Sambri I, Nusco E, Monaco C, Spampanato C, Polishchuk E, Saccone P, De Leonibus E, Ballabio A, Fraldi A. A highly secreted sulphamidase engineered to cross the blood-brain barrier corrects brain lesions of mice with mucopolysaccharidoses type IIIA. *EMBO Mol Med*. **2013**, 5(5):675-90.

[160]Wang D, El-Amouri SS, Dai M, Kuan C-Y, Hui DY, Brady RO, Pan D. Engineering a lysosomal enzyme with a derivative of receptor-binding domain of apoE enables delivery across the blood–brain barrier. *Proceedings of the National Academy of Sciences*. **2013**, 110(8):2999.

[161]Diaz-Perlas C, Oller-Salvia B, Sanchez-Navarro M, Teixido M, Giralt E. Branched BBB-shuttle peptides: chemoselective modification of proteins to enhance blood-brain barrier transport. *Chem Sci*. **2018**, 9(44):8409-15.

[162]Liu Y, Li J, Shao K, Huang R, Ye L, Lou J, Jiang C. A leptin derived 30-amino-acid peptide modified pegylated poly-l-lysine dendrigraft for brain targeted gene delivery. *Biomaterials*. **2010**, 31(19):5246-57.

[163]Tian X-H, Wang Z-G, Meng H, Wang Y-H, Feng W, Wei F, Huang Z-C, Lin X-N, Ren L. Tat peptide-decorated gelatin-siloxane nanoparticles for delivery of CGRP transgene in treatment of cerebral vasospasm. *Int J Nanomed*. **2012**, 8:865-76.

[164]Rousselle C, Clair P, Lefauconnier J-M, Kaczorek M, Scherrmann J-M, Temsamani J. New advances in the transport of doxorubicin through the blood-brain barrier by a peptide vector-mediated strategy. *Mol Pharmacol*. **2000**, 57(4):679-86.

[165]Neves-Coelho S, Eleuterio RP, Enguita FJ, Neves V, Castanho MARB. A new noncanonical anionic peptide that translocates a cellular blood-brain barrier model. *Molecules*. **2017**, 22(10):1753/1-/12.

[166]Singh K, Ejaz W, Dutta K, Thayumanavan S. Antibody Delivery for Intracellular Targets: Emergent Therapeutic Potential. *Bioconjugate Chem*. **2019,** Ahead of Print.

[167]Dang CV, Reddy EP, Shokat KM, Soucek L. Drugging the 'undruggable' cancer targets. *Nat Rev Cancer*. **2017**, 17(8):502-8.

[168]Smith GP. Filamentous fusion phage: novel expression vectors that display cloned antigens on the virion surface. *Science*. **1985**, 228(4705):1315-7.

[169]Nilvebrant J, Sidhu SS. Construction of synthetic antibody phage-display libraries. *Methods Mol Biol (N Y, NY, U S).* **2018**, 1701(Phage Display):45-60.

[170]Gaughan CL. The present state of the art in expression, production and characterization of monoclonal antibodies. *Mol Diversity*. **2016**, 20(1):255-70.

[171]Abdollahpour-Alitappeh M, Lotfinia M, Gharibi T, Mardaneh J, Farhadihosseinabadi B, Larki P, Faghfourian B, Sepehr KS, Abbaszadeh-Goudarzi K, Abbaszadeh-Goudarzi G, Johari B, Zali MR, Bagheri N. Antibody-drug conjugates (ADCs) for cancer therapy: Strategies, challenges, and successes. *J Cell Physiol*. **2019**, 234(5):5628-42.

[172]Tashima T. Effective cancer therapy based on selective drug delivery into cells across their membrane using receptor-mediated endocytosis. *Bioorg Med Chem Lett.* **2018**, 28(18):3015-24.

[173]Chalouni C, Doll S. Fate of antibody-drug conjugates in cancer cells. *J Exp Clin Cancer Res*. **2018**, 37:20/1-/12.

[174]Antman KH, Livingston DM. Intracellular neutralization of SV40 tumor antigens following microinjection of specific antibody. *Cell*. **1980**, 19(3):627-35.

[175]Blose SH, Meltzer DI, Feramisco JR. 10-nm Filaments are induced to collapse in living cells microinjected with monoclonal and polyclonal antibodies against tubulin. *J Cell Biol*. **1984**, 98(3):847-58.

[176]Berglund DL, Starkey JR. Introduction of antibody into viable cells using electroporation. *Cytometry*. **1991**, 12(1):64-7.

[177]Marrero MB, Schieffer B, Paxton WG, Schieffer E, Bernstein KE. Electroporation of pp60c-src antibodies inhibits the angiotensin II activation of phospholipase C-γ1 in rat aortic smooth muscle cells. *J Biol Chem*. **1995,** 270(26):15734-8.

[178]Kumar P, Tambe P, Paknikar KM, Gajbhiye V. Mesoporous silica nanoparticles as cutting-edge theranostics: Advancement from merely a carrier to tailor-made smart delivery platform. *J Controlled Release*. **2018,** 287:35-57.

[179]Baeza A, Vallet-Regi M. Targeted Mesoporous Silica Nanocarriers in Oncology. *Curr Drug Targets*. **2018**, 19(3):213-24.

[180]Maggini L, Cabrera I, Ruiz-Carretero A, Prasetyanto EA, Robinet E, De Cola L. Breakable mesoporous silica nanoparticles for targeted drug delivery. *Nanoscale*. **2016**, 8(13):7240-7.

[181]Guo H-C, Feng X-M, Sun S-Q, Wei Y-Q, Sun D-H, Liu X-T, Liu Z-X, Luo J-X, Yin H. Immunization of mice by Hollow mesoporous silica nanoparticles as carriers of Porcine circovirus type 2 ORF2 protein. *Virol J.* **2012**, 9:108.

[182]Roberts CJ, Davies MC, Tendler SJ, Williams PM, Davies J, Dawkes AC, Yearwood GD, Edwards JC. The discrimination of IgM and IgG type antibodies and Fab' and F(ab)2 antibody fragments on an industrial substrate using scanning force microscopy. *Ultramicroscopy*. **1996**, 62(3):149-55.

[183]Du X, editor. Biomacromolecule-gated mesoporous silica drug delivery systems for stimuli-responsive controlled release **2015**: *Scrivener Publishing LLC*.

[184]Karimi M, Mirshekari H, Aliakbari M, Sahandi-Zangabad P, Hamblin MR. Smart mesoporous silica nanoparticles for controlled-release drug delivery. *Nanotechnol Rev*. **2016**, 5(2):195-207.

[185]Wen J, Yang K, Liu F, Li H, Xu Y, Sun S. Diverse gatekeepers for mesoporous silica nanoparticle based drug delivery systems. *Chem Soc Rev*. **2017**, 46(19):6024-45.

[186]Yi S, Zheng J, Lv P, Zhang D, Zheng X, Zhang Y, Liao R. Controlled Drug Release from Cyclodextrin-Gated Mesoporous Silica Nanoparticles Based on Switchable Host-Guest Interactions. *Bioconjugate Chem*. **2018**, 29(9):2884-91.

[187]Gu J, Huang K, Zhu X, Li Y, Wei J, Zhao W, Liu C, Shi J. Sub-150nm mesoporous silica nanoparticles with tunable pore sizes and well-ordered mesostructure for protein encapsulation. *Journal of Colloid and Interface Science.* **2013**, 407:236-42.

[188]Garcia-Bennett AE, Kozhevnikova M, Koenig N, Zhou C, Leao R, Knoepfel T, Pankratova S, Trolle C, Berezin V, Bock E, Aldskogius H, Kozlova EN. Delivery of differentiation factors by mesoporous silica particles assists advanced differentiation of transplanted murine embryonic stem cells. *Stem Cells Transl Med.* **2013**, 2(11):906-15.

[189]Tarn D, Ashley CE, Xue M, Carnes EC, Zink JI, Brinker CJ. Mesoporous Silica Nanoparticle Nanocarriers: Biofunctionality and Biocompatibility. *Accounts of Chemical Research.* ***2013**, 46(3):792-801.*

[190]Wang Y, Gu H. Core-shell-type magnetic mesoporous silica nanocomposites for bioimaging and therapeutic agent delivery. *Adv Mater (Weinheim, Ger)*. **2015**, 27(3):576-85.

[191]Wang H, Covarrubias J, Prock H, Wu X, Wang D, Bossmann SH. Acid-Functionalized Magnetic Nanoparticle as Heterogeneous Catalysts for Biodiesel Synthesis. *J Phys Chem C*. **2015**, 119(46):26020-8.

[192]Lai C-Y, Trewyn BG, Jeftinija DM, Jeftinija K, Xu S, Jeftinija S, Lin VSY. A Mesoporous Silica Nanosphere-Based Carrier System with Chemically Removable CdS Nanoparticle Caps for Stimuli-Responsive Controlled Release of Neurotransmitters and Drug Molecules. *Journal of the American Chemical Society*. **2003**, 125(15):4451-9.

[193]Kalubowilage M, Covarrubias-Zambrano O, Malalasekera AP, Wendel SO, Wang H, Yapa AS, Chlebanowski L, Toledo Y, Ortega R, Janik KE, Shrestha TB, Culbertson CT, Kasi A, Williamson S, Troyer DL, Bossmann SH. Early detection of pancreatic cancers in liquid biopsies by ultrasensitive fluorescence nanobiosensors. *Nanomedicine (N Y, NY, U S)*. **2018**, 14(6):1823-32.

[194]Udukala DN, Wang H, Wendel SO, Malalasekera AP, Samarakoon TN, Yapa AS, Abayaweera G, Basel MT, Maynez P, Ortega R, Toledo Y, Bossmann L, Robinson C, Janik KE, Koper OB, Li P, Motamedi M, Higgins DA, Gadbury G, Zhu G, Troyer DL, Bossmann SH. Early breast cancer screening using iron/iron oxide-based nanoplatforms with sub-femtomolar limits of detection. *Beilstein J Nanotechnol.* **2016**, 7:364-73.

[195]Cheng Y-J, Luo G-F, Zhu J-Y, Xu X-D, Zeng X, Cheng D-B, Li Y-M, Wu Y, Zhang X-Z, Zhuo R-X, He F. Enzyme-Induced and Tumor-Targeted Drug Delivery System Based on Multifunctional Mesoporous Silica Nanoparticles. *ACS Applied Materials & Interfaces.* **2015**, 7(17):9078-87.

[196]Singh N, Karambelkar A, Gu L, Lin K, Miller JS, Chen CS, Sailor MJ, Bhatia SN. Bioresponsive Mesoporous Silica Nanoparticles for Triggered Drug Release. *Journal of the American Chemical Society.* **2011**, 133(49):19582-5.

[197]de la Torre C, Casanova I, Acosta G, Coll C, Moreno MJ, Albericio F, Aznar E, Mangues R, Royo M, Sancenón F, Martínez-Máñez R. Gated Mesoporous Silica Nanoparticles Using a Double-Role Circular Peptide for the Controlled and Target-Preferential Release of Doxorubicin in CXCR4-Expresing Lymphoma Cells. *Advanced Functional Materials.* **2015**, 25(5):687-95.

[198]Fathi S, Oyelere AK. Liposomal drug delivery systems for targeted cancer therapy: is active targeting the best choice? *Future Med Chem*. **2016**, 8(17):2091-112.

[199]Li Z, Tan S, Li S, Shen Q, Wang K. Cancer drug delivery in the nano era: an overview and perspectives (review). *Oncol Rep*. **2017**, 38(2):611-24.

[200]Ansari R, Mannan A. Liposomes As A Novel Drug Delivery System. *Int J Pharm Technol*. **2017**, 9(2):29735-58.

[201]Lasic DD, Barenholz Y, editors. Liposomes: Past, present, and future **1996**: *CRC*.

[202]Karanth H, Murthy RSR. pH-sensitive liposomes-principle and application in cancer therapy. *J Pharm Pharmacol.* **2007**, 59(4):469-83..

[203]Pezzoli D, Tallarita E, Rosini E, Candiani G. Characterization and investigation of redox-sensitive liposomes for gene delivery. *Methods Mol Biol (N Y, NY, U S)*. **2016**, 1445(Non-Viral Gene Delivery Vectors):217-33.

[204]Yavlovich A, Smith B, Gupta K, Blumenthal R, Puri A. Light-sensitive lipid-based nanoparticles for drug delivery: design principles and future considerations for biological applications. *Mol Membr Biol*. **2010**, 27(7):364-81. doi: 10.3109/09687688.2010.507788.

[205]Kono K, Ozawa T, Yoshida T, Ozaki F, Ishizaka Y, Maruyama K, Kojima C, Harada A, Aoshima S. Highly temperature-sensitive liposomes based on a thermosensitive block copolymer for tumor-specific chemotherapy. *Biomaterials*. **2010**, 31(27):7096-105.

[206]Milla P, Dosio F, Cattel L. PEGylation of proteins and liposomes: a powerful and flexible strategy to improve the drug delivery. *Curr Drug Metab*. **2012**, 13(1):105-19.

[207]Mozar FS, Chowdhury EH. Impact of PEGylated Nanoparticles on Tumor Targeted Drug Delivery. *Curr Pharm Des.* **2018**, 24(28):3283-96.

[208]Elkhodiry MA, Momah CC, Suwaidi SR, Gadalla D, Martins AM, Vitor RF, Husseini GA. Synergistic nanomedicine: passive, active, and ultrasound-triggered drug delivery in cancer treatment. *J Nanosci Nanotechnol.* **2016**, 16(1):1-18.

[209]Malalasekera AP, Bossmann SH, Zhu G. Magnetic Nanoformulations for Enhanced Drug Delivery and Retention. In: Bossmann SH, Wang H, editors. Magnetic Nanomaterials Applications in Catalysis and Life Sciences. *Croydon, UK: Royal Society of Chemistry*; **2017**. p. 221-39.

[210]Allen TM, Cullis PR. Liposomal drug delivery systems: From concept to clinical applications. *Adv Drug Delivery Rev*. **2013**, 65(1):36-48.

[211]Salatin S, Yari Khosroushahi A. Overviews on the cellular uptake mechanism of polysaccharide colloidal nanoparticles. *Jour of cel and mol med*. **2017**, 21(9):1668-86. Epub 2017/02/28.

[212]Guo C, Chen Y, Gao W, Chang A, Ye Y, Shen W, Luo Y, Yang S, Sun P, Xiang R, Li N. Liposomal nanoparticles carrying anti-IL6R antibody to the tumour microenvironment inhibit metastasis in two molecular subtypes of breast cancer mouse models. *Theranostics*. **2017**, 7(3):775-88.

[213]Subbarao NK, Parente RA, Szoka FC, Jr., Nadasdi L, Pongracz K. The pH-dependent bilayer destabilization by an amphipathic peptide. *Biochemistry*. **1987**, 26(11):2964-72.

[214]Liu K, Zheng L, Ma C, Gostl R, Herrmann A. DNA-surfactant complexes: self-assembly properties and applications. *Chem Soc Rev*. **2017**;46(16):5147-72.

[215]Wang S, Huttmann G, Zhang Z, Vogel A, Birngruber R, Tangutoori S, Hasan T, Rahmanzadeh R. Light-Controlled Delivery of Monoclonal Antibodies for Targeted Photoinactivation of Ki-67. *Mol Pharmaceutics*. **2015**;12(9):3272-81.

[216]Deng H, Song K, Zhao X, Li Y, Wang F, Zhang J, Dong A, Qin Z. Tumor Microenvironment Activated Membrane Fusogenic Liposome with Speedy Antibody and Doxorubicin Delivery for Synergistic Treatment of Metastatic Tumors. *ACS Appl Mater Interfaces.* **2017**, 9(11):9315-26.

[217]Buggins AGS, Levi A, Gohil S, Fishlock K, Patten PEM, Calle Y, Yallop D, Devereux S. Evidence for a macromolecular complex in poor prognosis CLL that contains CD38, CD49d, CD44 and MMP-9. *Br J Haematol*. **2011**, 154(2):216-22.

[218]Noda M, Oh J, Takahashi R, Kondo S, Kitayama H, Takahashi C. RECK: a novel suppressor of malignancy linking oncogenic signaling to extracellular matrix remodeling. Cancer *Metastasis Rev*. **2003**, 22(2-3):167-75.

[219]Basel MT, Shrestha TB, Troyer DL, Bossmann SH. Protease-Sensitive, Polymer-Caged Liposomes: A Method for Making Highly Targeted Liposomes Using Triggered Release. *ACS Nano*. **2011**, 5(3):2162-75.

[220]Jabin K, Husian Z, Ahmad M, Kushwaha P. Liposome: classification, preparation, and applications. *World J Pharm Pharm Sci*. **2018**, 7(9):1307-19.

[221]Sercombe L, Veerati T, Moheimani F, Wu SY, Sood AK, Hua S. Advances and challenges of liposome assisted drug delivery. *Front Pharmacol*. **2015**, 6:286/1-/13.

[222]Ahmed EM. Hydrogel: Preparation, characterization, and applications: A review. *J Adv Res*. **2015**, 6(2):105-21.

[223]Rahmati M, Mozafari M, Rahmati M, Mozafari M, Pennisi CP, Budd E, Mobasheri A, Budd E, Mobasheri A, Mobasheri A, Mobasheri A, Mozafari M. Biomaterials for Regenerative Medicine: Historical Perspectives and Current Trends. *Adv Exp Med Biol.* **2018**, 1119:1-19.

[224]Eskandari S, Guerin T, Toth I, Stephenson RJ. Recent advances in self-assembled peptides: Implications for targeted drug delivery and vaccine engineering. *Adv Drug Delivery Rev.* **2017**, 110-111:169-87.

[225]Mazza M, Patel A, Pons R, Bussy C, Kostarelos K. Peptide nanofibres as molecular transporters: from self-assembly to in vivo degradation. *Faraday Discuss*. **2013**, 166:181-94.

[226]https://www.cancer.gov/about-cancer/treatment/types/chemotherapy.

[227]Habibi N, Kamaly N, Memic A, Shafiee H. Self-assembled peptide-based nanostructures: Smart nanomaterials toward targeted drug delivery. *Nano Today*. **2016**, 11(1):41-60.

[228]Yishay-Safranchik E, Golan M, David A. Controlled release of doxorubicin and Smac-derived pro-apoptotic peptide from self-assembled KLD-based peptide hydrogels. *Polym Adv Technol*. **2014**, 25(5):539-44.

[229]Toft DJ, Moyer TJ, Standley SM, Ruff Y, Ugolkov A, Stupp SI, Cryns VL. Coassembled Cytotoxic and Pegylated Peptide Amphiphiles Form Filamentous Nanostructures with Potent Antitumor Activity in Models of Breast Cancer. *ACS Nano*. **2012**, 6(9):7956-65.

[230]Yapa AS, Wang H, Wendel SO, Shrestha TB, Kariyawasam NL, Kalubowilage M, Perera AS, Pyle M, Basel MT, Malalasekera AP, Manawadu H, Yu J, Toledo Y, Ortega R, Thapa PS, Smith PE, Troyer DL, Bossmann SH. Peptide nanosponges designed for rapid uptake by leukocytes and neural stem cells. *RSC Adv*. **2018**, 8(29):16052-60.

[231]Wang H, Yapa AS, Kariyawasam NL, Shrestha TB, Kalubowilage M, Wendel SO, Yu J, Pyle M, Basel MT, Malalasekera AP, Toledo Y, Ortega R, Thapa PS, Huang H, Sun SX, Smith PE, Troyer DL, Bossmann SH. Rationally designed peptide nanosponges for cell-based cancer therapy. *Nanomedicine (N Y, NY, U S)*. **2017**, 13(8):2555-64.

[232]Liechty WB, Kryscio DR, Slaughter BV, Peppas NA. Polymers for drug delivery systems. *Annu Rev Chem Biomol Eng*. **2010,** 1:149-73.

[233]Ding Z, Fong RB, Long CJ, Stayton PS, Hoffman AS. Size-dependent control of the binding of biotinylated proteins to streptavidin using a polymer shield. *Nature (London, U K).* **2001**, 411(6833):59-62.

[234]Lackey CA, Press OW, Hoffman AS, Stayton PS. A Biomimetic pH-Responsive Polymer Directs Endosomal Release and Intracellular Delivery of an Endocytosed Antibody Complex. *Bioconjugate Chem*. **2002**, 13(5):996-1001.

[235]Gdowski A, Ranjan A, Mukerjee A, Vishwanatha J. Development of biodegradable nanocarriers loaded with a monoclonal antibody. *Int J Mol Sci.* **2015**, 16(2):3990-5.

[236]Nouri FS, Wang X, Dorrani M, Karjoo Z, Hatefi A. A Recombinant Biopolymeric Platform for Reliable Evaluation of the Activity of pH-Responsive Amphiphile Fusogenic Peptides. *Biomacromolecules*. **2013**, 14(6):2033-40.

[237]Neuberg P, Kichler A. Recent developments in nucleic acid delivery with polyethylenimines. *Adv Genet*. **2014**;88:263-88.

[238]Didenko VV, Ngo H, Baskin DS. Polyethyleneimine as a transmembrane carrier of fluorescently labeled proteins and antibodies. *Anal Biochem.* **2005**, 344(2):168-73.

[239]Jiang T, Yu X, Carbone EJ, Nelson C, Kan HM, Lo KWH. Poly aspartic acid peptide-linked PLGA based nanoscale particles: Potential for bone-targeting drug delivery applications. *Int J Pharm (Amsterdam, Neth)*. **2014**, 475(1-2):547-57.

[240]Sipai ABM, Yadav V, Mamatha Y, Prasanth VV. Liposomes: an overview. *J Pharm Sci Innovation*. **2012**, 1(1):13-21.

Chapter 2 - Development of a Modified and Improved Cell Penetrating Peptide

1. Abstract

Cancer is the second leading cause of death worldwide, and no one is immune to this disease. Due to the lack of efficient cancer treatments, here we focus on development of a promising peptide that could be used as a primary nanocarrier to reach cancerous cells in a targeted manner. Understanding that secondary structures of peptides play important role in cellular uptake and penetration is essential. For this study peptides were modified by replacing an amino acid on a particular location to modify the predicted peptide structure and potentially generate a more effective cell penetrating peptide. Four modified cell penetrating peptides containing microtube-associated sequences (MTAS) with a modified amino acid in the sequence to what will be called WTAS and/or nuclear localization signals (NLS) were synthesized following the solid phase peptide synthesis protocol. Cellular uptake experiments were then conducted to demonstrate cell penetration by these peptides. The WTAS peptide was the candidate selected for further experiments due to better cellular uptake results. Confocal studies were conducted to confirm possible nuclear penetration of WTAS on two cell lines, B16F10 (cancerous cell line) and SIM-A9 (non-cancerous cell line). Results demonstrated that WTAS is able to penetrate both cell lines within a couple minutes, but it can only penetrate cell nuclei of B16F10. More studies need to be performed to clearly conclude that WTAS can penetrate cell nucleus for cancerous cells only, however WTAS is a promising peptide for an improved cancer treatment approach.

2. Background

2.1 Cancer Research Importance

Cancer, "an evil condition that spreads destructively", as is defined by the English dictionary, is a disease name used to describe uncontrolled division of abnormal cells in the body[1]. Normal cells tend to grow and divide as is required by the body, and once they become old or damaged, they die and are replaced by new cells. In contrast, cancer cells are abnormal cells that divide without stopping even when they are not needed, which leads to the formation of tumors, in most cancer cases except leukemia[2]. There are two types of tumors, benign, which do not invade or spread around the body, and malignant, which invade and spread to other organs. Upon removal of these tumors by means of surgery, benign tumors do not grow back, while malignant tumors often do[3]. Malignant tumors, also known as malignant neoplasms, arise due to genetic changes that control growth and division of cells, such as genetic and epigenetic mutations. These mutations can be inherited from ancestors or can be triggered due to certain environmental exposures (radiation, tobacco, and other chemicals)[2]. Cancer is a disease that knows no boundaries and does not discriminate against a specific ethnicity, skin color, gender, age, or social status; everyone is at risk!

Globally, cancer is the second leading cause of deaths, followed by heart diseases as the first cause. In 2015, cancer was responsible for 8.8 million deaths, which is approximately 1 in every 6[4]. Economically speaking, in 2010 the annual cost of cancer was estimated at $1.16 trillion dollars[4]. A more recent study has estimated 1,762,450 new cancer cases to arise in the US alone for 2019, from which 606,880 deaths will result, which is approximately a 35% death rate; in other words, 3 new cancer cases and 1 cancer death occurs every minute[5]. However, scientific research and new discoveries have given new hope for cancer patients. Currently, there are more

than 15.5 million American cancer survivors. These Americans have been victorious in their battle against cancer due to new screening methods, early diagnosis, and cancer treatments that have been discovered due to cancer research around the world[6].

2.2 Cell Penetrating Peptides and Essential Modifications for Effective Cellular Uptake and Delivery

The concept of using proteins for medical practices started with the approval of human insulin for diabetes treatment, back in 1980s[7]. Since then, proteins, peptides, and oligonucleotides have been investigated as potential therapeutic agents. These agents are usually highly specific and easier to advance to clinical trial than chemical drugs. A major drawback of these agents is their low membrane permeability due to hydrophilic properties, which becomes a major challenge when it comes to cross the blood-brain barrier and penetrate tissues throughout the body[7]. Opportunities to overcome these challenges were possible after identifying cell penetrating peptides with translocation capacities, in other words, peptides capable to cross tissues and cell membranes while transporting payloads[8-9]. In 2001, there were more than 10 FDA approvals for peptide therapeutics that emerged and entered the market[10], which shows the increase level of interest gained globally for this area of research.

Studies have demonstrated that structural properties of peptides as well as their interactions with membrane phospholipids play a major role in cellular uptake mechanism[11]. In 2010, Eiriksdottir et al. analyzed the structure and ability to interact with lipid layers of 10 well-known CPPs. Here, it was demonstrated that peptides that formed helix groups were able to insert spontaneously into lipid monolayer, which suggests spontaneous insertion into biological membranes[11]. Most CPP consist of cationic domains, which was considered to be essential for cellular penetrations. However, studies have demonstrated that amphiphilicity seemed to play a

bigger role in cellular entry than positive charge domains[11-12]. It is important to mention that a single point mutation and/or deletion of a single amino acid in a peptide chain could alter the amphipathic domain and weaken cellular uptake properties.

A major challenge faced when using peptides as drug delivery systems is their lack of specificity, and it has also been suggested that CPP internalization is limited to only a few cell types due to specific lipid composition required by peptides for penetration[7-8]. For this reason, the idea of using a secondary nanocarrier has been investigated to overcome these challenges. In 2017, Smith T. et al. developed a nanocarrier combining a peptide and polymer[13]. This peptide was an overlapped sequence containing two fragments, a nuclear localization signal peptide (NLS) and a microtube-associated sequence peptide (MTAS): *GRYLTQETNKVETYKEQ*<u>*PLKTPGKKKKGKP*</u>GKRKEQEKKKRRTR, (italicized=NLS and underlined=MTAS)[13]. In this study, this MTAS-NLS peptide containing 44 amino acids was used to synthesize nanoparticles coated with polyglutamic acid (PGA) containing a poly(β-amino ester) (PBAE) polymer and DNA to form a nanoparticle. For higher specificity, a targeting ligand was attached to the PGA coating layer, and in this study the nanocarrier was effective in carrying and introducing DNA into T cell nuclei[13].

Here, we report the design and synthesis of a modified MTAS-NLS which could be optimal for cellular uptake. After compiling information that is knows to be essential for cellular penetration by peptides, a series of substitution of one amino acid was conducted and a predicted structure was generated for each modified sequence. After selecting a modified peptide based from structure predictions, peptide was synthesized, characterized, and cell experiments were conducted to demonstrate enhanced cellular uptake.

3. Structure prediction for modified MTAS-NLS peptide

PEP-FOLD[14], a server designed to predict peptide structures from amino acid sequences, was utilized to generate a prediction for each modified peptide sequence. PEP-FOLD3, an updated on-line based program, was run for each peptide sequence shown below Table 4.

Original MTAS-NLS sequence:	
GRYLTQETNKVE**T**YKEQPLK**T**PGKKKKGKPGKRKEQEKKKRRTR	
Amino acids replacing T	Peptide sequence
Ala	GRYLTQETNKVE**A**YKEQPLK**A**PGKKKKGKPGKRKEQEKKKRRTR
Pro	GRYLTQETNKVE**P**YKEQPLK**P**PGKKKKGKPGKRKEQEKKKRRTR
Phe	GRYLTQETNKVE**F**YKEQPLK**F**PGKKKKGKPGKRKEQEKKKRRTR
Gln	GRYLTQETNKVE**Q**YKEQPLK**Q**PGKKKKGKPGKRKEQEKKKRRTR
Lys	GRYLTQETNKVE**K**YKEQPLK**K**PGKKKKGKPGKRKEQEKKKRRTR
Glu	GRYLTQETNKVE**E**YKEQPLK**E**PGKKKKGKPGKRKEQEKKKRRTR
Leu	GRYLTQETNKVE**L**YKEQPLK**L**PGKKKKGKPGKRKEQEKKKRRTR
Trp	GRYLTQETNKVE**W**YKEQPLK**W**PGKKKKGKPGKRKEQEKKKRRTR

Table 4. Modified peptide sequence after substitution of threonine (Thr) with another amino acid.

PEP-FOLD3 program is primarily used for linear peptides from 5 to 50 amino acids in length. For each analysis, the best model secondary structure prediction was obtained for all 7 amino acid sequences, shown in Figure 8. Based on this analysis, it was demonstrated that distinct structural changes where noticed after replacing a polar amino acid (T) at two different locations with various polar, nonpolar, or negatively charged amino acids (A, P, F, Q, K, E, L and W). Some of the predictions demonstrated distinct changes in how the peptide was folded, some of these included the formation of 3 α-helices, longer or shorter turns of α-helices, and the rotation in how the multiple helices face each other. The two predicted structures that gained attention were peptides substituted with Phe and Trp, where both of their α-helices were rotated to be almost parallel to each other, which could potentially facilitate direct cellular uptake as

demonstrated in previous studies[10-12]. Furthermore, on a well studied CPP, penetratin (peptide sequence: RQIKIWFQNRRMKWKK), studies have also demonstrated that tryptophan is an essential amino acid for cellular translocation and delivery of other small molecules[15]. The peptide sequence contains two W at position 6 and 14, and studies have demonstrated that while only W at position 14 is essential for cellular penetration, both are required for the transport and delivery of other bioactive molecules, such as shorter peptides or genetic materials[16]. Therefore, peptide sequence containing W was the selected peptide to be synthesized and studied.

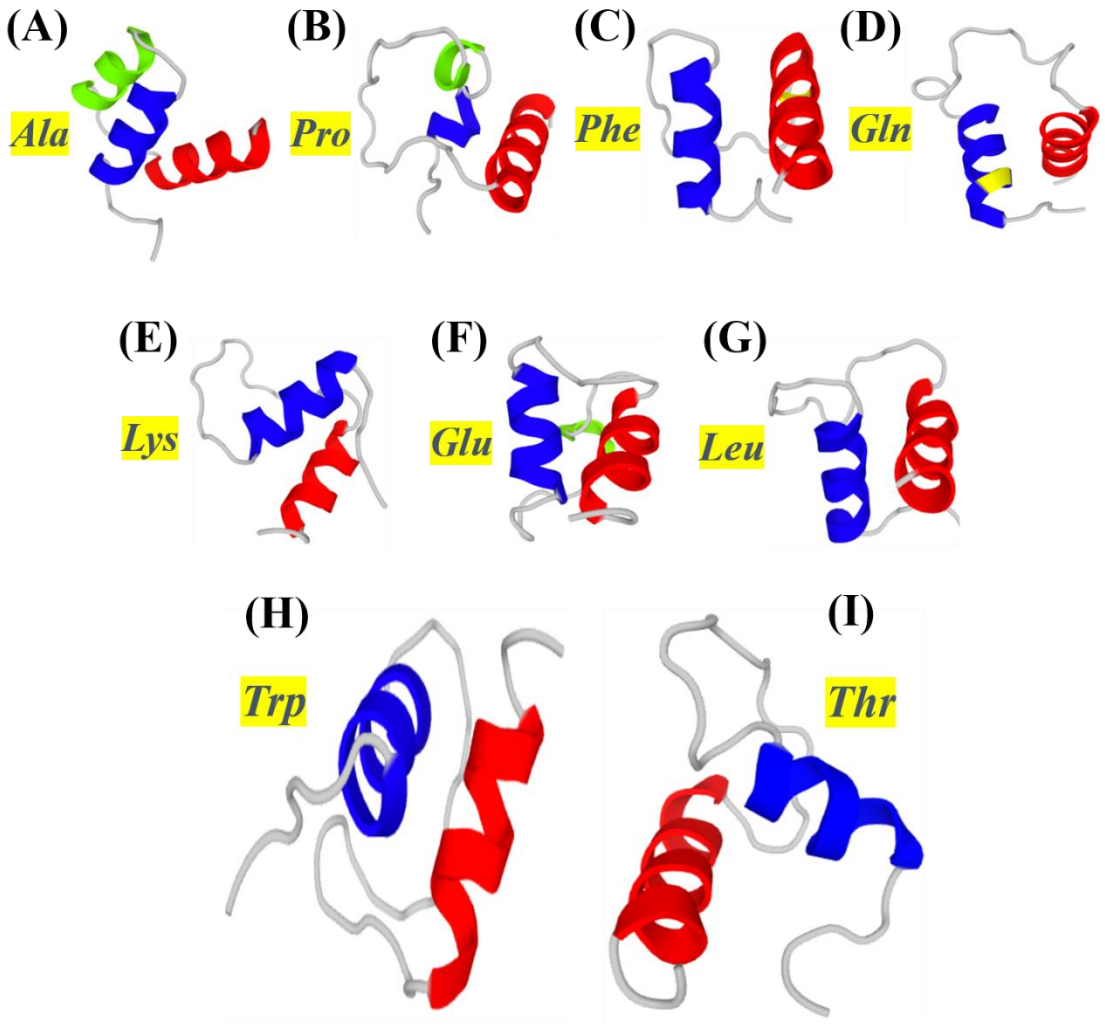

Figure 8. Structure predicted for original peptide MTAS-NLS (I) and after replacing Thr amino acid with (A)Ala, (B)Pro, (C)Phe, (D)Gln, (E)Lys, (F)Glu, (G)Leu, and (H)Trp.

4. Methodology

4.1 Solid Phase Peptide Synthesis

All peptides mentioned here (Table 5) were synthesized following the Fmoc (*N*-(9-fluorenyl)methoxycarbonyl) solid phase peptide synthesis procedure[17-18]. Briefly, a Wang or 2-ClTrt (2-chlorotrityl) resin containing the first amino acid is first swelled in dichloromethane (DCM) for 20 minutes and then washed with *N*,*N*-dimethylformamide (DMF) five times. After washing, a solution containing Fmoc-protected amino acid (resin:amino acid, 1:3 molar ratio) and O-Benzotriazole-N,N,N',N'-tetramethyl-uronium-hexafluoro-phosphate (HBTU) as a coupling agent (resin:HBTU, 1:29 molar ratio) dissolved in diisopropylethylamine (DIEA) and DMF was added to the resin and swirled for 30 minutes. Each amino acid was added two times to enhance addition of amino acid to the peptide chain. Before moving to the next amino acid, the last Fmoc-protected amino acid is deprotected using a 20% diethylamine solution and then washed with DMF to remove any excess diethylamine present. Each addition and deprotection of an amino acids is a cycle that is repeated until all amino acids on the peptide sequence are added. After synthesis was completed, peptides were labeled with rhodamine B, a fluorescent dye. Rhodamine B was added like another amino acid using HBTU and diisopropylethylamine, but the coupling reaction was left for 24 hours. After labeling the peptide with rhodamine B, peptide was then cleaved from the resin using trifluoroacetic acid, incubated for 3 hours and then precipitated and washed in cold ether. Peptide was then lyophilized overnight to remove any solvent.

Peptide Name	Peptide sequence
WTAS-NLS	GRYLTQETNKVEWYKEQPLKWPGKKKKGKPGKRKEQEKKKRRTR
NLS	GRYLTQETNKVETYKEQPLKTPGKKKKGK
WTAS	PLKWPGKKKKGKPGKRKEQEKKKRRTR
Polymer-based NLS	CGGPKKKRKVGG

Table 5. Peptide sequences for modified synthesized peptides.

4.2 WTAS Peptide Characterization

WTAS peptide was analyzed and purified by means of high performance liquid chromatography (HPLC – UltiMate 3000 by Thermo Scientific). Lyophilized peptide was dissolved in distilled water at a concentration of 3 mg/mL, and then filtered using 0.2 µM nylon filters. From this solution, 20 µL were injected into the HPLC column (Acclaim 300 from Thermo Fisher, 150 mm in length and 2.1 mm in diameter) to be analyzed. The solvent system used consisted of the following two solutions, A: water with 0.10% TFA and B: acetonitrile with 0.10% TFA. The gradient was run for 1-15 minutes with 5-80% solution B, and 15-20 minutes with 80% solution B. After identifying major product peak at 11.7 min, HPLC was repeated, and the major peak was collected in a separate vial. Collected peak was then re-injected to confirm purification of WTAS peptide.

A sample of WTAS peptide was sent to the University of Kansas for further mass spectrometry characterization by means of Matrix Assisted Laser Ionization Time-Of-Flight Mass Spectrometry (MALDI-TOF MS; Voyager DE STRT).

4.3 Cellular Uptake Experiments

Cellular uptake experiments were conducted for all four peptides synthesized, loading each peptide into six different types of cell lines. The six cell lines loaded with these peptides were: *i)* neural stem cells (NSC), *ii)* HeLa cells, *iii)* mouse glioma cells (GL26), *iv)* mouse melanoma cells (B16F10), *v)* mouse embryo fibroblast (STO), and *vi)* human lung carcinoma

(A549). All cell lines were seeded in a T-25 flask under the following media conditions: cell line *i)* was cultured in DMEM supplemented with 10% FBS, 5% horse serum, and 1% glutamine; cell lines *ii-iv*) were cultured in RPMI medium supplemented with 10% FBS; and cell lines *v-vi*) were cultured in DMEM supplemented with 10% FBS. After flask reached 70% confluency, cells were lifted with 0.1% trypsin-EDTA solution, re-plated in a 24-well plate with a density of 30,000/cm^2, and incubated overnight at 37°C. A solution with a concentration of 10 mg/mL was prepared for each of the 4 rhodamine B labeled peptides, separately, in sterile PBS (phosphate buffered saline solution), and these stock solutions were used to prepare the following concentration of peptides that were loaded into each cell line in duplicates: 70, 100, 150, 200 µM. After loading peptide solutions, cells were further incubated for 24 hours at 37°C. After incubation time with peptides, cells were washed with PBS three times, fixed with buffered neutral formalin (4% formaldehyde in phosphate buffered saline), and finally the cell nuclei were stained with Hoechst 33342 (1:1000 ratio of Hoechst:PBS) for 10 minutes. Cellular uptake was determined using a fluorescence microscope, where blue fluorescence corresponded to stained nucleus while red fluorescence corresponded to rhodamine B labeled peptides.

4.4 MTT Cell Proliferation Assay

Cytotoxicity of WTAS was assessed utilizing the MTT assay[19] on cell lines NSC, B16F10, and GL26. Cell culture conditions for these cell lines were the same ones described above. After reaching 70% confluency, cells were re-plated in a 96-well plate with a density 25,000/cm^2, and incubated overnight at 37°C. The following concentration series of WTAS were prepared in the same media used for the culture of each cell line: 0, 1, 2, 4, 6, 8, 10, 15, 25, 35, and 50 µM. Three replicates were prepared for each concentration plated. After incubating cells for 24 hours at 37°C, the peptide solution was removed from each well and replaced with a

solution containing 10 µL of MTT reagent (5 mg/mL in PBS) and 100 µL media, and plates where further incubated at 37°C for 4 hours. Then, 100 µL of 10% SDS in 0.01M HCl was added to each well and incubated overnight for 37°C. A plate reader was used to measure the absorbance at 550 nm and 690 nm to be used to calculate the cell proliferation percentage.

4.5 Confocal Imaging Experiments

Live and fixed confocal experiments were conducted using the Confocal Microscopy and Microfluorometry Core in the department of Anatomy and Physiology at Kansas State University. For these experiments, the confocal microscope used was Carl Zeiss 700, which consists of an inverted microscope with five objectives, 2.5x, 5x, 20x, and 40x (1.4 NA Oil), four lasers (blue-405 nm, cyan-488 nm, green-555 nm, and red-639 nm), two fluorescence emission detectors and one transmission detector[20].

B16F10 cells were plated in a glass bottom dish for confocal microscopy use with a density of 10,000/cm^2 and incubated overnight at 37°C. For fixed confocal imaging, cells were first loaded with 70 µM rhodamine B labeled peptide WTAS, incubated for 24 hours at 37°C, fixed with buffered neutral formalin (BFN) for 10 min, and then stained with Hoechst 33342 (1:1000 ratio of Hoechst:PBS) for 10 minutes. For live confocal imaging, B16F10 cells were plated in the same manner described above. After overnight incubation, cell nuclei were stained using Hoechst 33342 (1:500 ratio of Hoescth:RPMI) for 2 hours. After washing cells with PBS, they were loaded with 50 and 10 µM rhodamine B labeled peptide WTAS, separately, and images were captured immediately after.

SIM-A9 cells (mouse microglia cells), from Dr. Culbertson's lab, were also used for confocal imaging. Confocal experiments were semi-fixed, because these cells can grow both attached to the surface or floating in solution. In order to capture images of both attached and

suspended cells, 1 μM rhodamine B labeled peptide WTAS was directly added onto the same media used to re-plate cells and incubated overnight. After 24 hours incubation, cells were stained with Hoechst 33342 (1:200 ratio of Hoechst:DMEM F12 media) for 45 minutes. Very carefully, cells were washed and resuspended in PBS for imaging.

5. Results

5.1 WTAS Characterization and Peptide Structure Prediction

Rhodamine B labeled WTAS peptide was analyzed and purified by means of HPLC. Results indicated that a major product peak was present at around 11.7 min, with a few minor peaks as impurities. Major peak was then collected and re-analyzed to confirm successful purification of WTAS peptide (Figure 9).

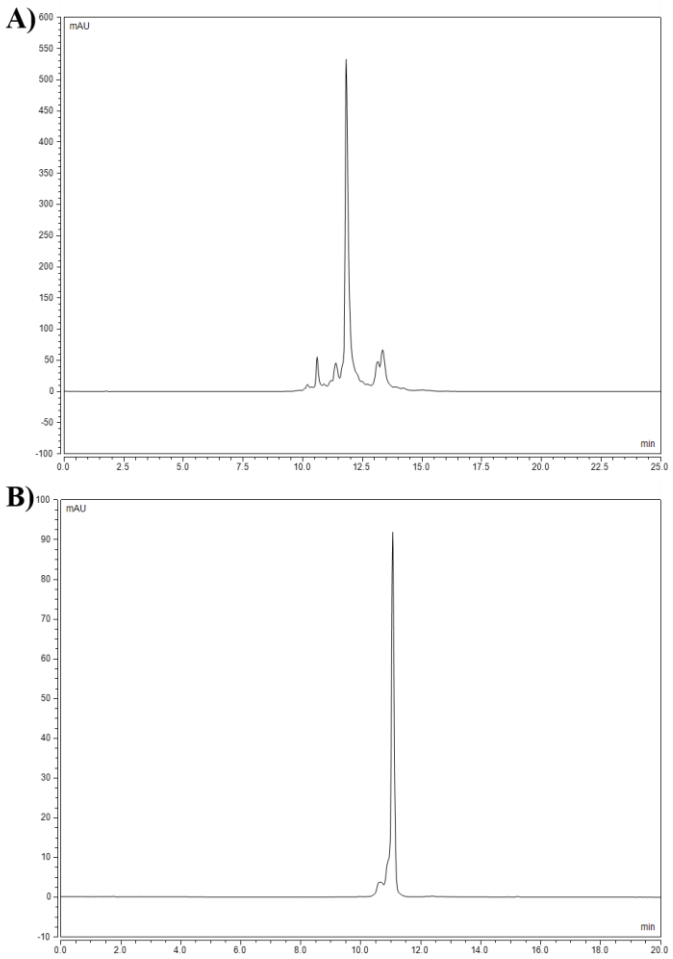

Figure 9. A) Crude and B) Purified rhodamine B labeled WTAS analyzed by HPLC.

WTAS labeled and unlabeled was also characterized by means of mass spectrometry. WTAS is relatively a long peptide sequence, and MS results identified shorter fragments of the peptide overlapping. For both labeled and unlabeled peptide, we were able to identify WTAS after assembling shorter fragments (Appendix A).

Peptide structure for WTAS peptide sequence alone was also predicted using PEP-FOLD software. Results demonstrated once again that after replacing Thr for Trp, the peptide is folded in half, forming like an "U" for random coil and one α-helix. This demonstrated that even for the truncated peptide sequence containing only WTAS part, distinct changes are notable.

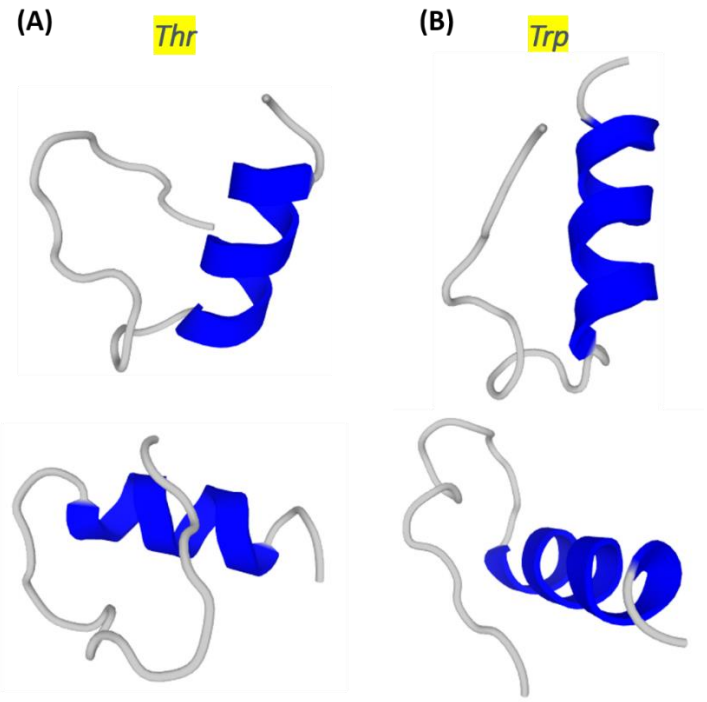

Figure 10. Predicted structure differences for MTAS and WTAS.

5.2 Cellular Uptake of WTAS peptide labeled with rhodamine B

Six cells lines, *i)* NSC, *ii)* HeLa, *iii)* GL26, *iv)* B16F10, *v)* STO, and *vi)* A549 were loaded with various concentrations of all four synthesized peptides, in order to determine cellular penetration after 24 hours. Fluorescent microscopy images indicated that all four peptides were successfully inserted in all six cell lines tested, for all concentrations loaded (images shown only for two cell lines, NSC and B16F10, at lowest peptide concentration of 80 μM, Figure 11). Cell morphology was affected for all cells tested with peptide 4 (polymer-based NLS), except for HeLa and B16F10 cells. These experiments demonstrated that cell penetration was more effective for peptide WTAS compared to the rest. These results also suggest possible penetration of cell nuclei, which will further be studied. Based on these results, WTAS peptide was the candidate selected to continue with further experiments.

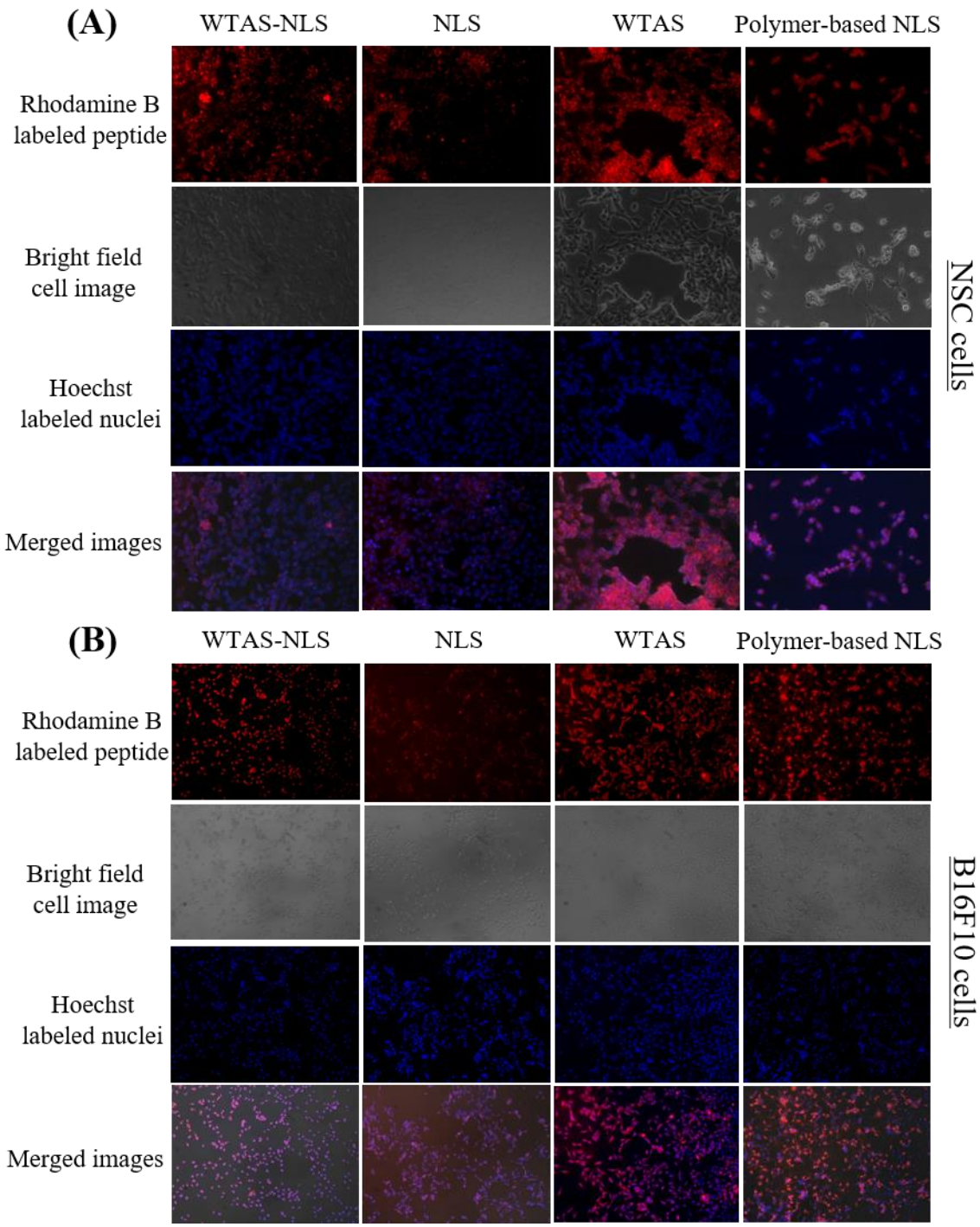

Figure 11. Fluorescent microscopy of NSC and B16F10 loaded with 70 μM of rhodamine B labeled peptides and cell nuclei stained with Hoechst.
(A) NSC cell line and (B) B16F10 cell line. For each section, showing rhodamine B labeled peptides inside of cells, bright field cell image, cell nuclei stained with Hoechst, and all 3 images merged in one.

5.3 Peptide Cytotoxicity

Cytotoxicity of WTAS peptide was determined by performing the classic MTT assay[19]. Cells were incubated with WTAS for 24 hours, and cell viability of three cell lines (NSC, B16F10, and GL26) was calculated. Results demonstrated that WTAS started to become slightly toxic to cells as the concentration was increased, and it was more noticeable on NSC compared to B16F10 and GL26. Toxicity levels were not very different when comparing WTAS unlabeled vs. WTAS labeled with rhodamine B. This data was processed using Graphpad Prism 5.0[21].

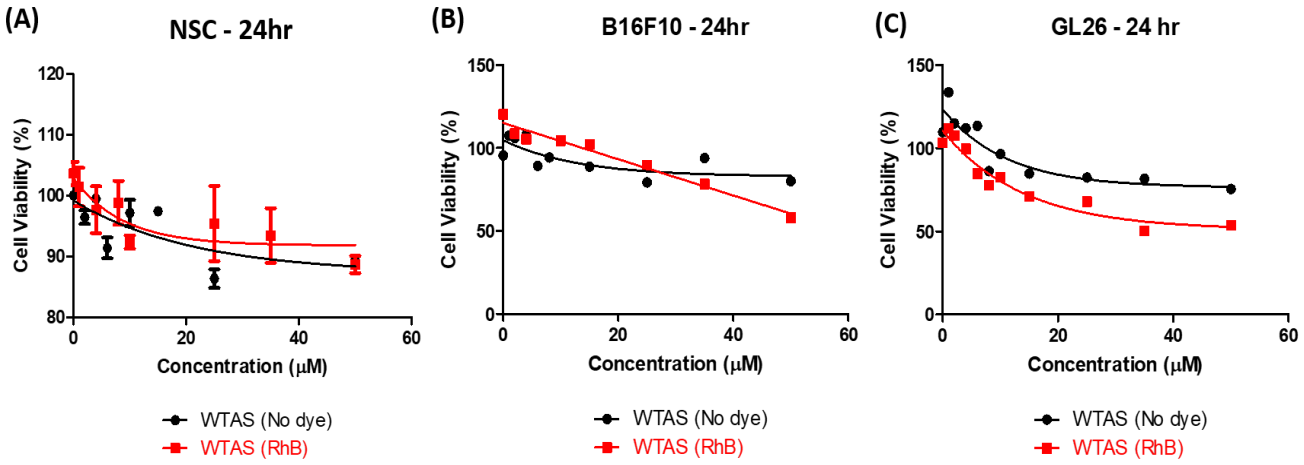

Figure 12. Cell viability percentage of (A) NSC, (B) B16F10, and (C) GL26.
Cells were incubated with WTAS for 24 hours at various concentrations ranging from 0 to 50 μM, measured by MTT assay.

5.4 Confocal Images Capture

In order to investigate possible penetration of WTAS peptide in cell nuclei, fixed and live confocal experiments were conducted using B16F10 cell line, which seemed to be the cell line to be better penetrated by WTAS peptide. For fixed confocal imaging, B16F10 cells were loaded with 70 μM of WTAS (red) in RPMI media and incubated overnight. Then, cells were fixed with BNF and nuclei were stained with Hoechst (blue). Focus stacking or 'Z-stacked' images (an

imaging method that combines multiple images taken at different focal distances) were captured to determine whether rhodamine B labeled WTAS was present in the cell nuclei or not. Results demonstrated that as the focal point remained focused on the nucleus (blue fluorescent signal), WTAS (red fluorescent signal) remained present, and as the focal point moved away from the nucleus, the red fluorescent signal started to disappear as well. These captured images confirmed the presence of WTAS peptide to be found primarily in the cell nuclei.

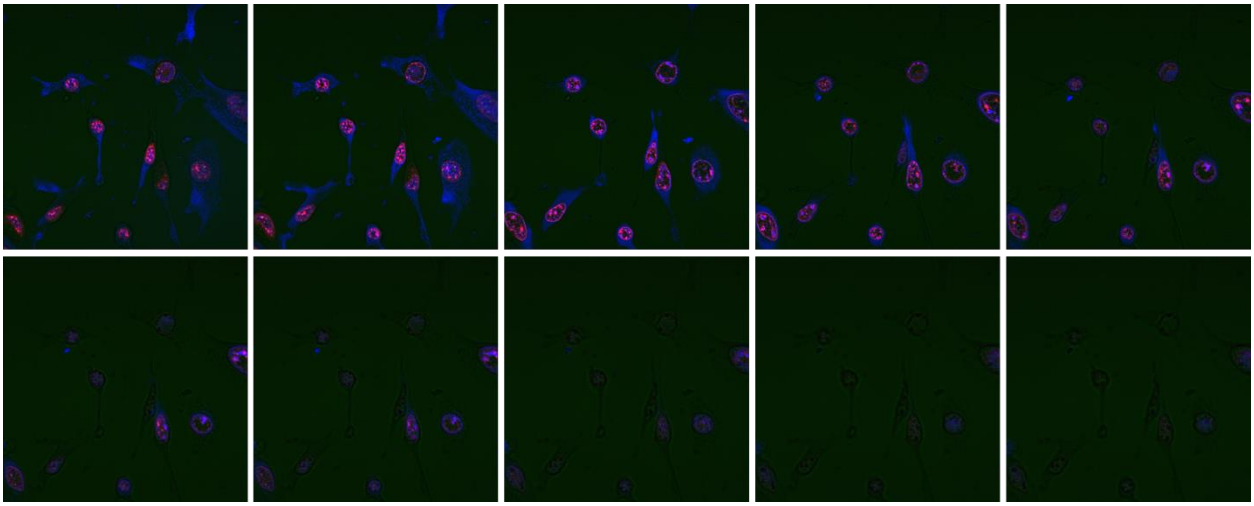

Figure 13. Z-stacked fixed confocal microscopy images of B16F10 cells after 24 hours incubation with rhodamine B labeled WTAS.
Blue corresponds to cell nuclei stained with Hoechst, and red corresponds to WTAS inside the cell. Images were captured with a focal point on cell nuclei and moving away from them.

Live confocal images were then captured. For this, cell nuclei were first stained, and later cells were loaded with 50 µM and 10 µM WTAS in RPMI, separately. Once the peptide solution was added to cells, images were captured immediately right after, every 30 seconds for 2 hours. Results demonstrated that WTAS was able to penetrate B16F10 cells immediately after coming into contact with them, and within 2 hours, WTAS had been taken up by most cells. These results also demonstrated how once WTAS is in the cell, it accumulates onto the nuclear cell membrane and then moves into the nucleus. This was repeated loading cells with 10 µM, and

results were similar, demonstrating that after 2 hours most cells had encapsulated WTAS peptide.

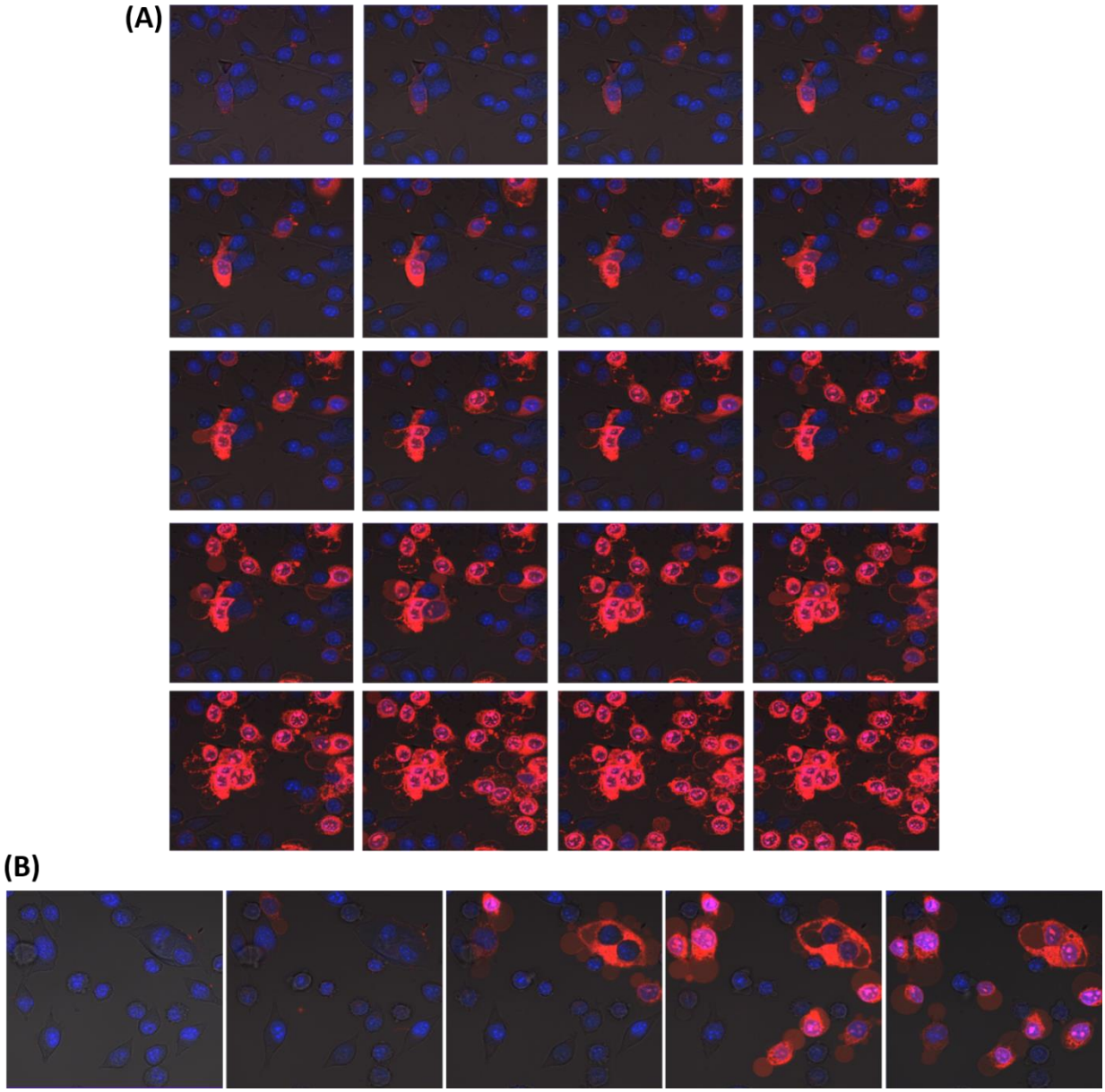

Figure 14. Live confocal microscopy images of B16F10 cells after 2 hours of incubation with WTAS at a concentration of (A)50 µM and (B)10 µM.
Blue corresponds to cell nuclei and red corresponds to WTAS inside the cell. Images were captured every 30 seconds for a total of 2 hours.

Semi-fixed confocal studies were also conducted on a second noncancerous cell line, SIM-A9. This relatively new cell line can grow in both manners, floating in solution or attached to the surface. To be able to capture images from cells floating and attached, cells were not fixed to avoid the excess washings. Cells were incubated with 1 µM rhodamine B labeled WTAS, and Z-stacked images were captured after staining cell nuclei with Hoechst. Results demonstrated that while WTAS still maintains the ability to penetrate this cell line, it cannot be further taken into the cell nuclei like it does on B16F10 cancerous line, which was observed on both attached and suspended cells.

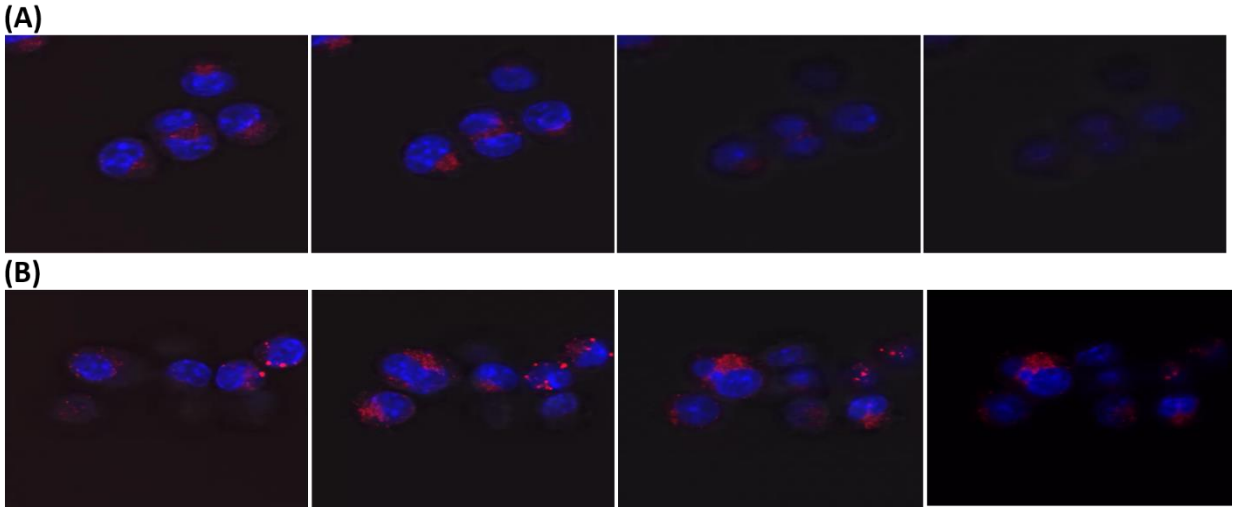

Figure 15. Z-stacked confocal microscopy images of SIM-A9 cells after 24 hours incubation with a 1µM concentration of WTAS.
(A) Cells attached to surface, (B) Cells suspended in solution. Blue corresponds to cell nuclei and red to WTAS peptide.

6. Conclusion

This second chapter describes the approach taken to design an optimized cell penetrating peptide by replacing a polar amino acid, Threonine (T), by an amphipathic nonpolar amino acid, Tryptophan (W). The substitution of this amino acid generated a peptide chain structure with two α-helices nearly parallel to each other for WTAS-NLS, and a less twisted/hindered structure for WTAS, which could play an important role in cell penetration. Four peptides were synthesized,

and after cell penetration studies, WTAS became the candidate peptide for further studies due to its better cell penetration properties. Cytotoxic studies demonstrated that WTAS toxicity in cells increases at higher concentrations. Live and fixed confocal studies demonstrated that WTAS is capable to only penetrate cells, but it can also reach the cell nuclei at low concentrations within a few minutes after exposure in B16F10 cell line. Confocal studies were also carried using a second cell line, this time noncancerous cells. Results demonstrated that WTAS was able to penetrate SIM-A9 cells, but it failed at penetrating the cell nuclei, for either cells attached to the bottom surface of the plate or cells suspended in solution. These results demonstrate that this peptide could be a promising as a component of a cancer specific drug delivery system, one which could reach the nucleus of cancerous cells only. More studies need to be conducted in order to determine if WTAS is truly cancer specific for cell nucleus penetration or if there are other factors in glioma cells which prevent the penetration of WTAS into the nucleus.

7. References

[1]http://www.dictionary.com/browse/cancer

[2]https://www.cancer.gov/about-cancer/understanding/what-is-cancer

[3]https://www.cancercenter.com/whats-the-difference-benign-and-malignant-tumors

[4]http://ww.who.int/news-room/fact-sheets/detail/cancer

[5]https://www.cancer.org/research/cancer-facts-statistics/all-cancer-facts-figures/cancer-facts-figures-2019.html

[6]Siegel R. L., Miller K. D., and Jemal A. Cancer Statistics, 2018. *A Cancer Jour for Clinic* **2018;**68(1):7-30.

[7]Guidotti G., Brambilla L., and Rossi D. Cell-Penetrating Peptides: From Basic Research to Clinics. *Trend in Pharmacological Sciences.* **2017**, 38(4):406-424.

[8]Raucher D. and Ryu J. S. Cell-Penetrating Peptides: Strategies for Anticancer Treatments. *Trends in Molecular Medicine.* **2015**, 21:560-570.

[9]Bechara C. and Sagan S. Cell-Penetrating Peptides: 20 years later, where do we stand? *FEBS Letters.* **2013**, 587:1693-102.

[10]Milletti, F. Cell-penetrating peptides: classes, origin, and current landscape. *Drug Discovery Today.* **2012**, 17(15/16):850-860.

[11]Eiriksdottir, E., Konate, K., Langel, U., Divita, G., and Deshaayes, S. Secondary structure of cell-penetrating peptides control membrane interaction and insertion. *Biochimica et Biophysica Acta.* **2010**, 1119-1128.

[12]Scheller, A., Oehlke, J., Wiesner, B., Dathe, M., Krause, E., Beyermann, M., Melzig, M., and Bienert, M. Structural requiremtns for cellular uptake of α-helical amphipathic peptides. *Journal of Peptide Science.* **1999**, 5:185-194.

[13]Smith T. T., Stephan S. B., Moffett H. F., McKnight L. E., Ji W., Reimann D., Bonagofski E., Wohlfahrt M. E., Pillai S. P. S., and Stephan M. T. *In Situ* Programming of Leukaemia-Specific T Cells Using Synthetic DNA Nanocarriers. *Nature Nanotechnology.* **2017**, 12(8):813-820.

[14]http://mobyle.rpbs.univ-paris-diderot.fr/cgi-bin/portal.py#forms::PEP-FOLD

[15]Dom, G., Shaw-Jackson, C., Matis, C., Bouffioux, O., Picard, J. J., Prochiantz, A., Mingeot-Leclercq, M-P., Brasseur, R., and Rezsohazy, R. Cellular uptake of antennapedia

penetratin peptides is a two-step process in which phase transfer precedes a tryptophan-dependent translocation. *Nucleic Acids Research.* **2003**, 31(2):556-561.

[16]Watson, G. M., Kulkarni, K., Brandt, R., Del Borgo, M. P., Aguilar, M-I., and Wilce, J. Shortened penetrating cell-penetrating peptide is insufficient for cytosolic delivery of a Grb7 targeting peptide. *ACS OMEGA.* **2017**, 2:670-677

[17]Wang H., Udukala D. N., Samarakoon T. N., Basel M. T., Kalita M., Abayaweera G., Manawadu H., Malalasekera A., Robinson C., Villanueva D., Maynez P., Bossmann L., Riedy E., Barriga J., Wang N., Li P., Higgins D. A., Zhu G., Troyer D. L., and Bossmann, S. H. Nanoplatforms for Highly Sensitive Fluorescence Detection of Cancer-Related Proteases. *Photochemistry & Photobiology Sciences.* **2014**, 13:231–240.

[18]Duro-Castano A., Conejos-Sanchez I., and Vicent M. Peptide-Based Polymer Therapeutics. *Polymers.* **2014**, 6(2):515-551.

[19]Stockert, J. C.; Blazquez-Castro, A.; Canete, M.; Horobin, R. W.; Villanueva, A., MTT assay for cell viability: Intracellular localization of the formazan product is in lipid droplets. *Acta Histochem.* **2012,** *114* (8), 785-796.

[20]https://www.k-state.edu/cobre/confocal_core/Confocal-Zeiss-700.html

[21]https://www.graphpad.com/support/prism-5-updates/

Chapter 3 - Combination of Anti-Cancer Peptide and Cell/Nucleus Penetration Peptide to Develop an Improved Therapeutic Peptide.

1. Abstract

Cancer is a disease divided into more than 200 different and unique types of cancer, where each type requires a different approach for treatment. Currently, most common cancer treatments are narrowed to surgery, chemotherapy, and/or radiation. With the help of cancer research and technology, new promising approaches for cancer treatment are being developed. For this study, we combined two unique peptides previously synthesized in our research group, an anti-cancer therapeutic peptide (SA-D-K_6L_9-AS), and a cell/nucleus penetrating peptide (WTAS). WTAS- SA-D-K_6L_9-AS was synthesized following the solid phase peptide synthesis procedure, and it was analyzed by HPLC and mass spectroscopy. Cytotoxicity effects of the new generated peptide were tested on B16F10 and GL26 cell lines, and results demonstrated that toxicity was not altered after addition of WTAS. Also, confocal studies were conducted to determine cellular uptake and confirm possible interaction of WTAS-SA-D-K_6L_9-AS with the mitochondria in the GL26 cell line. Lastly, cell experiments were conducted using a necrosis/apoptosis detection kit to determine the killing mechanism of cancerous cells used by the new synthesized peptide.

2.Background

2.1 Current Cancer Treatment Options

Cancer, as many other diseases, does not distinguish ethnicity, skin color, gender, age, or social status, it targets about everyone in both humans and animals. It is important to note that cancer is not only one disease, but it is broken into more than 200 different and unique types of cancer, where each type requires a different approach for treatment. This is one of the many challenges faced when trying to develop a cure for cancer. Currently, the most common treatments for cancer include: surgery, chemotherapy, and radiation. Surgery has been used for cancer for many years, and it is used to prevent, diagnose, stage, and treat cancer[1]. Preventive surgery is the removal of a body tissue or organ that could become cancerous; biopsy is the removal of a small piece of tissue which is then tested to determine the diagnosis; stage surgery is the procedure done to determine the stage of cancer and how far it has spread[1]. Surgery to treat cancer is the complete removal of a cancerous tumor in the body[1]. Surgery always comes with some risks, such as: excess bleeding, damage to other tissues/organs, reaction to drugs used during or after surgery, and not to mention pain, possible infections, and slow recovery after surgery. Another common treatment for cancer is chemotherapy, which is the use of drugs to treat cancer throughout the entire body, being effective at killing cancerous cells that have metastasized[1]. The major side effects for chemotherapy is the collateral damage these drugs cause to normal and healthy cells, which results in weakness of the immune system and consequent infections, anemia, as well as weight and hair loss and fertility problems[1]. Radiation therapy is another common treatment for cancer[1.] This treatment option involves the use of x-rays, gamma rays, implanted radioisotopes, electron beams, or proton beams to destroy or damage cancerous cells. Radiotherapy is often effective in shrinking early stage tumors[1].

However, radiation therapy does not reach all parts of the body, and the side effects include the risk of developing a second cancer as well as nausea, vomiting, diarrhea, and weight loss, etc. For many years, these have been the only options for cancer treatment. Fortunately, due to cancer research, newer treatment modalities have arisen, for example: *i)* targeted therapy, which differentiates between normal and cancer cells and attacks the latter in a targeted manner, *ii)* immunotherapy, which recruits immune system components to fight cancer cells, and *iii)* stem cell transplants, which replace cells destroyed by cancer or chemotherapy with immature blood cells[1]. Even though newer techniques for cancer treatments have been developed, major scientific discoveries at the molecular level are opening the door for more effective and promising cancer treatments.

2.2 Development of SA-D-K6L9-AS Therapeutic Peptide

Cancer research around the world has improved both cancer detection and treatments, like development of therapeutic peptides. K_6L_9 (LKLLKKLLKKLLKLL) was originally an antibacterial peptide originally designed to kill bacteria[3]. This sequence was composed of six polar lysine and nine hydrophobic leucine, in order to develop a peptide featuring both positive charge and hydrophobic segments, with both being ideal components to facilitate interaction with negatively charged bacterial cell envelopes[3-4]. Later, this peptide was modified into D-K_6L_9 by replacing some L-amino acids with D-amino acids (italics/underlined) as shown in this peptide sequence LK*L*LK*K*L*LK*KLL*K*LL, which was aimed to protect the early degradation of this peptide by proteases like trypsin or proteinase K. D-K_6L_9 resulted in a more effective antibacterial peptide against 4 gram-positive and 4 gram-negative bacteria[5]. This peptide became popular for possible cancer approaches, after discovering that D-K_6L_9 was not a bacterial targeting peptide only, but it rather targeted the plasma membrane[5]. D-K_6L_9 was a peptide with

positive charge residues that targeted the plasma membrane, which was ideal to be used to target negative surface charge of most cancerous cells, as we know now.

Multiple studies have demonstrated D-K_6L_9 to be successful at killing cancerous cells in prostate, breast, and pancreatic cancer cell lines[6]. However, results have demonstrated that D-K_6L_9 does not only target cancerous cells but is equally toxic to healthy cells. With the goal of developing an improved therapeutic peptide, a previous graduate student in our group, Jing Yu, developed a modified version of D-K_6L_9 by adding two amino acids (serine and alanine) to both C- and N- terminal sides of the peptide, generating SA-D-K_6L_9-AS (SALK*L*LK*K*L*LK*KLL*K*LLAS). This modification was aimed to enhance solubility of peptide in aqueous buffers and increase toxicity. The 3D structure of SA-D-K_6L_9-AS was determined, and MTT assays demonstrated that SA-D-K_6L_9-AS had a higher toxicity than D-K_6L_9, with LC50 values being 5-10 times lower for SA-D-K_6L_9-AS. Also, it was demonstrated that SA-D-K_6L_9-AS peptide interacted with the cell membrane to then be internalized into the cytoplasm and localized in the mitochondria within a few minutes[7]. Unfortunately, just like with D-K_6L_9, SA-D-K_6L_9-AS is equally toxic to both healthy and cancerous cells, which indicates the need of a secondary nanocarrier that could be cancer cell target specific.

For our next approach, we wanted to combine this therapeutic peptide, SA-D-K_6L_9-AS, with the modified cell/nuclear penetrating peptide described in chapter 1 to possibly generate an improved and targeting therapeutic peptide.

3. Methodology

3.1 Solid Phase Peptide Synthesis and Characterization

WTAS-SA-D-K_6L_9-AS was synthesized by means of solid phase peptide synthesis, which is fully described in Chapter 2,[8-9] using a 2-ClTrt resin containing Arg amino acid. The

sequence for this peptide consisted of WTAS and then continued synthesizing D-SA-K_6L_9-AS as follows, from N- to C- terminus (resin in bold):

SALK*L*LK*K*L*LK*KLL*K*LLASPLKWPGKKKKGKPGKRKEQEKKKRRT**R**. After completing synthesis of this peptide, rhodamine B was coupled to the *N*-terminal serine (S) on the sequence, following the peptide coupling procedure, and incubating for 24 hours. After cleaving peptide from resin, it was analyzed by HPLC (UltiMate 3000 by Thermo Scientific) and mass spectroscopy (Appendix B).

3.2 MTT Cell Proliferation Assay

Cytotoxic effects of WTAS-SA-D-K_6L_9-AS and SA-D-K_6L_9-AS peptides were determined and compared on GL26 and B16F10 cell lines utilizing the MTT assay[10]. For this, both cell lines use the same cell culture media, RPMI supplemented with 10% FBS serum. Once 70% confluency was reached, cells were re-plated in a 96-well plate with a density of 25,000/cm^2 and incubated overnight at 37°C. Cells where then incubated for 24 or 48 hours with the following concentration series of WTAS-SA-D-K_6L_9-AS prepared in same media used for culture: 0, 2, 4, 6, 8, 10, 15, 25, 35, and 50 µM. Three replicates were prepared for each concentration tested. After incubation, peptide solution was replaced with 10 µL of MTT reagent (5 mg/mL in PBS) and 100 µL media for each well, and plates where then incubated at 37°C for 4 hours. Then, 100 µL of 10% SDS in 0.01M HCl was added to each well, and cells were incubated overnight for 37°C. Absorbance was measured at 550 and 690 nm using a plate reader, and cell proliferation percentages were then calculated.

3.3 Live Confocal Imaging for Cellular Uptake and Mitochondria Co-Staining

Live confocal imaging was used to determine cellular uptake of WTAS-SA-D-K_6L_9-AS. For this, GL26 cells were re-plated at a density of 10,000/cm^2 and incubated overnight at 37°C.

After overnight incubation, cell nuclei were stained with Hoechst 33342 (1:200 ratio of Hoechst:RPM) and then loaded with 5 μM rhodamine B labeled peptide WTAS-SA-D-K_6L_9-AS. Images were captured right after the peptide solution was added.

In order to determine if WTAS-SA-D-K_6L_9-AS has a similar ability to SA-D-K_6L_9-AS of targeting the mitochondria, MitoTracker Green FM (λ_{ex} = 490 nm, λ_{em} = 516 nm; from Invitrogen by Thermo Fischer Scientific)[11] was used to stain the mitochondria in GL26 cells, and cells were then loaded with WTAS-SA-D-K_6L_9-AS labeled with rhodamine B. For live confocal experiments, GL26 were re-plated in a 35 mm glass bottom dish (MatTek Corporation) at a density of 10,000/cm^2 and incubated overnight at 37°C. Cells were treated with 100 nM of MitoTracker Green FM for 35 minutes (using growth media and conditions), and then washed with PBS to remove any excess stain. A solution of 5 μM rhodamine B labeled peptide WTAS-SA-D-K_6L_9-AS was prepared in culture media and loaded to GL26 cells. Images were captured immediately after the peptide solution had been added.

3.4 Necrosis and Apoptosis Assay

Necrosis vs. apoptosis kit assay (Biotium) was utilized to determine and differentiate if cells killed by WTAS-SA-D-K_6L_9-AS die through necrosis (premature death of cells) or apoptosis (programmed cell death). This kit contains 4 components: Annexin V binding buffer, CF®488A Annexin V (λ_{ex} = 490 nm, λ_{em} = 515 nm, detection stain for apoptotic cells), ethidium homodimer III (λ_{ex} = 522 nm, λ_{em} = 593 nm, detection stain for necrotic cells), and Hoechst 33342 (λ_{ex} = 350 nm, λ_{em} = 461 nm, detection stain for heathy cells)[12]. This kit differentiates between necrotic and apoptotic cells in the following manner: for apoptotic cells, phosphatidylserine is transferred from the inner to the outer side of the plasma membrane for it to be recognized to trigger phagocytosis. Annexin V is a high affinity binding protein for

phosphatidylserine, so once this protein is exposed on the cell surface, apoptotic cells will be stained with green fluorescence. On the other side, necrotic cells result in the loss of both organelles and plasma membranes into the surrounding environment. Ethidium homodimer III is a nucleic acid probe with a high positive charge, which makes it impermeable to either live or early apoptotic cells and will only stain necrotic cells with red fluorescence[12]. For this experiment, GL26 cells were re-plated in a 96-well black wall/clear bottom plate at a density of 30,000/cm^2 and incubated overnight at 37°C. Cell were treated with 5 µM of unlabeled WTAS-SA-D-K_6L_9-AS peptide prepared in cell culture media, and incubated for 3 hours at 37°C. Then, cells were washed with PBS, stained for 15 minutes with 5 µL of each necrosis/apoptosis/healthy reagent solution kit mixed in annexin V binding buffer, and finally washed and covered with annexin V binding buffer. A fluorescence microscope was utilized to capture images and identify healthy, necrotic, and apoptotic cells.

4. Results

4.1 Characterization of WTAS-SA-D-K_6L_9-AS

Rhodamine B labeled WTAS-SA-D-K_6L_9-AS peptide was analyzed and purified by means of HPLC. Results indicated that a major product peak was present at around 12.4 min, with a couple minor peaks as impurities on the surrounding areas. The major peak was then collected and re-analyzed to confirm successful purification of WTAS-SA-D-K_6L_9-AS peptide (Figure 16).

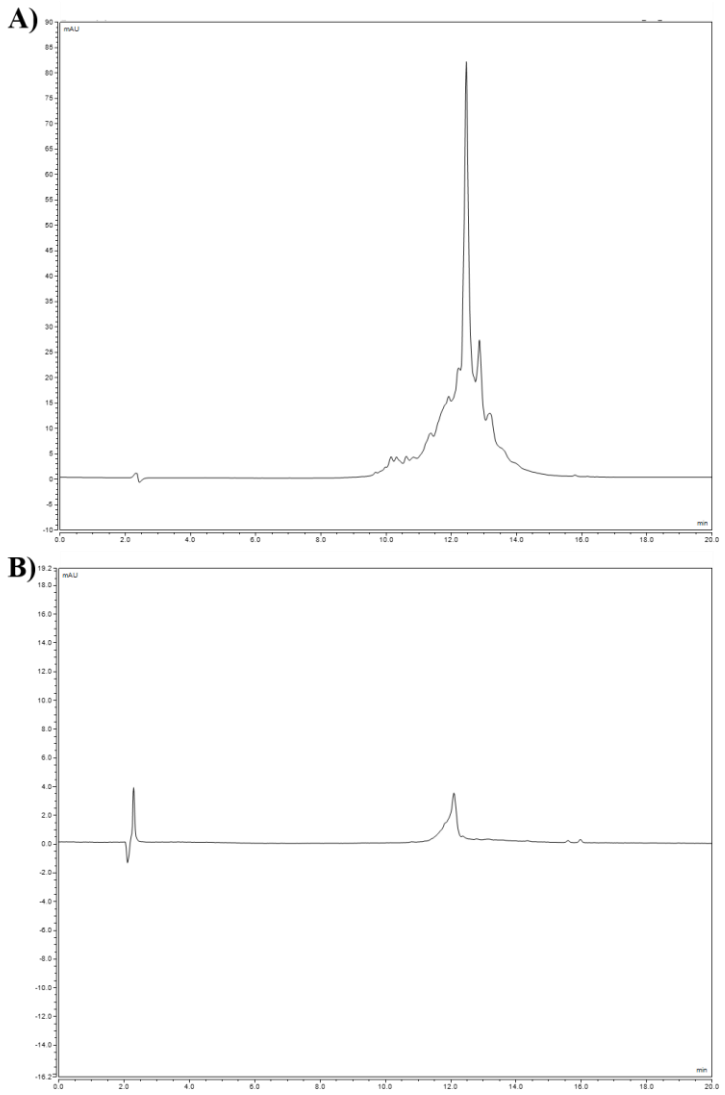

Figure 16. A) Crude and B) Purified rhodamine B labeled WTAS-SA-D-K_6L_9-AS analyzed by HPLC.

4.2 WTAS-SA-D-K_6L_9-AS Peptide Cytotoxicity

Cytotoxic effects of WTAS-SA-D-K_6L_9-AS and SA-K_6L_9-AS peptide were determined on B16F10 and GL26 cell lines, which was performed following the MTT assay[10]. For this experiment, cytotoxicity was tested for both 24- and 48-hour incubation time, separately. Results demonstrated that both peptides were equally toxic on both cell lines, meaning that toxicity of SA-D-K_6L_9-AS was not affected after adding WTAS, even though WTAS alone was relatively

nontoxic. Toxicity of both peptides was tested for both 24 and 48 hours, and toxicity remained similar for both incubation times for GL26 cells, but for B16F10, toxicity seemed to decrease slightly for WTAS-SA-D-K_6L_9-AS labeled and unlabeled peptides but remained similar for SA-D-K_6L_9-AS. Data was processed using Graphpad Prism 5.0 program[13].

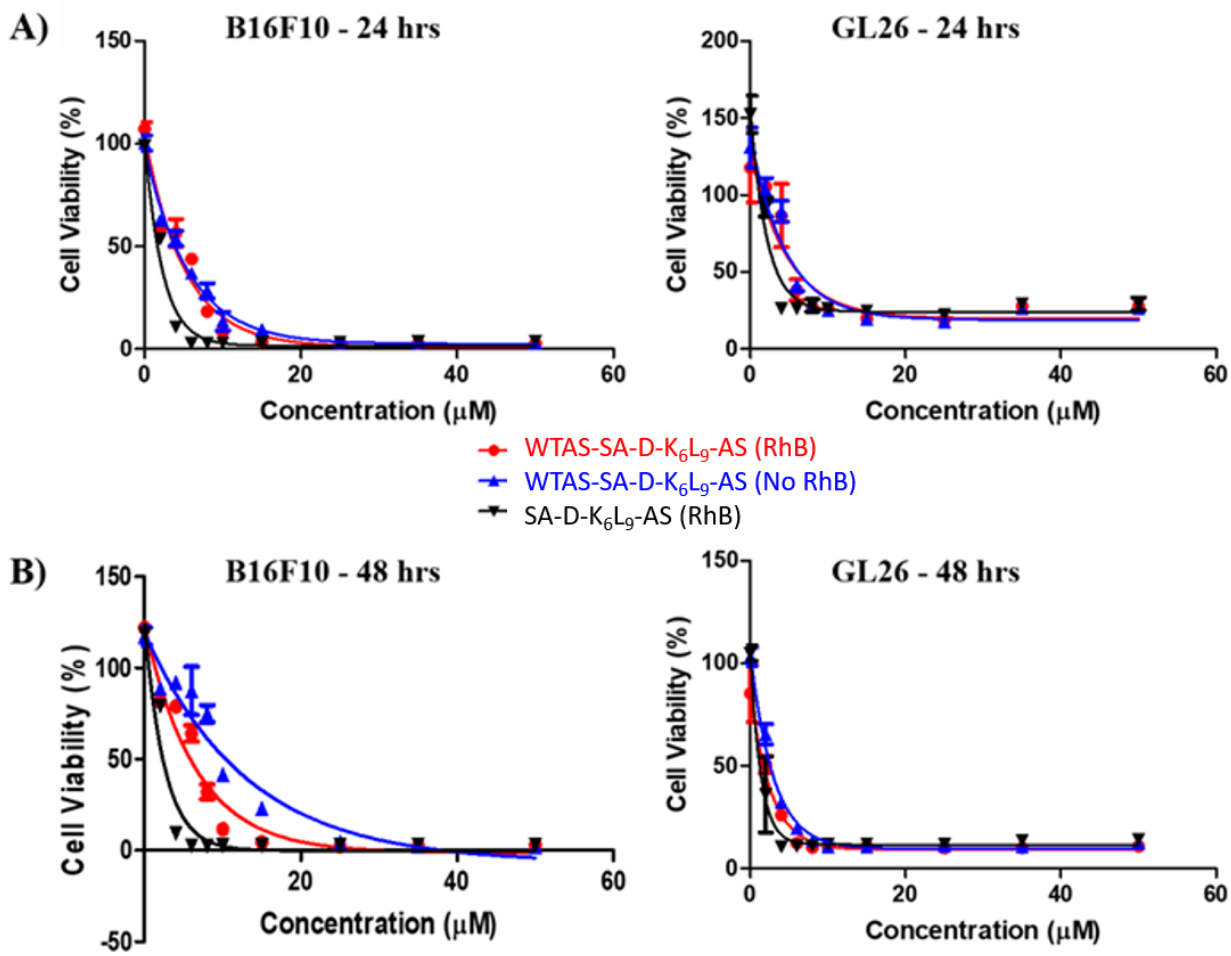

Figure 17. Cell viability percentages for B16F10 and GL26 incubated with WTAS-SA-D-K_6L_9-AS and SA-D-K_6L_9-AS peptides for both A) 24 hours and B) 48 hours.

4.3 Live Confocal Images for Cellular Uptake and Mitochondria Co-Stained.

Live confocal experiments were conducted to determine cellular uptake and confirm if WTAS-SA-D-K_6L_9-AS peptide had the ability to target the mitochondria in GL26 cells, just like SA-D-K_6L_9-AS peptide did. For cellular uptake, after staining the nuclei of GL26 cells with Hoechst and loading them with 5 μM rhodamine B-labeled WTAS-SA-D-K_6L_9-AS peptide,

images were captured for 2 hours every 30 seconds. Results demonstrated that WTAS-SA-D-K_6L_9-AS was taken up by the cell immediately after being loaded, and it was able to get into the cytosol as well as the nucleus.

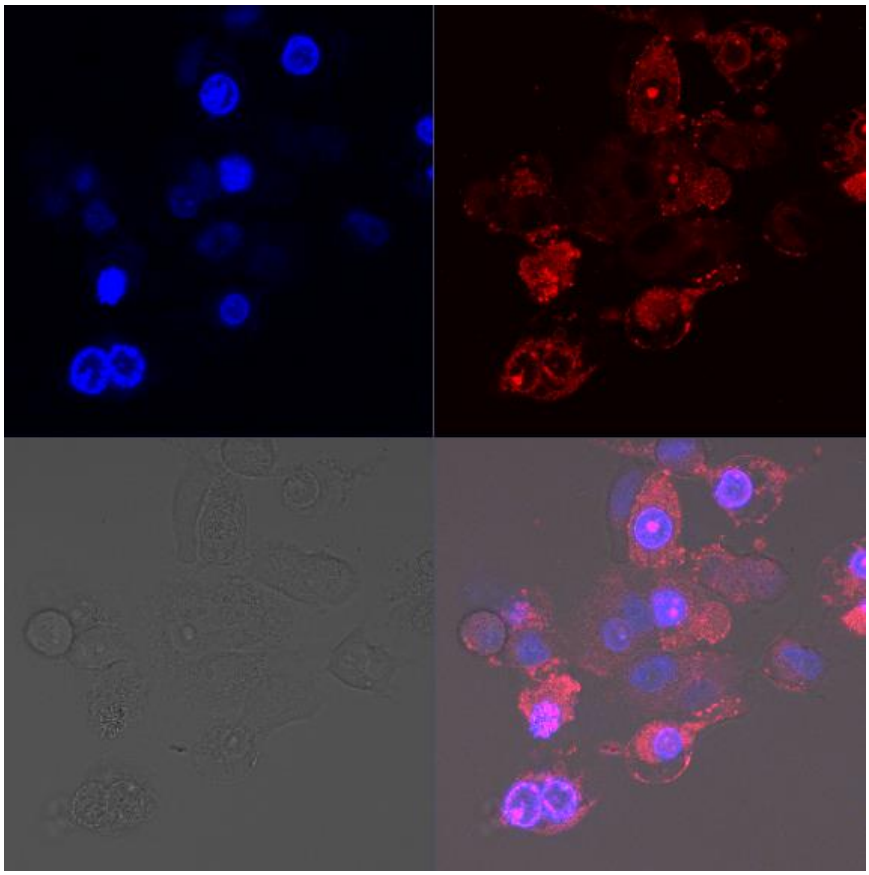

Figure 18. Live confocal images demonstrating uptake of rhodamine B labeled WTAS-SA-D-K_6L_9-AS peptide by GL26 cells.
Blue corresponds to cell nuclei stained with Hoechst, and red corresponds to WTAS-SA-D-K_6L_9-AS inside GL26 cell.

To determine possible targeting of mitochondria, re-plating GL26, MitroTracker Green FM was used to stain the mitochondria in cells and then loaded with 5 µM rhodamine B-labeled WTAS-SA-D-K_6L_9-AS peptide. Images were captured every 60 seconds for 2 hours immediately right after, and result confirmed that indeed WTAS-SA-D-K_6L_9-AS peptide remained the capacity to target the mitochondria in these cells. Images demonstrate that red fluorescence

corresponding to WTAS-SA-D-K_6L_9-AS peptide overlapped with the green fluorescence corresponding to MitroTracker Green FM.

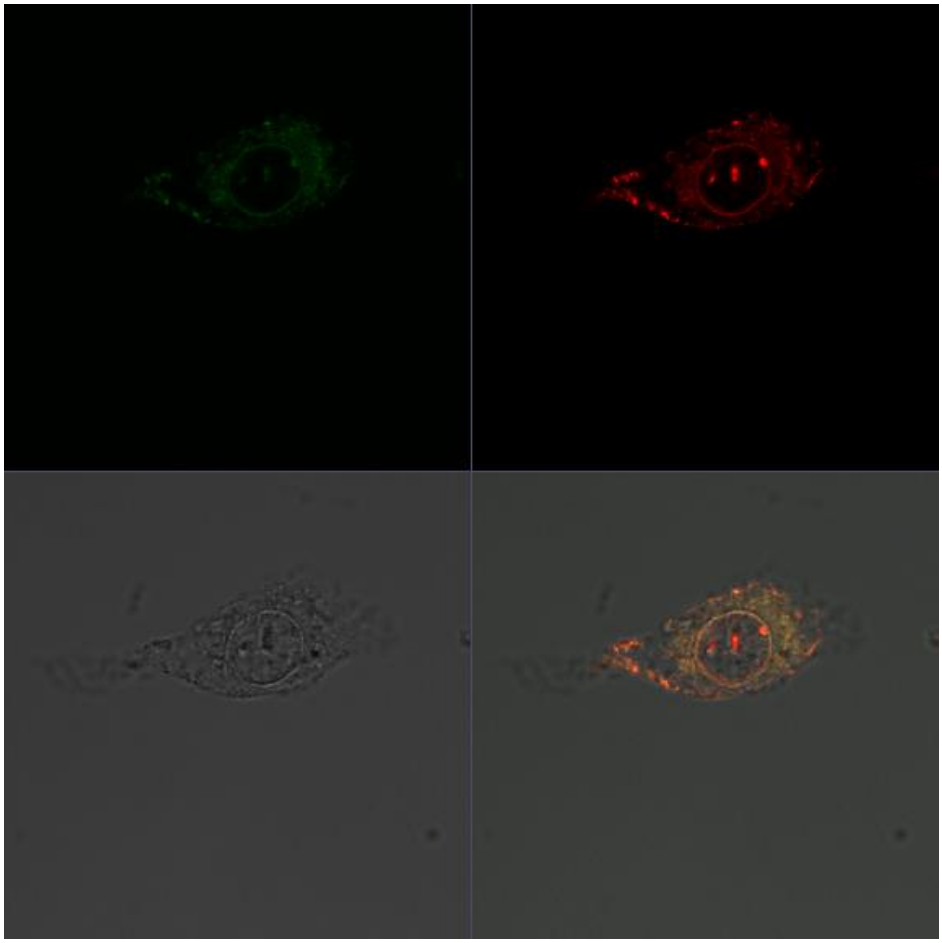

Figure 19. Confocal microscopy images of GL26 stained with MitroTracker Green FM and loaded 5 µM of rhodamine B labeled WTAS-SA-D-SA-K_6L_9-AS peptide.
Green corresponds to mitochondria stained in GL26 cells, and red corresponds to WTAS-SA-D-K_6L_9-AS inside cells.

4.4 Necrosis vs. Apoptosis Results

The killing mechanism used by WTAS-SA-D-K_6L_9-AS was determined after using a necrosis/apoptosis kit to differentiate between necrotic, apoptotic, and healthy cells. Cells were exposed to 5 µM of unlabeled WTAS-SA-D-K_6L_9-AS peptide for only 3 hours, and cells were then stained with each reagent in the kit to distinguish between necrotic, apoptotic, and healthy cells. Results demonstrated that on control wells, cells which were not exposed to WTAS-SA-D-

K_6L_9-AS peptide, only healthy cells were stained and present in the well. With cells that had been exposed to 5 μM of unlabeled WTAS-SA-D-K_6L_9-AS peptide, results demonstrated that a lower number of healthy cells had been identified, while now there were a large number of necrotic cells, but no apoptotic cells identified. These results confirm that WTAS-SA-D-K_6L_9-AS peptide kills GL26 cells by necrosis pathway. This finding is surprising, because cell peptides that kill exclusively via the necrotic pathway are rare. SA-D-K_6L_9-AS kills via apoptosis (major pathway) and necrosis (minor pathway). It is our hypothesis that necrosis occurs due to interference of WTAS-SA-D-K_6L_9-AS with the enzymatic machinery of the nucleus as the mitochondria is not specifically targeted by WTAS-SA-D-K_6L_9-AS, as this peptide targets the mitochondria but is also localized everywhere else in the cytoplasm and nucleus of cells.

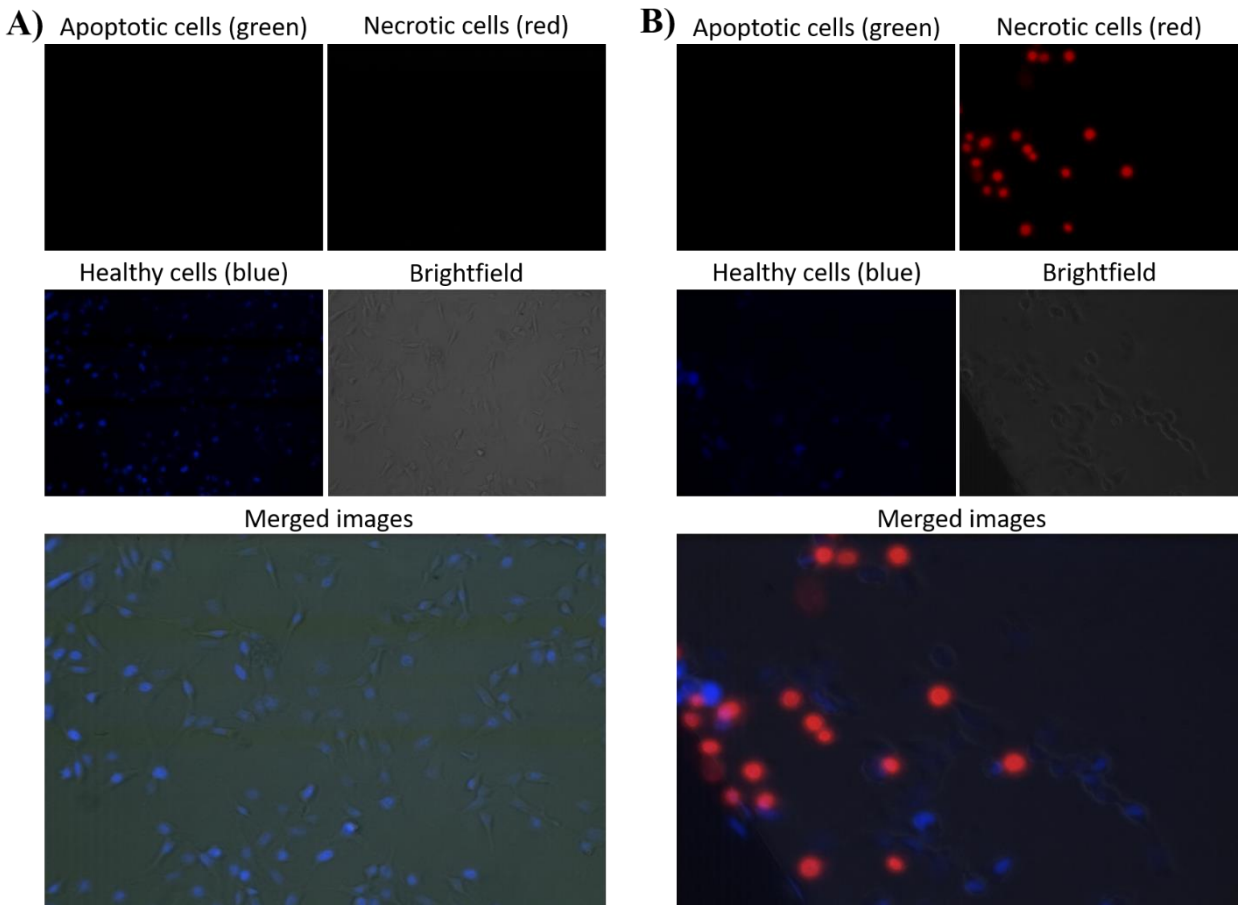

Figure 20. Mechanism used by WTAS-SA-D-K_6L_9-AS to kill GL26 cells, either by necrosis or apoptosis pathways.
A) Control cells, not treated with peptide, showed only healthy cells present (blue). B) Cells exposed to WTAS-SA-D-K_6L_9-AS, showed both healthy (blue) and necrotic (red) cells present.

5. Conclusion

This second chapter describes the development of a therapeutic peptide by combining two unique peptides previously synthesized in our lab. Here, WTAS was synthesized, and SA-D-K_6L_9-AS was further grown into the peptide chain to generated WTAS-SA-D-K_6L_9-AS, which was characterized and analyzed by both HPLC and mass spec. Cytotoxic studies demonstrated that toxicity levels remained similar to those of SA-D-K_6L_9-AS alone, which indicated that they were not affected by the addition of WTAS, which is a relatively nontoxic peptide. Live confocal

experiments demonstrated that WTAS-SA-D-K_6L_9-AS peptide targeted the mitochondria after being internalized into the cytosol of GL26 cells, which demonstrated similar mechanism used by SA-D-K_6L_9-AS alone to enter and kill cells. Lastly, fluorescent microscopy experiments determined that WTAS-SA-D-K_6L_9-AS kills GL26 cells via necrosis pathway only.

6. Reference

[1]http://www.cancer.org/treatment/treatmentsandsideeffects/treatmenttypes/

[2]https://www.macmillan.org.uk/information-and-support/understanding-cancer/cancer-and-cell-types.html

[3]Silhavy, T. J.; Kahne, D.; and Walker, S. The bacterial cell envelope. *Cold Spring Harb Perspect Biol.* **2010,** 2(5): a000414.

[4]Papo, N.; Oren, Z.; Pag, U.; Sahl, H.-G.; and Shai, Y. The consequence of sequence alteration of an amphipathic alpha-helical antimicrobial peptide and its diastereomers. *J. Biol. Chem.* **2002,** 277(37):33913-33921.

[5]Braunstein, A.; Papo, N.; and Shai, Y., In vitro activity and potency of an intravenously injected antimicrobial peptide and its DL amino acid analog in mice infected with bacteria. *Antimic agents and chem.* **2004,** 48(8): 3127-3129.

[6]Papo, N.; Seger, D.; Makovitzki, A.; Kalchenko, V.; Eshhar, Z.; Degani, H.; and Shai, Y., Inhibition of tumor growth and elimination of multiple metastases in human prostate and breast xenografts by systemic inoculation of a host defense–like lytic peptide. *Cancer research.* **2006,** 66(10): 5371-5378.

[7]Yu, J., and Bossmann, S. H. *Structure determination, mechanistic study, and safe delivery of an anti-cancer peptide* (Doctoral dissertation thesis). **2018**.

[8]Wang H., Udukala D. N., Samarakoon T. N., Basel M. T., Kalita M., Abayaweera G., Manawadu H., Malalasekera A., Robinson C., Villanueva D., Maynez P., Bossmann L., Riedy E., Barriga J., Wang N., Li P., Higgins D. A., Zhu G., Troyer D. L., and Bossmann, S. H. Nanoplatforms for Highly Sensitive Fluorescence Detection of Cancer-Related Proteases. *Photochem & Photobio Sciences.* **2014**, 13:231–240.

[9]Duro-Castano A., Conejos-Sanchez I., and Vicent M. Peptide-Based Polymer Therapeutics. *Polymers.* **2014**, 6(2):515-551.

[10]Stockert, J. C.; Blazquez-Castro, A.; Canete, M.; Horobin, R. W.; Villanueva, A., MTT assay for cell viability: Intracellular localization of the formazan product is in lipid droplets. *Acta Histochem.* **2012,** *114* (8), 785-796.

[11]Presley, A. D.; Fuller, K. M.; Arriaga, E. A., MitoTracker Green labeling of mitochondrial proteins and their subsequent analysis by capillary electrophoresis with laser-induced fluorescence detection. *J. Chromatogr. B: Anal. Technol. Biomed. Life Sci.* **2003,** 793(1), 141-150.

[12]https://biotium.com/product/apoptotic-necrotic-healthy-cells-quantitation-kit-plus/

[13]Stockert, J. C.; Blazquez-Castro, A.; Canete, M.; Horobin, R. W.; Villanueva, A., MTT assay for cell viability: Intracellular localization of the formazan product is in lipid droplets. *Acta Histochem.* **2012,** *114* (8), 785-796.

Chapter 4 - Development of Novel Gene Delivery System Composed of Two Nanocarriers: A Cell Penetrating Peptide (WTAS) and a Nontoxic Polymer (PBAE)

1. Abstract

Major concerns have arisen due to the approach of using viral vectors for gene therapies, which include cancer resistance, development of new cancers, and even systemic deaths. For this reason, researchers have focused on the alternative of using a nonviral gene delivery for gene therapy approaches. In this study, a novel gene delivery nanocarrier has been developed, composed of a cell penetrating peptide called WTAS as a primary nanocarrier and a poly(β-amino ester) (PBAE) polymer as a secondary nanocarrier. PBAE polymer has been widely studied as an alternative vehicle for gene delivery, which has become a hot research topic due to its biodegradable and nontoxic properties. Here, PBAE polymer is used to protect WTAS peptide from an early degradation while further facilitating the transportation into cells. WTAS is a peptide that has been demonstrated to penetrate cell nuclei within a few minutes after exposure, which makes it an ideal candidate to transport genetic materials into the nucleus of cells. PBAE-WTAS nanocarrier was assembled, and cytotoxic studies demonstrated low toxicity against three cell lines (SIM-A9, B16F10, and GL26). Cell transfection experiments were carried using GL26 cells, and these studies demonstrated a successful transfection rate of PBAE-WTAS loaded with GFP pDNA. This study describes a promising gene delivery nanocarrier, which could be further modified to transport a variety of genetic materials as well as being target specific, which could be used to target multiple diseases such as bacterial infections and viruses, not only cancer based.

2. Background

2.1 Gene Delivery Therapy

Most diseases, including cancer, are caused due to a specific genetic or epigenetic mutation, which can be inherited or triggered by environmental factors. Novel therapeutic strategies for many diseases have emerged through understanding this paradigm along with considerable advancements in genomics and discoveries at the molecular level. Cancer gene therapy is a technique intended to modify, delete, or replace any mutated genes that causes a disease, for instance cancer in this case[1]. Gene therapy implies an approach of inserting genetic materials, such as DNA (deoxyribonucleic acid) or RNA (ribonucleic acid), into the nucleus of cells to alter the genetic instructions in cells to be effective against mutated genes that cause a disease, like cancer[2]. This approach comes with a major drawback, not only because "naked DNA" and RNA are very unstable, but also because of the difficulty to transport them inside the body while protecting early degradation before reaching the targeted area. For this reason, pharmaceutical and therapeutic research have focused on finding suitable nanocarriers to fight multiple diseases.

2.2 Multiple Nanocarriers used for Gene Delivery Approaches

There is a critical need of a more effective treatment for cancer, one that would have a lower cost and could lead to less side effects for patients. Important drugs against cancer, as well as promising gene therapeutic agents, have been discovered in laboratories worldwide, but these cancer therapeutic candidates have not made it to the clinic due to the lack of a drug delivery system that could protect, transport, and manage the release of these drugs into specific targets in the body without damaging other organs[3]. Due to this need, a wide variety of potential gene

therapy delivery nanocarriers have been investigated, which include viruses, liposomes, and polymers.

In the middle 1950s, physicians discovered signs of improvement in cancer patients that had recently been vaccinated or suffered from a viral infection[4]. From here, oncolytic virotherapy became the new idea to combat cancer disease. Oncolytic virotherapy uses the approach of replicating competent viruses to select, lyse, and destroy only cancerous cells[4]. Specifically, the mechanism of destruction of cancerous cells by oncolytic viruses is broken into two main mechanisms: killing host cells in tumors directly and triggering host's immune response to attack infected tissues. The first mechanism was supported by a recent study that demonstrated the effectiveness of an oncolytic herpes simplex virus-1 that was engineered to kill glioma tumor cells[5]. The second one has been supported by multiple studies that have observed a rapid immune response taking place upon viral infection to fight and remove viruses from the body[6]. Even though more than 50% of gene therapies that are underway in clinical trials use viral vectors, concerns have arisen due to intrinsic safety risks, such as cancer resistance, the development of new cancers, and even systemic deaths caused by this approach[7]. Due to these concerns, nonviral gene delivery approaches have been developed and investigated[6-7].

An alternative and common nonviral nanocarrier for drug delivery are liposomes[8]. Liposomes are phospholipid vesicles consisting of lipid bilayers that have the ability to encapsulate and transport different payloads, including both hydrophobic and hydrophilic drugs; this is a promising alternative to virus delivery system because they also are non-toxic, biocompatible, and biodegradable[8]. The unique ability to encapsulate both hydrophobic and hydrophilic molecules is achieved by the insertion of hydrophobic molecules into the bilayer membrane and encapsulation of hydrophilic molecules in the aqueous center of liposomes. Even

though liposomes are the most common used nonviral delivery system, the challenges faced by this approach include poor selectivity, low percent delivery, and tedious and expensive processes methods used for liposome preparation[9]. Aiming to develop a novel drug delivery system, other nonviral vectors like polymers have emerged as an alternative approach[10].

The application of polymers includes: drug delivery systems, tissue engineering, implantation of devices and artificial organs, prosthesis, dentistry, and bone repair, among others[10]. For their application in drug delivery systems, polymers are often a backbone of the drug delivery system that protects the drug from degradation, improves the drug's stability, and controls its release rate once the desired part of the body is reached. Diffusion, degradation, and swelling are the three mechanisms by which drug is released from a polymer[11]. Diffusion takes place when the drug is diffused through pores from the polymer matrix into the surrounding environment. Degradation occurs when a polymer is degraded in the body and exposes the drug into the reached area; biodegradable polymers are ideal drug delivery system because there is not a need to be removed from the body after releasing the drug. Lastly, when a drug delivery device is desiccated, swelling occurs once the dry device is in contact and absorbs water or any other body fluid and swells. By swelling, it enables the drug to diffuse through the swollen areas into the surroundings[11]. Polymers can be assembled as spheres, loading payloads on the polymer matrix or polyplex, that is self-assembling based on opposite charges from polymer and payload, as well as capsules, loading payloads in the inner aqueous core or on the surface. Different types of synthesized polymers have been effective nanocarriers of multiple payloads, including chemically synthesized drugs, and genetic material like DNA and siRNA (short-interference RNA)[12]. Examples of synthesized polymers include cyclodextrin, poly(lactic-co-glycolic acid), chitosan, polyethylenimine, poly-L-lysine, and the promising poly(β-amino ester) [12].

2.3 PBAE Polymer

Poly(β-amino ester), PBAE, was first developed in 2000 by David Lynn and Robert Langer[13]. Since then, this polymer has gained interest for gene delivery due to its biodegradability under physiological conditions, reduced toxicity with a half-life of only a few hours, ability to trigger DNA release within cells, and its structural diversity potentials[13-15]. These polymers can be synthesized to have primary, secondary, or tertiary amines and cleavable ester bonds. These characteristics are important to determine their function; for example, it has been demonstrated that amines are able to bind to anionic DNA and enable endocytosis, while polymer degradation occurs through ester linkages[14]. With the purpose of identifying the best PBAE polymer, a variety of monomers with modification on the backbone, side chains, and end-capped groups have been synthesized and studied[15]. A study demonstrated that the polymer structure is essential for gene delivery, especially any modification on the end-capped group is crucial for cellular uptake and transfection[15]. Here, end-capped groups containing secondary amines resulted in enhanced cellular uptake and transfection, while secondary and tertiary amines can buffer the acidification inside of endosomes to elongate the polymer degradation, so they can be released from the endosome[15]. Surprisingly, this study demonstrated that particle size, charge, and molecular weight did not have major effects on either uptake and transfection[15]. In another study, the same end-capping group was used to synthesize a PBAE polymer, and then self-assembled with DNA to be tested in human glioblastoma cells. Here, it was demonstrated that nanocarrier successfully transfected brain tumor cells with high specificity, which shows the potential this polymer could have to cross the blood brain barrier[16]. PBAE polymers have gained interest as a new hope against cancer to be used as a nanocarrier.

3. Methodology

3.1 PBAE Polymer Synthesis

PBAE polymer was synthesized following a two-step reaction synthesis via a Michael addition by conjugating amines and acrylates[15]. For the first step of this reaction, 1,4-butanediol diacrylate was reacted with 3-amino-1-propanol using a 1.15:1 ratio for both reactants respectively. Reaction was heated and refluxed at 90°C for 24 hours. In order to determine optimal capping reaction conditions, cysteine (10% per mass weight) was used as a temporary end-capping reagent, so that sulfur could be measured using inductively coupled plasma mass spectrometry (ICP-MS, which is used to detect metals at very low concentrations[17]). Once sulfur was quantified and reaction conditions optimized, the second-step or end-capping reaction proceeded. For this reaction, tris(2-aminoethyl)amine (10% per mass weight) was reacted with polymer (step 1 final product) for 2 hours at room temperature using tetrahydrofuran (THF). After the two hours, capped polymer was precipitated and washed in cold ether (5 equivalents of cold ether per 1 equivalent of capped polymer reaction solution). After multiple washings, product was dried under high vacuum for 2 days to remove any solvent present. These two-step reaction schemes are summarized in Figure 21.

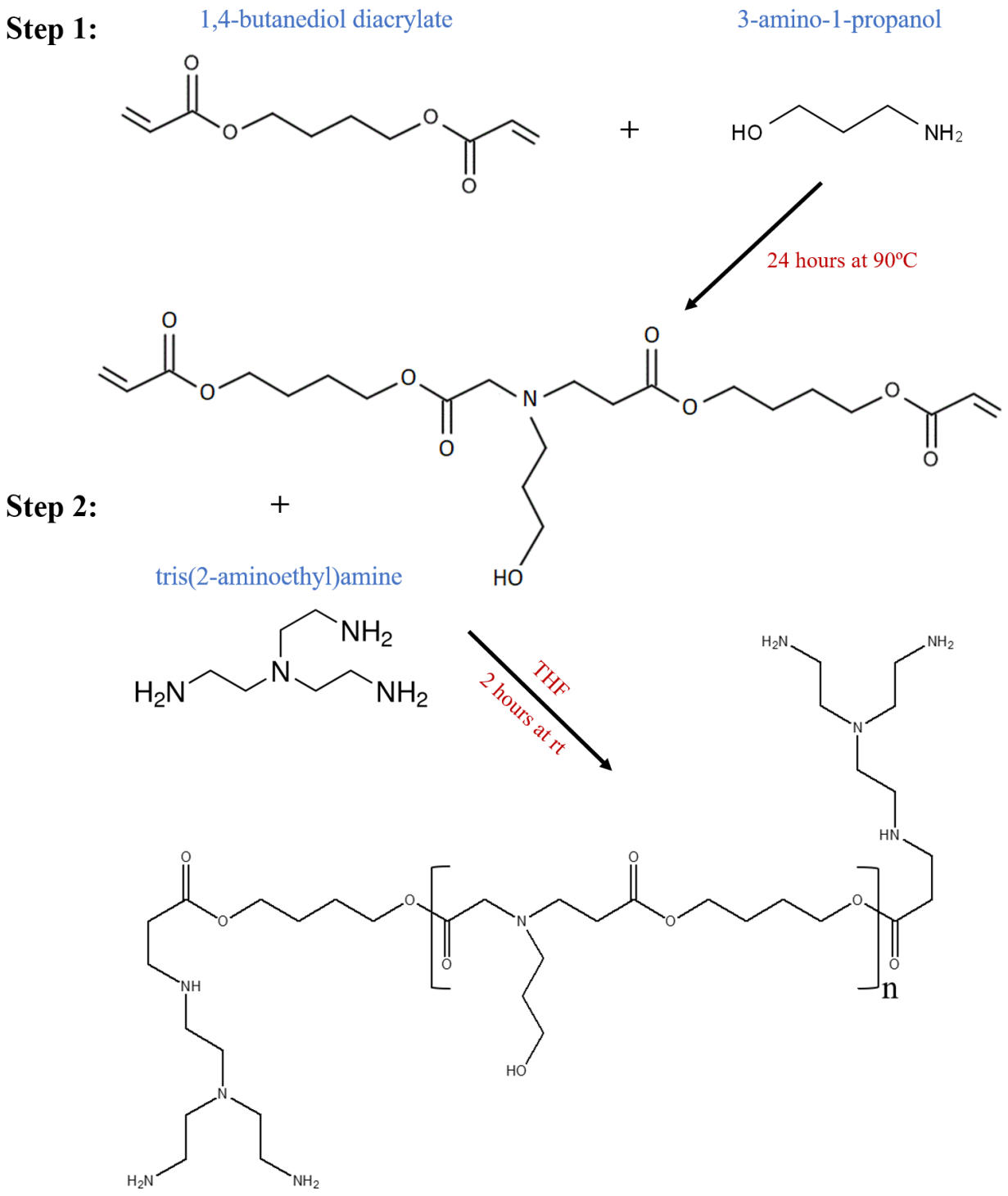

Figure 21. Scheme for the two-step reaction synthesis of the PBAE polymer.

3.2 Characterization of Synthesized PBAE Polymer

After each reaction synthesis, all intermediates and final products were characterized by ^{1}H-, ^{13}C- NMR, and mass spectrometry (MS) (see Appendix C). In order to determine optimal reaction conditions for end-capping reaction, ICP-MS was used to quantify the sulfur (S) present after capping PBAE with cysteine as a temporary end-cap. Once final product was synthesized and capped, the Dynamic Light Scattering (DLS) and zeta potential surface charge were measured using the instrument ZetaPALS, Brookhaven Instruments Corp., Holtsville, NY.

3.3 Assembly of Nanocarrier PBAE-WTAS

One equivalent of PBAE polymer, 4 equivalents of rhodamine B-labeled WTAS peptide, and 4 equivalents of EDC (*N*-ethyl-*N*'-(3-dimethylaminopropyl)carbodiimide hydrochloride) and DMAP (4-dimethylaminopyridine) were dissolved and stirred in deoxygenated PBS buffer (pH 7.4) for 48 hours under argon atmosphere. After 48 hours, product was purified by dialysis using a membrane tubing with a molecular weight cut off of 3500 Da, against distilled water, until all unreacted peptide was washed off. Final product collected from the membrane bag was lyophilized. (Figure 22)

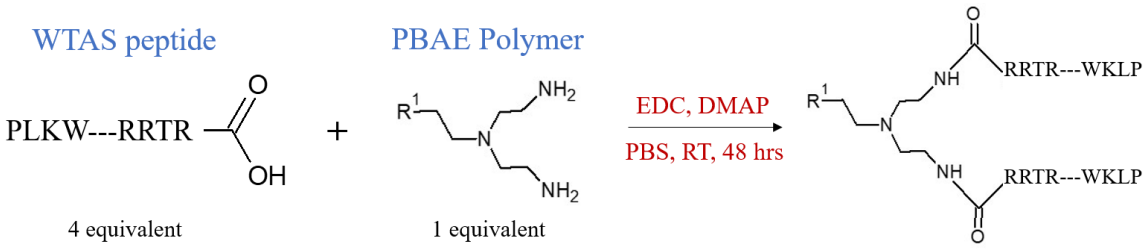

Figure 22. Scheme for assembly of nanocarrier containing PBAE polymer and WTAS peptide.
R^1 represents the remaining chain length and end-capped groups of PBAE polymer.

3.4 MTT Cell Proliferation Assay

Cytotoxicity of PBAE alone as well as the nanocarrier assembled with WTAS was assessed utilizing the MTT cell proliferation assay[18]. Cell lines used for this assay were SIM-A9 (noncancerous microglia cells), B16F10 (mouse melanoma cells), and GL26 (mouse glioma cells). SIM-A9 cells were seeded in a T-75 flask and cultured in DMEM-F12 supplemented with 10% FBS heat inactivated, 5% horse serum heat inactivated, and 1% penicillin-streptomycin. B16F10 and GL26 were seeded in a T-25 flask and cultured in RPMI medium supplemented with 10% FBS. After cells had reached a 70% confluency, they were re-plated in a 96-well plate with a density of 30,000/cm^2 and incubated overnight at 37°C. Concentration series of polymer alone (PBAE) and nanocarrier assembled (PBAE-WTAS) (0, 0.001, 0.01, 0.02, 0.04, 0.08, 0.1, 0.2, 0.4, 0.8, and 1 mg/mL) were prepared by dissolving each component in the same media required for each cell line. Cell were incubated with each component solution for 24 hours at 37°C. After this, cells were washed with PBS, 10 µL of MTT reagent (5 mg/mL in PBS) mixed with 100 µL media were added to each well and further incubated at 37°C for 4 hours. Finally, 100 µL of 10% SDS in 0.01M HCl was added and plates were incubated overnight for 37°C. Absorbance at 550 nm and 690 nm was quantified using a plate reader, and cell proliferation percentages were calculated.

3.5 Transfection Experiments

3.5.1 Optimizing conditions for positive charge nanocarrier

Surface charge plays an important role in cellular uptake[20], and for this reason zeta potential was measured over time after loading PBAE-WTAS with a plasmid DNA bioengineered to express the green fluorescent protein (GFP), which was synthesized in Dr. Troyer's lab. Two concentrations of PBAE-WTAS (0.2 and 0.6 mg/mL) were incubated with

500 ng of GFP pDNA for a total of 3 ½ hours, and zeta potential readings were collected after 1, 2, 3, and 3 ½ hours of incubation. This experiment narrowed down the window of concentrations and incubation times to use during the cellular experiments.

3.5.2 Cellular transfection experiments

Transfection experiments were conducted using GL26 cell line, because PBAE-WTAS showed a lower cytotoxicity for these cells compared to the others. After reaching a 70% confluency, GL26 were re-plated in a 48-wells plate at a density of 25,000/cm^2 and incubated overnight at 37°C. A concentration of 0.5 mg/mL of PBAE-WTAS was prepared using RPMI supplemented with 5% FBS serum. In a small 1.5 mL conical vial, 800 ng GPF pDNA were mixed with 0.5 mg/mL of PBAE-WTAS nanocarrier and incubated for 30 minutes at room temperature. After 30 min, cells were then loaded with media solution containing nanocarrier and DNA, and cells were incubated for 30 hours at 37°C. Then, new media (RPMI supplemented with 10% FBS) was added to cells, and a fluorescence microscope was used to check for transfection for the following 24, 48, and 72 hours.

4. Results

4.1 PBAE Polymer Characterization

All intermediates and final PBAE products were characterized by NMR (1H- and 13C-) and MS, which are found in Appendix C. In order to determine optimal reaction conditions for end-capping reaction, sulfur was measured after using cysteine as a temporary capping reagent. The highest yield of sulfur quantified by ICP-MS present in the intermediate product corresponded to polymer with reactants ratio of 1.15:1, and for the reaction conditions using 10% cysteine (per weight) dissolved in THF and reacted for 2 hours at room temperature. Based on these ICP-MS results (Table 6), these reaction conditions were utilized to capped PBAE with

tris(2-aminoethyl)amine. After synthesizing final PBAE polymer, DLS and zeta potential were measured using the ZetaPALS instrument. DLS showed an average diameter of 1635.9 nm and a zeta potential of 7.12 mV, which based on the charge and large size, possible aggregation of polymer is suggested. Therefore, diameter was further analyzed using the Malvern Panalytical NanoSight LM10 instrument, to obtain a more accurate diameter size. NanoSight results demonstrated a wide range of diameter size, which demonstrated aggregation of PBAE polymer into big clusters while measuring. The average diameter size calculated was 293.9 nm (Figure 23).

PBAE polymer Sample	Measured Sulfur concentration (mg/L)	Total Sulfur present in 5 mL of sample	
		mass (mg)	# of moles
1.15:1 ratio	68.591	0.342	1.069×10^{-5}

Table 6. Sulfur measured through ICP-MS.

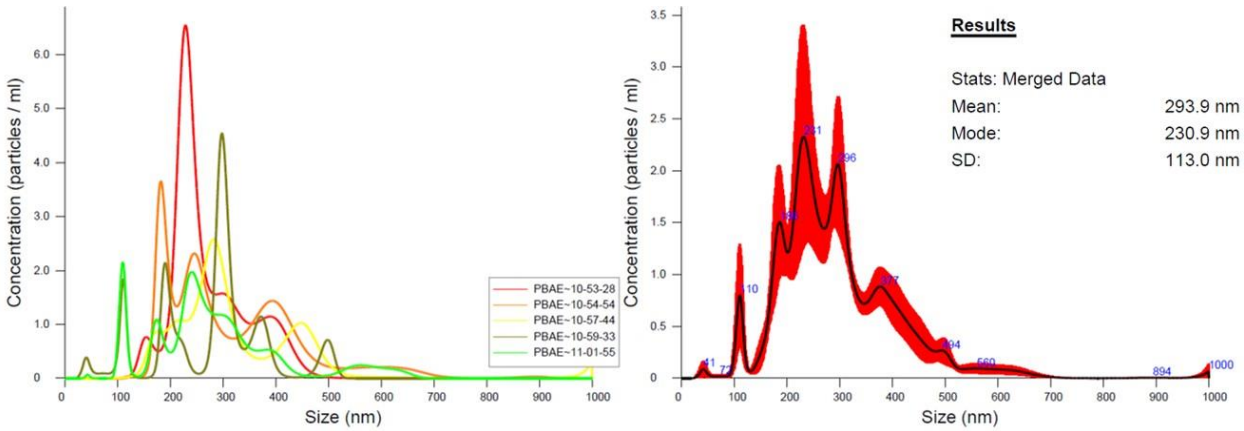

Figure 23. Range of PBAE polymer diameter size measured by NanoSight.

4.2 PBAE Polymer Cytotoxicity

Cell viability percentage of three cell lines, SIM-A9, B16F10, and GL26, was determined following the classic MTT assay[18]. After 24 hours incubation of cells with each component at various concentrations, results demonstrated that PBAE polymer alone has a lower toxicity compared to the nanocarrier assembled PBAE-WTAS. PBAE polymer alone demonstrated higher toxicity for SIM-A9 and B16F10 cells at higher concentrations (around 0.5 mg/mL), while remained nontoxic for GL26 cells. PBAE-WTAS nanocarrier demonstrated a close to 50% cell viability at concentrations between 0.1-1 mg/mL, with the highest toxicity for SIM-A9 cells and similar toxicity for B16F10 and GL26. This data was processed using Graphpad Prism 5.0[19].

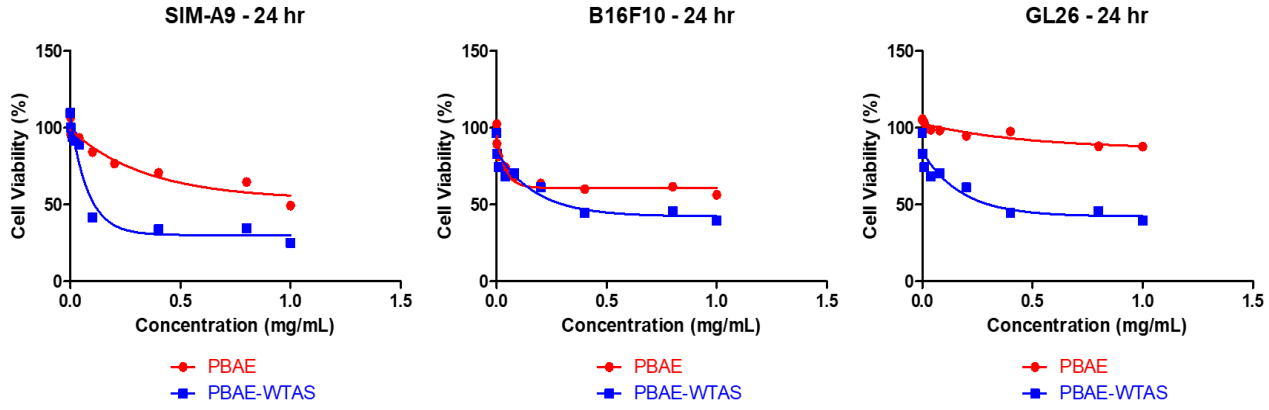

Figure 24. Cell viability for SIM-A9, B16F10, and GL26 cell lines treated with PBAE polymer alone and PBAE-WTAS assembled nanocarrier.

4.3 Cellular Transfection Experiments

4.3.1 Zeta potential measured over time after loading nanocarrier with pDNA

After PBAE-WTAS nanocarrier was completely assembled, it was loaded with GFP plasmid DNA, and surface charge was measured over time in order to determine optimal concentrations between pDNA and the nanocarrier to obtain a positive charge, which would be ideal for cellular uptake. Since DNA is anionic, two different concentrations of the nanocarrier

were loaded with 500 ng pDNA, and zeta potential was measured over a course of 3 ½ hours. Results (Table 7) demonstrated that surface charge remained positive during the 3 ½ hours when the nanocarrier concentration was higher, whereas for the lower nanocarrier concentration, the positive charge decreased over time.

Incubation time (hour)	**Zeta Potential (mV) PBAE-WTAS nanocarrier with 500 ng GFP pDNA**	
	0.2 mg/mL nanocarrier	0.6 mg/mL nanocarrier
1	1.42	16.44
2	0.31	2.67
3	-0.04	8.19
3 ½	-0.82	9.55

Table 7. Zeta potential measured for nanocarrier loaded with pDNA during a 3 ½ hours incubation time.

4.3.2 Effective transfection experiments using GL26 cells

GL26 cells were successfully transfected with PBAE-WTAS under the following conditions: 0.5 mg/mL PBAE-WTAS loaded with 800 ng GFP pDNA, and RPMI supplemented with 5% FBS (half the serum used for normal grow conditions). After treating cells with transfection reagents, normal grow media was used and replaced daily to maintain cells healthy. Transfected cells were visible within the next 40 hours after treatment and remained alive and fluorescent up to after 80 hours post treatment. Experiments with these conditions have been repeated multiple times, and an efficient transfection has been notable. Figure 22 shows the images captured for GL26 cells successfully transfected with PBAE-WTAS using a fluorescence microscopy at a 40X magnification.

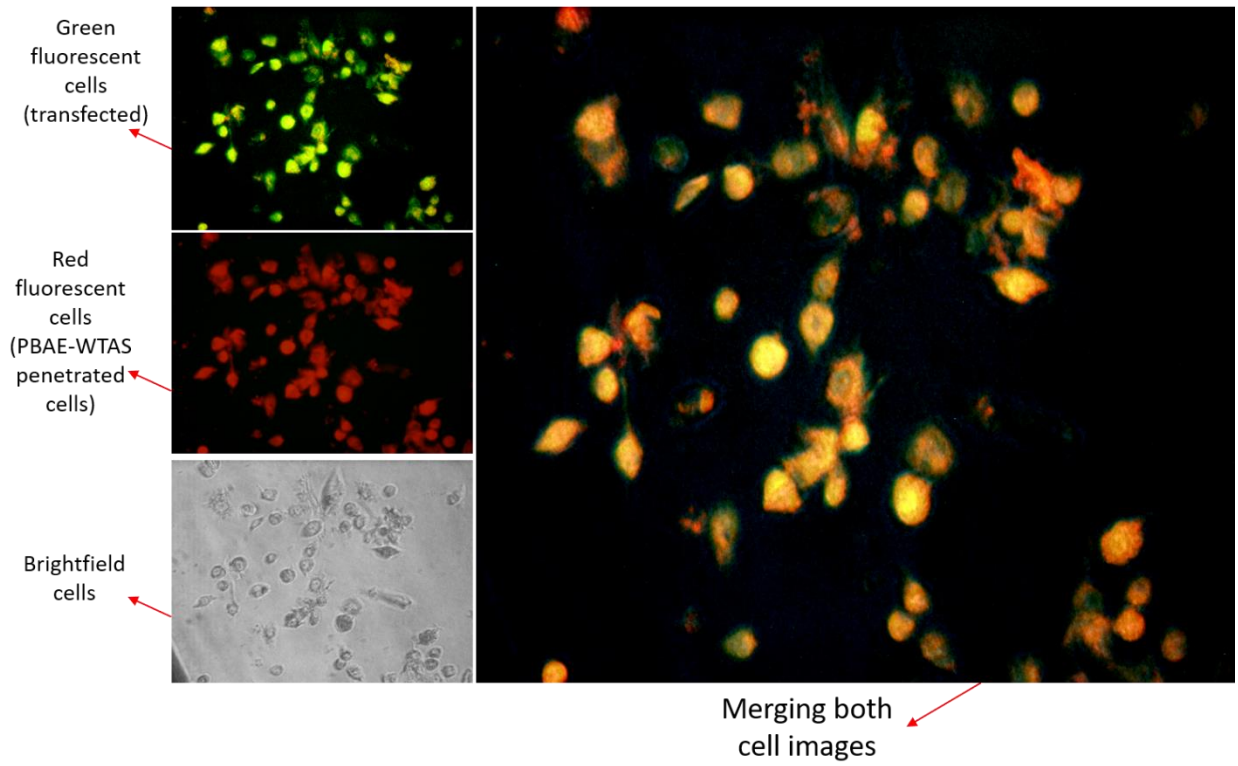

Figure 25. GL26 cells transfected with PBAE-WTAS.
Green fluorescence represents cells that were successfully transfected, red fluorescence represents penetration of PBAE-WTAS (WTAS labeled with rhodamine B), brightfield shows cells with no fluorescence light, and merged image demonstrates overlapping of red and green fluorescent cells. Images captured after 40 hours post transfection treatment, at a magnification of 40X.

5. Conclusion

This chapter describes the design of a novel gene delivery nanocarrier composed of a cell penetrating peptide (WTAS) as the primary nanocarrier and PBAE polymer as the secondary nanocarrier. In order to overcome early degradation of WTAS under physiological conditions, PBAE polymer was used to generate a more stable gene delivery system. The synthesis of PBAE polymer as well as the assembly of PBAE-WTAS nanocarrier are fully described and characterized. NanoSight results demonstrated that PBAE polymer aggregates to form larger clusters, and the calculated average size was determined to be 293.9 nm with a positive surface

charge of 7.12 mV. After assembling PBAE-WTAS nanocarrier, cytotoxic studies were conducted to determine safe concentrations to be used during cellular transfection experiments. Cytotoxic experiments demonstrated PBAE polymer alone is not toxic; however, once assembled with WTAS toxicity increases at higher concentrations. Based on cell viability results, cell transfection experiments were conducted using GL26, the cell line that showed a lower cytotoxic effect towards PBAE-WTAS nanocarrier. Before conducting transfection experiments, conditions required to generate a positive charge nanocarrier assembled with DNA were determined. For this, it was demonstrated that a higher concentration of PBAE-WTAS nanocarrier needed to be incubated for no longer than 1 hour in order to maintain the maximum positive surface charge. Once ideal conditions were generated (0.5 mg/mL of PBAE-WTAS incubated with 800 ng GFP pDNA for 30 min), transfection experiments were conducted. After 40 hours post transfection treatment, cells were successfully transfected.

6. References

[1]Amber M. H. Gene Therapy for Cancer: Present Status and Future Perspective. *Molecular and Cellular Therapies*. **2014**, 2(27):1-19

[2]Riesz, Megan. How is gene therapy being used to treat cancer? *Nada-Farber Cancer Institute.* **2018,** https://blog.dana-farber.org/insight/2018/04/gene-therapy-used-treat-cancer/

[3]Gandhi K. J., Deshmane S. V., and Biyani K. R. Polymers in Pharmaceutical Drug Delivery System: A Review. *International Journal of Pharmaceutical Sciences Review and Research*. **2012**, 14(2):57-66.

[4]Kelly E., and Russell S. J. History of Oncolytic Viruses: Genesis to Genetic Engineering *Molecular Therapy*. **2017**, 15(4), 651–659.

[5]Goetz1 C., Dobrikova E., Shveygert M., Dobrikov M., and Gromeier M. Oncolytic Poliovirus Against Malignant Glioma. *Future Virology*. **2011**, 6(9):1045–1058.

[6]Eisenstein S., Chen S. H., and Pan P. Y. Immune Cells: More than Simple Carriers for Systemic Delivery of Oncolytic Viruses. *Oncolytic Virotherapy*. **2014**, 3:83–91.

[7]Green J. J., Langer R., and Anderson D. G. A Combinatorial Polymer Library Approach Yields Insight into Novniral Gene Delivery. *Accounts of Chemical Research*. **2007**, 41(6):749-759.

[8]Sawant R.R., and Torchilin V.P. Liposomes as 'Smart' Pharmaceutical Nanocarriers. *Soft Matter*. **2010**, 6(17):4026-4044.

[9]Secombe L., Verati T., Moheimani F., Wu S. Y., Sood A. K., and Hua S. Advances and Challenges of Liposome Assisted Drug Delivery. *Frontiers in Pharmacology.* **2015**, 6(286):1-13.

[10]Vicky V. M. Introduction to Polymeric Drug Delivery. *Internet Journal of Medicinal Update*. **2010**, 5(2):1-2.

[11]Farokhzad O. C. Nanotechnology for Drug Delivery: The Perfect Partnership. *Expert Opinion on Drug Delivery*. **2008**, 5(9):9217-929.

[12]Cun D., Jensen L. B., Nielsen H. M., Moghimi M., and Foged C. Polymeric Nanocarriers for siRNA Delivery: Challenges and Future Prospects. *Journal of Biomedical Nanotechnology.* **2008**, 4(3):1-18.

[13]Lynn D. D., and Langer R. Degradable Poly(β-amino esters): Synthesis, Characterization, and Self-Assembly with Plasmid DNA. *Journal of the American Chemical* Society. **2000**, 122(44):10761-10768.

[14]Green J. J., Langer R., and Anderson D. G. A Combinatorial Polymer Library Approach Yields Insight into Nonviral Gene Delivery. *Account of Chemical Research.* **2008**, 41(6):749-759.

[15]Sunshine J. C., Peng D. Y., and Green J. J. Uptake and Transfection with Polymeric Nanoparticles are Depended on Polymer End-Groups Structure, but Largely Independent of Nanoparticle Physical and Chemicals Properties. *Molecular Pharmaceutics.* **2012**, 9:3375-3383.

[16]Beranl G. M., LaRiviere M. J., Mansour N, Pytel P., Cahil K. E., Voce D. J., Kang S., Spretz R., Welp U., Noriega S. E., Nunez L., Larsen G. F., Weichselbaum R. R., and Yamini B. Convection-Enhanced Delivery and in Vivo Imaging of Polymeric Nanoparticles for the Treatment of Malignant Glioma. *Nanomedicine.* **2013**, 10(1):149-157.

[17]Allabashi R., Stach W., de la Escosura-Muniz A., Liste-Calleja L, and Merkoci A. ICP-MS: A Powerful Technique for Quantitative Determination of Gold Nanoparticles without Previous Dissolving. *Journal of Nanoparticle Research.* **2008**, 11:2003-2011

[18]Stockert, J. C.; Blazquez-Castro, A.; Canete, M.; Horobin, R. W.; Villanueva, A., MTT assay for cell viability: Intracellular localization of the formazan product is in lipid droplets. *Acta Histochem.* **2012,** *114* (8), 785-796.

[19]https://www.graphpad.com/support/prism-5-updates/

[20]Yu B., Zhang Y., Zheng W., Fan C., and Chen T. Positive surface charge enhances selective cellular uptake and anticancer efficacy of selenium nanoparticles. *Inorg Chem.* **2012**, 51(16):8956-8963

Chapter 5 - Summary and Future Studies

1. Summary of Results

Therapeutic peptides have become a hot topic of interest for approaches to fight against multiple disease such as virus and bacterial infections as well as cancer[1-3]. These peptides have the ability to act as different enzymes in order to accomplish the job needed, and some can also be used to transport payload into cells. However, the use of therapeutic peptides alone comes with major drawbacks, as they have a low stability under physiological conditions and can be degraded rapidly by multiple proteases present in the human body, some have cytotoxicity effects, and they also lack specificity and their internalization into cells might be limited to only a few cell types[3,4]. In order to overcome these limitations, the strategy of developing nanoparticles conjugated or coated with peptides has been investigated as means to protect peptides from an early degradation while facilitating both transportation and delivery of these into cells[1,5]. Currently, this strategy has become one of the most promising approaches to combat any disease.

In our study we describe the successful design and development of an effective cell penetrating peptide, WTAS, which is a peptide containing a microtubule associated sequence. For this peptide, different amino acids were replaced on a specific location in the peptide sequence and the structure was predicted. The replacement of threonine with tryptophan generated a predicted structure where the α-helix and the random coil were 'folded in half' and less hindered. WTAS was synthesized and characterized, and results demonstrated successful synthesis and labeling of WTAS with rhodamine B, a fluorescent tag. Cytotoxic studies demonstrated that WTAS toxicity in cells increased at higher concentrations. Live and fixed confocal studies demonstrated that WTAS is able to penetrate B16F10 cancerous cells at low

concentrations within a few seconds, and further reached the cell nucleus in a matter of a couple minutes after exposure. Confocal studies were also conducted on SIM-A9, a noncancerous cell line, and results demonstrated that WTAS is still capable to penetrate these cells, but it is not able to penetrate the cell nucleus even after 24 hours. WTAS became an interesting peptide with unique properties, for this reason it was further investigated to develop an anti-cancer peptide and a gene delivery nanocarrier.

D-SA-K_6L_9-AS is a peptide with a high toxicity for both cancerous and noncancerous cells. WTAS peptide was combined with this toxic peptide to create WTAS-D-SA-K_6L_9-AS peptide. The goal of this was to develop a peptide to combine both unique properties for each peptide; high toxicity and ability to rapidly penetrate cell nuclei. Cytotoxicity effect remained the same as the one for D-SA-K_6L_9-AS alone, which demonstrated that toxicity levels were not altered upon addition of WTAS. Live confocal studies demonstrated that WTAS-D-SA-K_6L_9-AS did not lose the ability to target the mitochondria after penetrating the GL26 cells, which was discovered for D-SA-K_6L_9-AS. Lastly, it was discovered that WTAS-D-SA-K_6L_9-AS used the necrosis pathway only to kills GL26 cells within 3 hours at relatively low concentrations.

Finally, poly(β-amino ester) (PBAE) polymer was successfully synthesized, and the final product was capped to contain two secondary amine groups, which has been demonstrated to enhance both cellular uptake and transfection in previous studies[4]. After characterizing this polymer via ^{1}H- and ^{13}C-NMR, MS, and NanoSight, it was assembled with WTAS by coupling the amine groups on the polymer with the carboxyl group on WTAS. Cytotoxic studies demonstrated that PBAE polymer alone was nontoxic to cells; however, once it was assembled to WTAS, the toxicity was increased at higher concentrations. Then, cell transfection experiments were conducted. For this, PBAE-WTAS nanocarrier was self-assembled with a

plasmid DNA engineered to express GFP, and previous test experiments were conducted to determine optimal conditions and concentrations of both nanocarriers and DNA were required for transfection experiments. After establishing ideal conditions (0.5 mg/mL of PBAE-WTAS nanocarrier, 800 ng GFP pDNA, and incubation time of 30 minutes), transfection experiments were successful and within 40 hours over 90% cells had been successfully transfected.

2. Discussion and Future Research

Development of an effective cell penetrating peptide was an attractive strategy to exploit and improve multiple pathways for cancer treatments. The sequence of a peptide is crucial not only for the structure determination, but even for the function of a peptide. Here, it was determined that replacement of a single amino acid in the peptide sequence changed both structure and function for WTAS. Results demonstrated that WTAS was able to penetrate cells and reach cell nuclei in cancerous cells rapidly, which was not the case for noncancerous cells. One of the very next steps will be to conduct more confocal cellular uptake experiments in multiple cell lines (cancerous and noncancerous) to determine if WTAS nucleus penetration is cancer specific or cell line specific. Depending on these results, WTAS could further be tested in mouse models growing cancer tumors for cancer detection approaches.

WTAS is a relatively long peptide, containing a total of 27 amino acids; therefore, another next step would be to synthesize shorter fragments of WTAS and determine if cell penetration is maintained. Different studies have demonstrated that truncated versions of a longer peptides can maintain the functionality, whether it is cell penetration or antimicrobial activity[5-7]. For this reason, it would be interesting to determine if that could be case for WTAS, and the efficacy of cell and nucleus penetration is maintained for a shorter fraction of WTAS.

After identifying the actual fragment in WTAS to be responsible for cellular uptake, WTAS could become a base-like model to be combined with many other peptides for different approaches such as disease detection and/or treatments.

WTAS was combined with an anti-cancer peptide, D-SA-K_6L_9-AS, and for this section, further experiments must be conducted. Here, two peptides with unique functions were combined, and these functions were maintained in the longer peptide synthesized, WTAS-D-SA-K_6L_9-AS. However, this peptide was still nonspecific and remained highly toxic for all cell lines. Therefore, a secondary nanocarrier, like a polymer or nanoparticle, should be synthesized around WTAS-D-SA-K_6L_9-AS to transport and deliver this peptide to a targeted site.

Another future step would be to combine WTAS with a chemotherapeutic drug, like doxorubicin, to develop a more effective and targeted drug. Doxorubicin is one of the most common chemotherapeutic drugs used against various cancer types, but just like with many other drugs, it lacks cancer specificity and kills both healthy and cancerous cells. Recently, a major side effect discovered for the use of doxorubicin is cardiotoxicity, in other words, damage to the heart muscles[8]. In order to continue using an effective drug against cancer, it should be modified so that it can be more target specific and used even at lower doses. For this reason, WTAS could be combined with doxorubicin to possibly be more cancer specific and even used at lower doses compared to the ones used currently.

Lastly, WTAS was used to develop a novel gene delivery system. Here, it was demonstrated that PBAE-WTAS was effective in transfecting cancerous cells. However, this is just the first step, where a base model nanocarrier was developed. The PBAE polymer can be coated with a target ligand and the genetic material can be replaced by another plasmid DNA or even siRNA (small interfering Ribonucleic Acid), in order to develop a more disease specific

nanocarrier. As of right now, all experiments completed have been *in vitro*; therefore, *in vivo* experiments are also required to be completed.

4. References

[1]Acar H, Ting JM, Srivastava S, La Belle JL, Tirrell MV. Molecular engineering solutions for therapeutic peptide delivery. *Chem Soc Rev*. **2017**, 46(21):6553-69.

[2]Zuconelli CR, Brock R, Adjobo-Hermans MJW. Linear Peptides in Intracellular Applications. *Curr Med Chem*. **2017**, 24(17):1862-73.

[3]Raucher D. Tumor targeting peptides: novel therapeutic strategies in glioblastoma. *Curr Opin Pharmacol*. **2019**, 47:14-9.

[4]Sunshine J. C., Peng D. Y., and Green J. J. Uptake and transfection with polymeric nanoparticles are depended on polymer end-groups structure, but largely independent of nanoparticle physical and chemicals properties. *Mol Pharmaceutics* **2012**, 9:3375-3383

[5]Guidotti G., Brambilla L., and Rossi D. Cell-Penetrating Peptides: From Basic Research to Clinics. *Trends Pharmacol Sci*. **2017**, 38(4):406-424.

[6]Eskandari S., Guerin T., Toth I., and Stephenson R. J. Recent advances in self-assembled peptides: implications for targeted drug delivery and vaccine engineering. *Advanced Drug Delivery Reviews.* **2017**, 110:169-187.

[7]Perez-Peinado C., Dias S. A., Domingues M. M., Benfield A. H., Freire J. M., Radis-Baptista G., Gaspar D., Castanho M. A. R. B., Craik D. J., Henriques S. T., Veiga A. S., and Andreu D. Mechanism of bacteral membrane permeabilization by crotalicidin (Ctn) and its fragment Ctn(15-34), antimicrobial peptides from rattlesnake venom. *The American Society for Biochemistry and Molecular Biology*. **2018**, 293(5):1536-1549.

[8]Thorn C. F., Oshiro C., Marsh S., Hernandez-Boussard T., McLeod H., Klein T. E., and Altman R. B. Doxorubicin pathways: pharmacodynamics and adverse effects. *Pharmacogenet Genomics*. **2012**, 21(7):440-446.

Appendix A - For Chapter 2

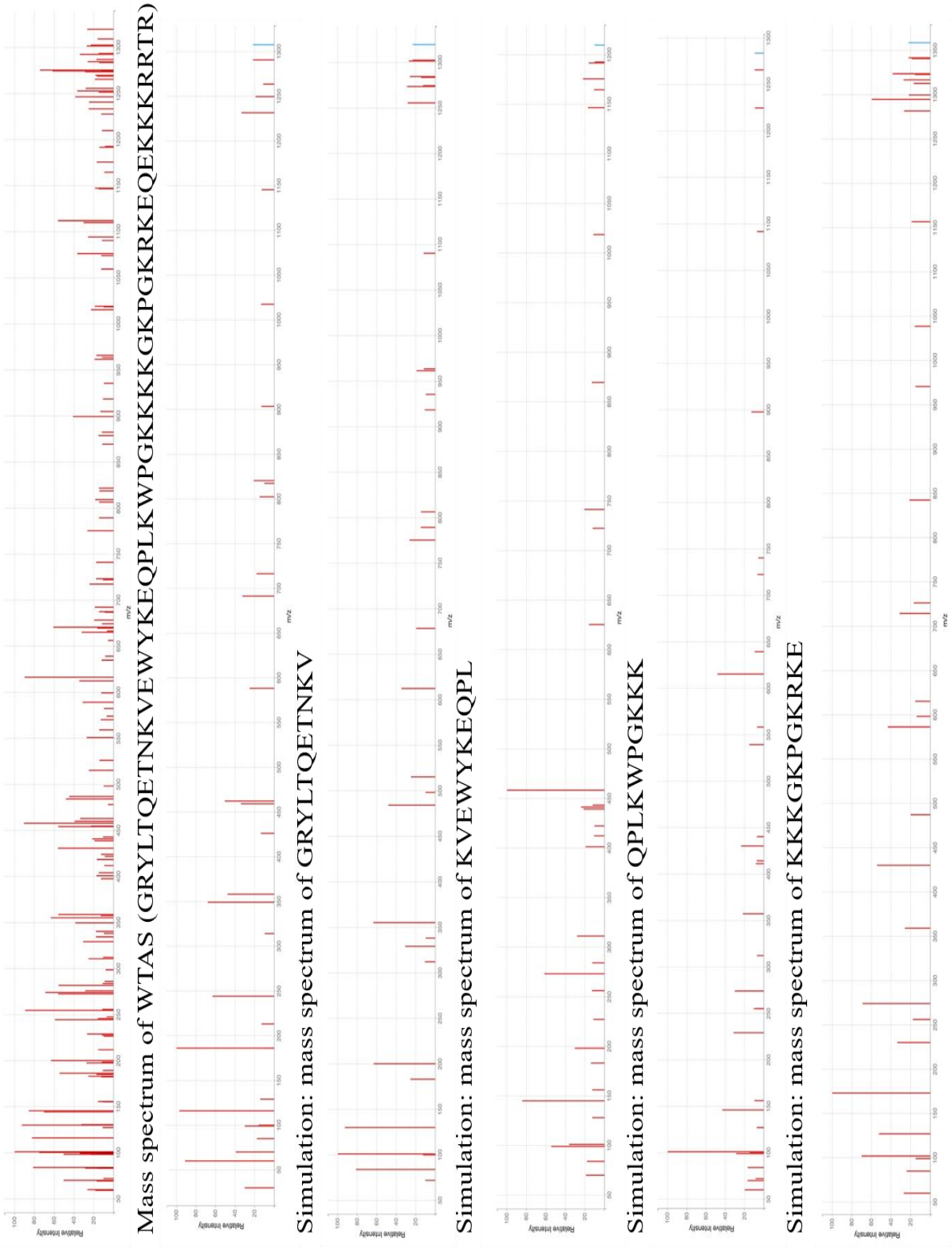

Figure A.1. MS results for unlabeled WTAS, and simulation for detected fragments.

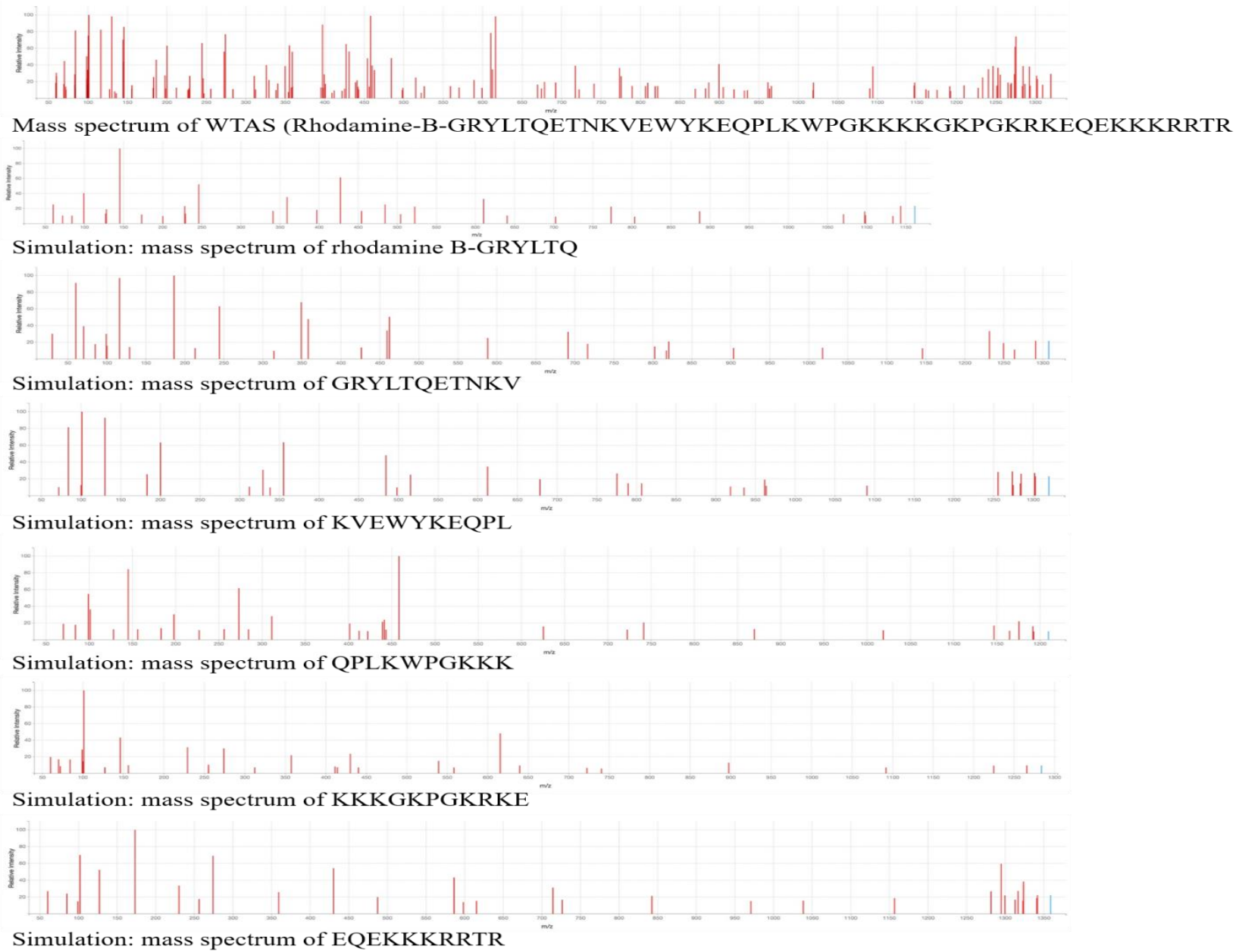

Figure A.2. MS results for rhodamine B labeled WTAS, and simulation for detected fragments.

Appendix B - For Chapter 3

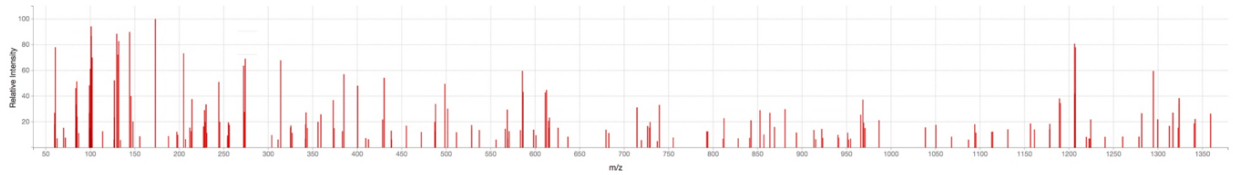

Mass spectrum of SALKLLKKLLKKLLKLLASPLKWPGKKKKGKPGKRKEQEKKKRRTR

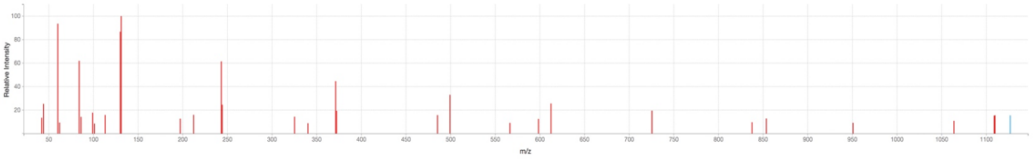

Mass spectrum of SALKLLKKLL

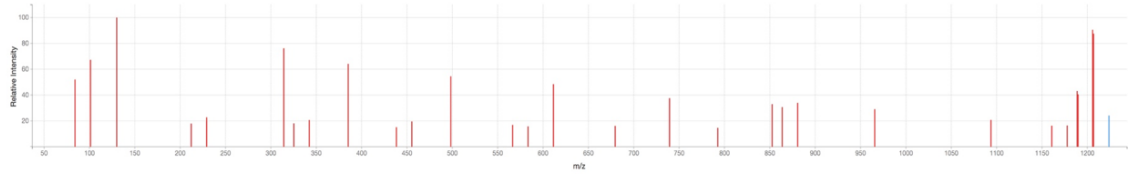

Mass spectrum of KKLLKLLASPL

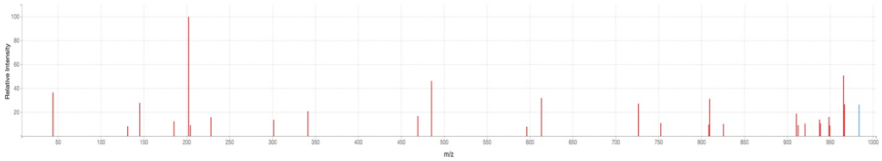

Mass spectrum of ASPLKWPGK

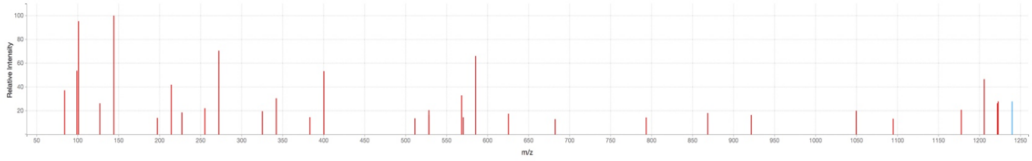

Mass spectrum of KLKWPGKKKK

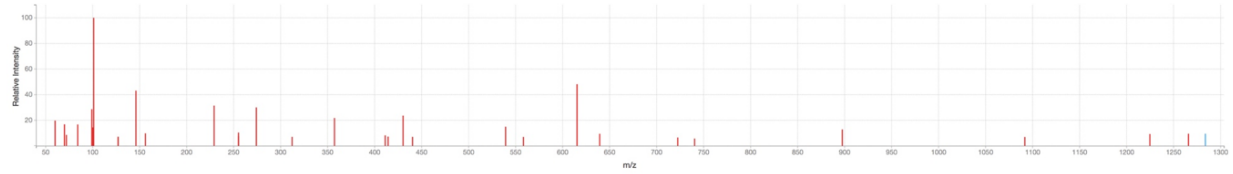

Simulation: mass spectrum of KKKGKPGKRKE

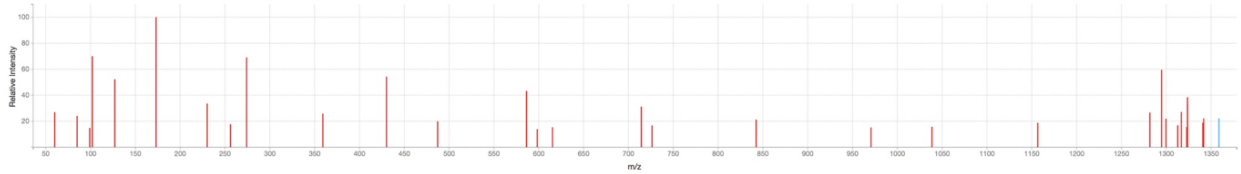

Simulation: mass spectrum of EQEKKKRRTR

Figure A.2. MS results for WTAS-D-SA-K_6L_9-AS, and simulation for detected fragments.

Appendix C - For Chapter 4

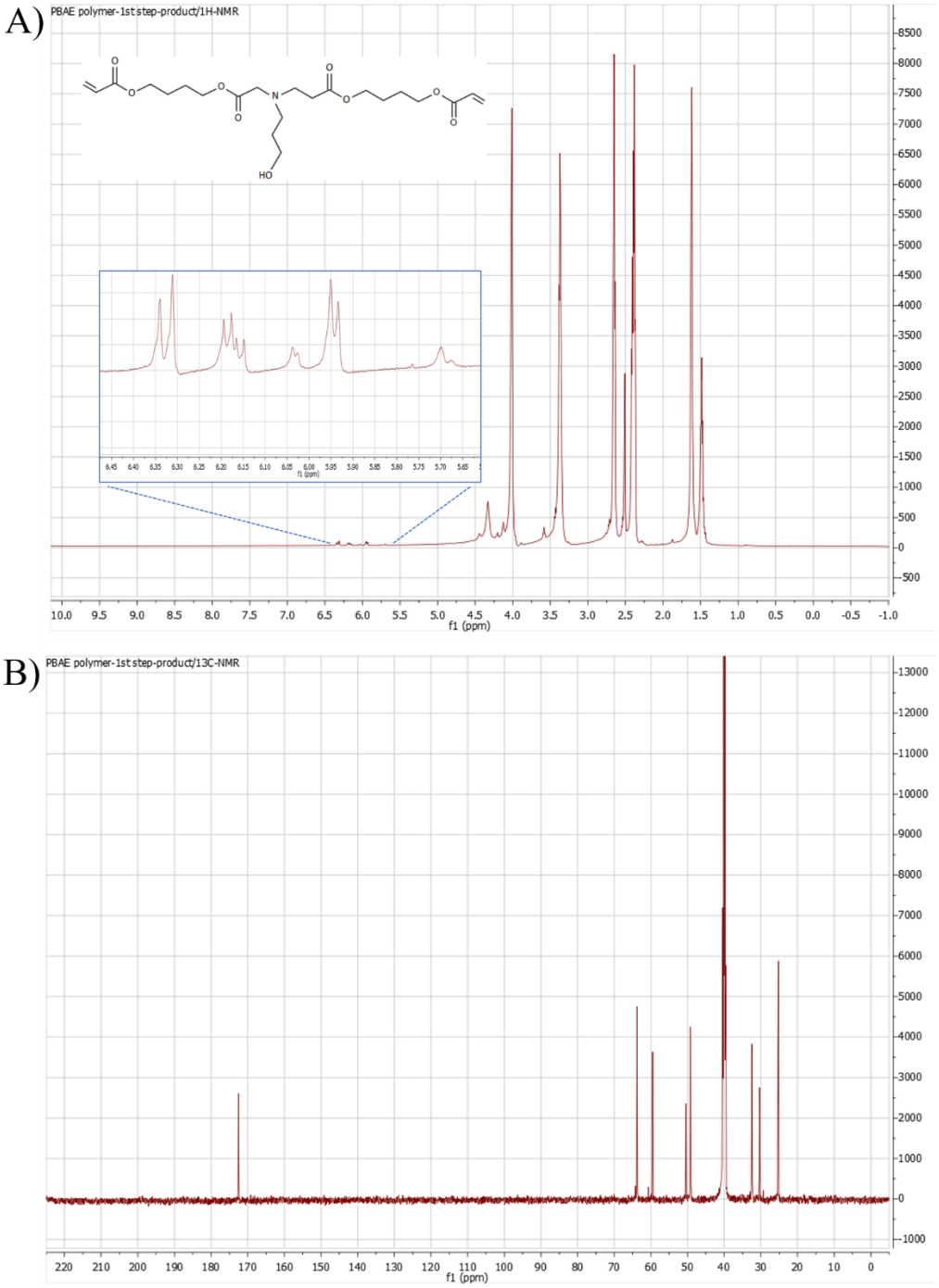

Figure C.1. A) ^{1}H- and B) ^{13}C-NMR of 1st reaction step, intermediate from PBAE polymer synthesis.

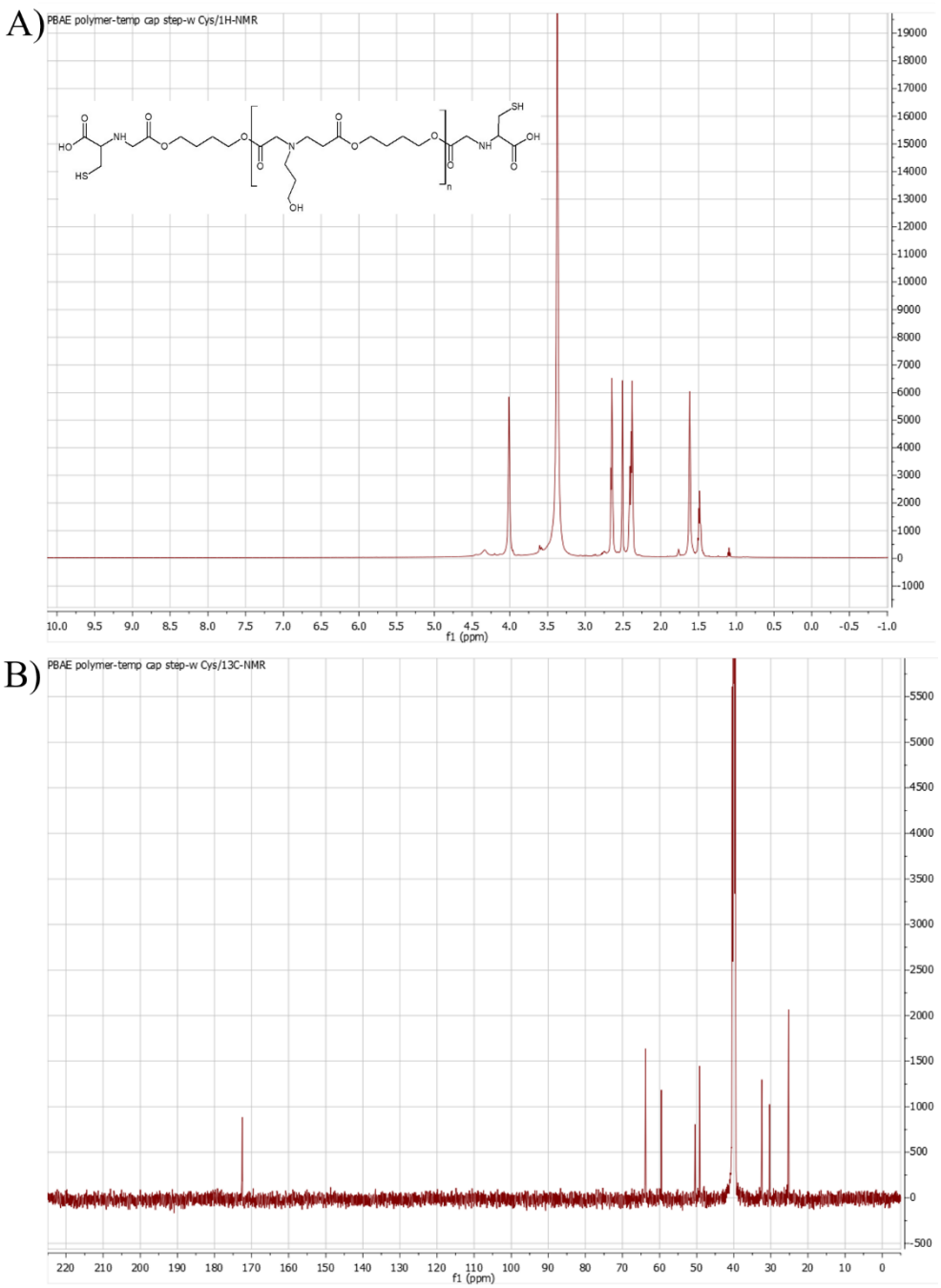

Figure C.2. A)^{1}H- and B)^{13}C-NMR of 2nd reaction step, adding the temporary end-cap group of cysteine from PBAE synthesis.

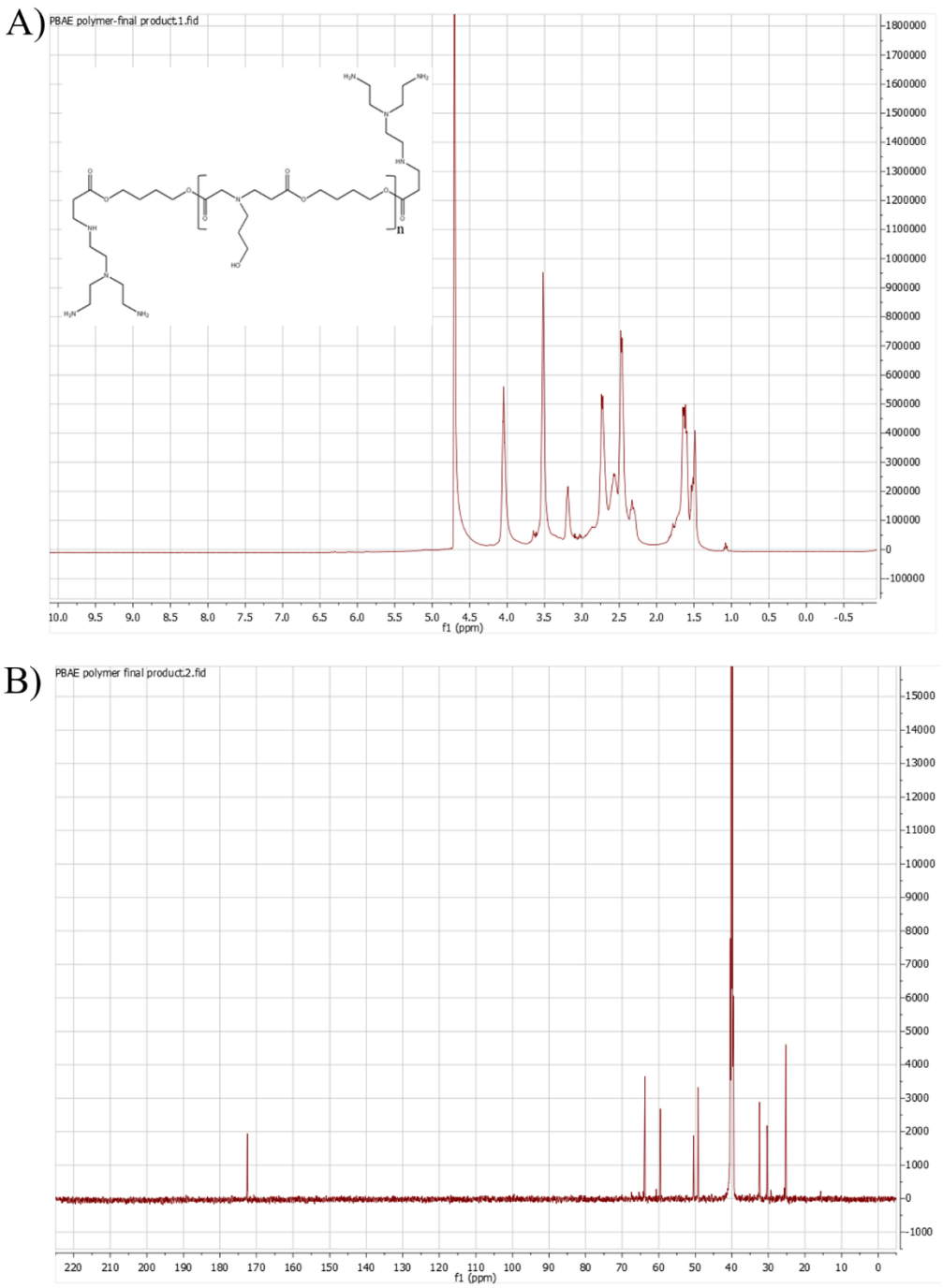

Figure C.3. A)^{1}H- and B)^{13}C-NMR of 2nd reaction step, final product from PBAE polymer synthesis.

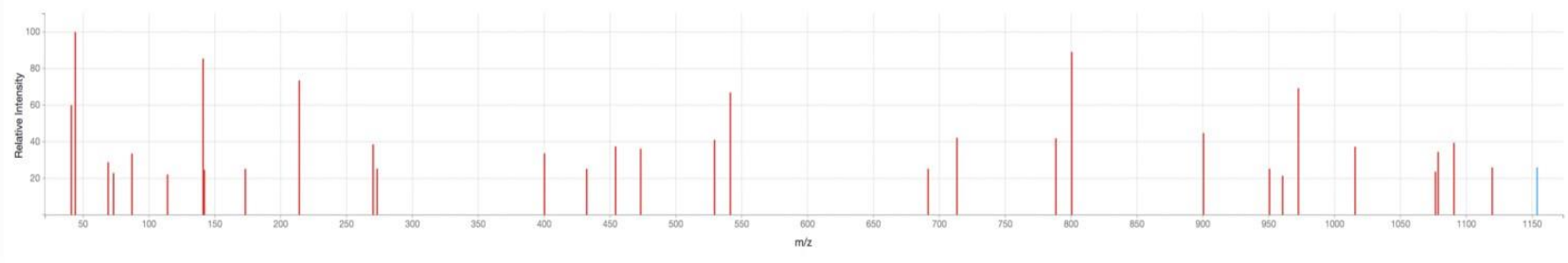

Chemical Formula: $C_{53}H_{97}N_7O_{19}$ Exact Mass: 1135.68 Molecular Weight: 1136.39m/z: 1135.68 (100.0%), 1136.69 (57.3%), 1137.69 (16.1%), 1138.69 (3.0%), 1136.68 (2.6%), 1137.69 (2.5%), 1138.69 (2.2%), 1137.68 (1.5%), 1137.69 (1.4%), 1136.69 (1.1%)Elemental Analysis: C, 56.02; H, 8.60; N, 8.63; O, 26.75

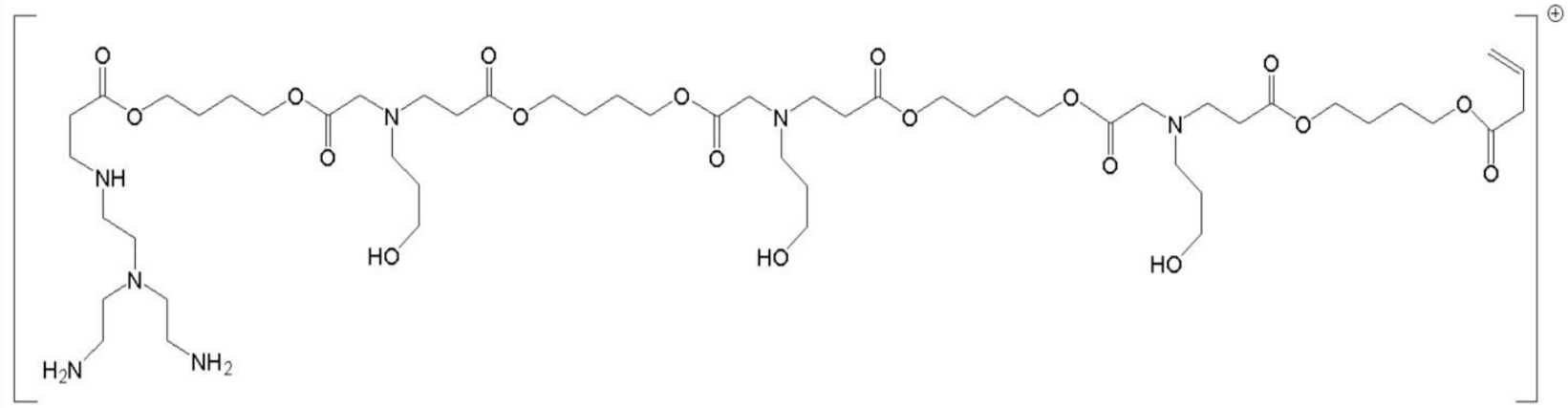

Figure C.4. MS results for PBAE polymer, largest fragment detectable.